PLANAR SLIDING OF A RIGID BODY WITH DRY FRICTION: LIMIT SURFACES AND DYNAMICS OF MOTION

A Dissertation

Presented to the Faculty of the Graduate School

of Cornell University

in Partial Fulfillment of the Requirements for the Degree of

Doctor of Philosophy

by

Suresh Goyal

January 1989

PLANAR SLIDING OF A RIGID BODY WITH DRY FRICTION: LIMIT SURFACES AND DYNAMICS OF MOTION

Suresh Goyal, Ph.D.
Cornell University 1989

We present a relation between friction 'load' (force and torque) and slip 'motion' (displacement and rotation) for a rigid planar object sliding on a flat surface, where the distribution of the normal contact forces between the object and the supporting surface is assumed to be known *a priori* and the friction is assumed to be independent of slip rate. Every point of frictional contact is assumed to obey a 'maximum work inequality', which generalizes Coulomb friction. Then in analogy with the 'maximum plastic work inequality' in classical plasticity, the relation between the total frictional load and slip motion for the given slider also obeys a 'load motion inequality'.

The full relation between the frictional load and the slip motion for an object can thus be described by a convex limit surface in load space, with the instantaneous motion direction (in conjugate motion space) being normal to this surface, where it is smooth. The object's limit surface can be found by Minkowsky addition of the limit surfaces of the individual contact points or by other simple means. Attention is focussed on the cause of the occurrence of vertices on the limit surface (where motion is not unique for a given load) and flat regions (where load is not unique for a given motion). In the special case of isotropic friction, the possible frictional loads for the given object are also fully characterized by a single scalar function of the relative position of the center of rotation, which is called the moment function.

A few special types of contacts are considered in more detail: sliders with discrete points of isotropic support, points of contact which are wheels or skates, and symmetric distributions of contacts of these types.

The limit surface gives insight into certain aspects of sliding motion: the propensity for sliders to rotate about points of support; the uniqueness of incipient motion associated with a given applied load when inertia is involved; and the existence of special final motion directions (in body axes), independent of initial conditions, for all rigid planar objects slowed by dry friction.

Biographical Sketch

The author was born in the town of Bhatinda, Punjab, in India, on December 6^{th}, 1960. His primary and secondary education was in various schools in India. He was awarded the B.Tech. degree in Mechanical Engineering by the Indian Institute Of Technology, Kharagpur, India, in May 1982; his final thesis being on the development of low cost reading aids for sightless people.

The M.S. degree in Mechanical Engineering was awarded him by the University Of Iowa, Iowa City, in August 1984; his thesis was on the kinematics of the lumbar spine.

From the fall of 1984 he has been enrolled in the Ph.D. program in Mechanical Engineering at Cornell University, Ithaca, with a research concentration in the fields of Mechanics, Friction and Robotics.

For my angelic sister, **Reena**

Acknowledgements

First and foremost, I would like to thank my thesis advisor Andy Ruina for sharing with me his insights and knowledge in Mechanics, which made the writing of this dissertation possible. Dr. Jim Papadopoulos contributed a great amount to this research through novel ideas, discussions and help with some proofs; I am thankful to him. I am indebted to Dr. John Hopcroft for his moral and financial support, and for encouraging me to work with Andy. Acknowledgements are due to Dr. Dean Taylor for chairing my special committee, for financial support, and for the use of the computing facilities at IMAP; Dr. James Thorpe for serving on my special committee and for his kindness during my A-exam.

I also greatly appreciate the support and friendliness of Dr. Bruce Donald, Dr. Subrata Mukherjee and Dr. Chris Hoffmann.

A special mention here to Dr. Frank Rizzo for his faith and encouragement, and his spiritual guidance.

My warmest acknowledgements to my dear friends Michael O'Donnell, George Freij, Daniela Rus, Kanwardip Singh, David Boss, Dennis McGowan, Pooja Sinha, Beena Upadhyay, Maria de Miguel, Edith Klein, Veronique Hervouet, Nadine Aubry, Mona Singh, Edelle O'Donnell, Coeli Barry, Ashish Verma, Patrick Stephenson, Partha Banerjee and Parvinder Ahluwalia, to mention just a few; they treated me most special and were there for everything.

I would like to acknowledge the help of Kapil Mathur with computing; Christine Van Borm, Dave O'Neill, Bill Horn and Richard Warkentin with figures. Special thanks to Olga Peschansky for her help in translating the Russian literature. I appreciate the efforts of Katrin Elbert and Valerie Jobin in carefully reading this dissertation.

Most important, I would like to thank my wonderful and devoted parents for their immense love, and for what they mean to me.

This research was supported at various periods through research and teaching assistantships; a grant from the Emerson Electric Company and COMEPP; and the PYI award of Andy Ruina from the NSF.

Table of Contents

List of Figures

Chapter 1

Introduction

Because mechanical systems with dry frictional contact are generally non-conservative and are also not governed by linear equations, they do not usually fall into the appealing structures of either Lagrange's equations or linear systems theory. However, within the context of more restrictive assumptions, certain interesting, and perhaps useful results about the mechanics of slip can be obtained. This dissertation concerns itself with the following restricted problem.

1.1 Problem Statement

1. *A rigid planar body slides on a horizontal planar surface.*
2. *The contact normal force (or pressure) distribution is known* a priori.
3. *The friction force or traction at each contact point depends on normal force (or pressure) and direction of relative motion.*
4. *Frictional forces are independent of the magnitude of the slip rate and also of the slip rate history.*
5. *The dependence of friction force on direction is consistent with a maximum work inequality. The maximum work inequality generalizes Coulomb friction to include anisotropic contacts mediated by skates and wheels.*

Extra assumptions sometimes used are:

6. *Isotropy of friction. This yields standard Coulomb friction at each point.*
7. *Proportionality of friction force (or traction) on normal force (or pressure).*
8. *Uniformity of properties over the surface.*

Subject to the assumptions mentioned above, our central concerns are:

1. Is there a simple representation of the overall relation between the total friction load (force and moment) due to arbitrary motions (velocity and rotation rate) of the rigid body?
2. What general conclusions may be drawn about the dynamics of free or forced sliding of an arbitrary slider?

1.2 Motivation

According to Jellett [1872], development of the 'Theory of Friction' should be an integral part of Rational Mechanics. One task in this development is the formulation of constitutive laws for frictional slip between sliding surfaces. This task could include postulation of laws that define friction forces at a point as a function of slip, slip rate, loading conditions, time effects or any other state variables; experimental test of such laws [e.g. referenced in Oden and Martins 1984], or the micro-mechanical investigation of the causes of such laws [e.g. Tabor 1981].

Another task, is understanding the implications of particular friction laws on the overall behaviour of sliding objects. This study addresses the motion of rigid bodies with particularly simple friction laws. In particular, it is centered on the result that for certain simple friction laws, the overall frictional load and motion relationship for a planar slider is completely characterized by an appropriate closed and convex surface. Moreover, the symmetries of these surfaces and their geometrical properties provide useful insights into the dynamics of sliding.

One possible application of this study is in 'robotic motion planning', where sliding occurs in the manipulation of objects. Some desirable instances of 'sliding motion' are discussed by Mason [1985] where manipulation of a solid object by a robot hand may involve relative slip without full direct control of all possible degrees of freedom of the sliding object. Another application could be in the numerical simulation of the dynamic motion of rigid bodies with dry friction [Lötstedt 1981, Jean and Pratt 1985, Jean and Moreau 1986], a few examples of which are presented later. An interesting application is in finding the stable motions of planar sliders during free sliding, special cases of which, like the motion of rings and discs are discussed in Ishlinskii et al. [1981] and Voyenli and Eriksen [1985].

1.3 The Friction Law

The primary friction law that we use is due to Coulomb [1785], Da Vinci [referenced in Dowson 1979], and Amontons [1699] and is stated as follows: *during slip the frictional force is directly proportional to the normal force and opposes motion.* In the theory that we develop for the overall load-motion relationship, the assumption of an isotropic coefficient of friction implicit in this law can be generalized to also include all friction laws which satisfy a maximum work inequality, to be discussed later. We assume that such a friction law applies at every 'point' of contact, whether it is a differential element in a distributed contact region, or a point carrying a finite non-zero load. Besides Coulomb friction, anisotropic frictional behaviour modeled as contacts mediated by wheels or skates also obeys the maximum work inequality.

1.4 Central Result

Assuming a known motion, a Coulomb type friction law that obeys the maximum work inequality, and known values for the contact pressure and friction coefficient everywhere, the total friction force and moment can be found by summation or integration over the region of contact. In some sense, the entire presentation that follows is a discussion of

that sum and its properties. This sum, for arbitrary motions, can be described using a 'limit surface' (LS) which fully characterizes the relation between the motion and the total friction force and torque acting on a given object.

> *For any body sliding on a plane with known normal forces and a friction law that obeys the 'maximum work inequality', the relationship between the friction force and the motion is characterized by a surface in three dimensional load space (two components of force and the torque). During slip, the loads are on this surface and the direction of motion, in three dimensional motion space (two components of linear velocity and the angular velocity) is the normal to this surface (where it is smooth). When no slip is occuring, the loads are within or on the surface.*

The surface just described is the limit surface (LS) for the slider. The relation between motion and the LS, if as described above, is called normality.

1.5 Friction And Plasticity

The above normality principle is more or less directly quoted from classical plasticity. In fact, rate independent friction has an intertwined relation with plasticity theory. Friction is variously used as (*a*) a metaphor for, (*b*) an example of, (*c*) a counter example of, and (*d*) something to be explained by plasticity; as reviewed in Michalowski and Mroz [1978]. Frictional slip is (*a*) analogous to plastic deformation in that both involve (more or less) rate independent dissipation; the analogy can be made more precise when particular friction and plasticity laws are considered. If one thinks of slip as an extremely localized continuum deformation, then 'frictional slip' is (*b*) an example of inelastic (plastic) deformation. For the case of isotropic friction, and a finite number of support points between the slider and the supporting surface, our problem is precisely equivalent to the failure of a frictionless lap joint held by plastic rivets or bolts, a problem discussed e.g. by McGuire [1968]. Also, as pointed out by an anonymous reviewer, there is a correspondence between the problems analyzed here (those that use isotropic friction) with torsion and shear of a very short prismatic bar (or bars) made of ideally plastic material.

On the other hand, if the normal load is included as a variable, common friction laws violate the maximum plastic work postulate which is often assumed in plasticity, so that friction is a (*c*) counter example to plasticity in this regard. The micro-mechanics of friction is still not totally understood, but it is commonly held that (*d*) plastic deformation of the adjoining solids during slip is part of the micro-mechanics of frictional dissipation [e.g. Tabor 1981].

1.6 Limitations Of Model

This study does have its limitations. Though obviously of interest in practice (especially in robotic motion planning), the way in which external loading is applied to the sliding object, say with the possibly frictional contact of a pushing finger, is not considered here.

Nor do we consider the set of all possible contact pressure distributions consistent with a given center of gravity and region of contact as in Mason [1985] and Peshkin [1985, 1986]. Instead, we discuss only the overall load-motion relation for a given contact

pressure distribution. The requirement that this distribution be known *a priori* can be a severe restriction. In practice, the exact contact pressure distribution between contacting surfaces is almost always statically indeterminate; and there is insufficient information about surface deviation from flatness and deformation laws for the solid even to calculate this pressure distribution. In the illustrative examples that we use, simple normal pressure distributions have been chosen.

Also entirely neglected here are rate and memory effects in the friction laws. Such effects are surely important for the examination of stability (stick-slip and vibrations, e. g. Ruina 1983, 1985).

1.7 Literature Review

The literature surveyed briefly below is fairly sharply divided into the following categories based on the interests of the authors. The main lines of thought are friction laws, plasticity and friction, normality, moment function, dynamics of slip and motion planning in robotics.

1.7.1 Some Background On Friction Laws

The following works deal with the specification and review of friction laws.

Da Vinci [referenced in Dowson 1979], Amontons [1699] and Coulomb [1785] are credited with stating the simple friction law that is normally used under the name of Coulomb friction [Dowson 1979]. Tabor [1981] presents a comprehensive review of the current understanding of frictional processes; emphasizing the three main elements involved: the true area of contact, the area over which the atoms on one surface are within the repulsive fields of the other; the nature and strength of the interfacial bonds formed at the regions of contact; and the way in which the material around the contacting regions is sheared and ruptured during sliding, separation of material some distance away from the interface, and the ploughing of the softer material by harder asperities.

Oden and Martins [1984] critically review a large body of experimental and theoretical literature on friction laws as a basis for numerically modeling dynamic friction phenomenon like stick-slip motion, dynamic sliding and friction damping.

Ruina [1983, 1985] states and reviews some experimentally motivated state variable constitutive laws where the friction force is a function of slip rate and state variables, with particular emphasis on relations useful for stability analysis, e.g. stability of steady slip and incipient slip from a state of rest.

Papers dealing with the directional dependence of friction (anisotropy) are discussed in a later section.

1.7.2 Plasticity And Friction

Some precepts from the theory of classical plasticity as applied to this work, and their application towards friction phenomenon are investigated by the following authors.

In a series of papers on plasticity, Drucker [1951, 1954, 1959, 1964] postulates the Drucker's stability postulate or the maximum plastic work inequality and interprets it in terms of the 'stability' (meaning different things for different materials) of an elastic-plastic material under certain dead loading conditions. He also establishes that the postulate implies convexity and normality of the yield criterion for the material.

Savvin [1962, 1969] uses some of Zhukovskii's [1948] results to discuss the equilibrium between applied loads and dry frictional reactions (Coulomb friction) in rectangular frictional joints and couplings. McGuire [1968] analyzes the behaviour at plastic yield of a frictionless lap joint held by plastic rivets or bolts, based on Drucker's stability postulate, which is similar to the above problem.

In order to find approximate solutions for friction tractions in contact problems with dry friction, Kalker [1971] assumes the following minimum principle. For a given slip motion, the associated friction traction distribution (from the set of all possible friction traction distributions that satisfy the constitutive law of Coulomb friction) over the contacting area, is that which minimizes the difference between the power dissipated by the Coulomb traction generated by the slip and the power produced by the applied loads.

Inspired by the theory of classical plasticity, Curnier [1984] presents a general theory of friction that allows the incorporation of the dependence of the friction forces on the normal load, the initial roughness of the contacting surfaces and the subsequent wear of these surfaces. By choosing different potentials for frictional yield to determine the condition for slip, and for slip velocity to determine sliding directions at slip, the theory obeys normality of the slip velocity from the slip potential (not the normality we use). The condition of contact impenetrability is achieved as a by-product through the specification of penalty matrices. For contacting surfaces that are not microscopically flat, the theory is limited to small amounts of slip.

1.7.3 Normality

The following papers either deal with friction laws that obey normality, or argue against the application of normality to friction in general.

Moreau [1974, 1979] lays down the mathematical foundations of convex analysis as applicable to friction laws that obey convexity and normality. Though not widely referenced, he seems to be the only one to extend these ideas from Coulomb friction to anisotropic frictional behaviour caused by contact with wheels between the slider and the supporting surface. He clearly distinguishes between the psuedo-potential from which the friction force is derivable (by differentiation) and the dissipation potential (power dissipated to frictional forces), and points out possible relations between the two. Stating the friction law with a limit curve and a maximum work inequality, he shows its interpretation as principles of maximum and minimum dissipation, i.e. the friction force corresponding to a given motion is the one that maximizes the power dissipated to friction and the motion corresponding to a given friction force is the one which minimizes frictional dissipation. He also states certain principles governing the frictional load motion relation for sliders moving under constraints.

Michalowski and Mroz [1978] discuss the analogies between plastic flow rules for perfectly plastic materials and the sliding rules for perfectly rigid bodies with dry contact friction. They detail the case of orthotropic friction caused by wedge asperities, each of which is like a particle moving on an inclined plane with Coulomb friction. Their model does not result in normality for the overall frictional behaviour in terms of frictional tractions and velocities in the horizontal plane. They conclude that there is no reason that in general normality would apply to anisotropic frictional contact.

Zmitrowicz [1981 and personal communication] argues strongly against the applicability of normality to anisotropic dry friction in general.

Ziegler [1981], on the other hand, argues towards the fundamental thermodynamic validity of normality in thermomechanical phenomenon. He refutes the objections raised against it (including those of Michalowski and Mroz [1978]) by showing that:

1. The models used to check normality are too simple and do not correctly model reality, hence they are not conclusive.
2. Normality in motion space does not necessarily imply normality in load space.
3. Care must be taken in the formulation of the dissipation function.

1.7.4 Moment Function

The moment function is the moment of the frictional forces about the instantaneous center of rotation (COR) as a function of the position of the COR, for planar sliders with Coulomb friction. The moment function has been investigated by the following authors.

Zhukovskii [1948, the text is in Russian] (Zhukovskii actually died in 1921) studies the equilibrium between in-plane external loads and frictional forces for a planar slider with given normal pressure distribution and spatially uniform Coulomb friction. He seems to be the first to formulate the idea of the moment function and to show that the friction force can be obtained from it by differentiation. He also states that the moment surface approximates a circular cone centered at the center of pressure, at distances far removed from this center. He also observes that the friction force is maximum for pure translation of the slider, when the friction force and moment can be replaced by a single force passing through the center of mass of the slider. He proves that the COR when a pure moment is applied (called the pole of friction or the center of twist) cannot be outside the convex hull of the contact area.

For support distributions that are not confined to a line, he proves that the center of twist is unique and the moment function has a minimum at that point. He also proves that if the moments of all possible frictional force distributions (due to all possible motions of the slider) are taken about the center of twist, then the maximum of these moments is the one corresponding to the frictional force distribution obtained due to rotation of the slider about the center of twist.

Following up on his work, Shvedenko [1986] states and presents a proof of an *incorrect* theorem that all moment surfaces are surfaces of revolution about a vertical axis passing through the unique center of twist. Equation 1.6 in the proof of theorem 1 in his paper is incorrect.

The present author's independent development of the moment function approach largely duplicates Zhukovskii's [1948] contributions, except for certain new results regarding construction of moment surfaces and their relation to limit surfaces, all discussed in later chapters.

1.7.5 Slider Dynamics

The following authors have concerned themselves with the dynamics of slip in systems with dry friction.

Wittenburg [1970] analyzes the planar sliding of homogenous plates of constant thickness on a horizontal plane, with different friction laws. He plots the trajectories of motion in phase space, of the free sliding of a symmetric bar supported at its ends with Coulomb

friction. From these he shows that the bar comes to rest with final motion being rotation about one of the ends, and that there is a finite duration of time (before it stops), during which the bar purely rotates about this end.

Ishlinskii et al. [1981] analyze the free sliding of a uniformly supported ring, a uniformly supported disk, and a symmetric bar supported at its ends, all with a spatially uniform Coulomb friction coefficient. They show analytically the existence of final attracting motions for the ring and the disk, and demonstrates through numerical integration that the bar comes to rest in rotation about a point of support. They give an incorrect value for the position of the final attracting centers of rotation of the uniformly supported disk. Voyenli and Eriksen [1985] arrive analytically at similar but correct results for the ring and the disk (without reference to Ishlinskii et al. [1985]).

Lötstedt [1981] analyzes the problem of existence and uniqueness of solutions to the equations governing the motion of two dimensional rigid body systems, moving in mutual frictional contact (both point contact and line segment contact) with Coulomb friction. He presents examples of cases where the solution is non-unique or where shocks might occur; and using mathematical programming results he derives certain sufficient conditions for existence and uniqueness of solutions.

Jean and Pratt [1985] analyze the dynamics of motion of a finite set of perfectly rigid bodies subjected to holonomic constraints and to frictional constraints due to contact between bodies. The applicable dry friction law is the one proposed by Moreau [1974] which obeys convexity and normality, although they restrict their study to Coulomb's law. They formulate the problem as a quasi-variational inequality arising from the dissipational character of the system and the form of the friction law, and prove theorems about the existence of solutions.

Jean and Moreau [1986] develop numerical algorithms for determining the dynamics of systems in the presence of constraints and dry friction (that obeys convexity and normality), paying special attention to the occurrence of shocks. Amongst other examples, they simulate the chattering motion of a solid body elastically driven along a plane wall with Coulomb friction.

Jellett's [1872] text seems to be one of the earliest texts devoted solely to the theory of friction, touching upon topics like friction laws, equilibrium between applied forces and frictional forces, and the dynamics of motion of objects with dry friction. Prescott [1923] gives a pragmatic rationale for using Coulomb friction, despite its limitations, and shows the non-uniquenesses that arise in the load motion relation for some simple sliders with point supports. MacMillan [1936] coins the term 'center of friction' for translation with Coulomb friction and sums the frictional forces and their moments during sliding of some simple sliders. All three of these authors note the tendency of sliders to rotate about one of their discrete points of support.

1.7.6 Motion Planning For Robotic Applications

Erdmann [1984] studies the motion of a two dimensional polyhedral object sliding on a frictionless supporting surface, but touching other two dimensional polyhedral objects (vertex on an edge contact or edge on a vertex contact) at a finite number of points with Coulomb friction. The normal force at each point of contact is allowed to vary. He develops a configuration space projection of the Coulomb friction cone at each point of frictional contact by generalizing the notion of friction force to include also their moment about a

reference point, and calling it the generalized friction cone, which is similar to the limit surface described in our work.

He shows that the overall generalized friction cone for a slider with multiple contacts is the Minkowsky sum of the individual generalized friction cones for each point of contact. He then shows methods for determining the frictional reactions at the contacts for a given applied load on the slider, and thence determining the corresponding motion.

He also highlights some motional ambiguities that can occur from the above model in the form of:

1. Non-uniqueness of the decomposition of the frictional reactions for a slider with multiple contact points and a given applied load.
2. Situations where maintaining contact or breaking contact between the slider and the constraining object are both acceptable solutions.

The above results are then generalized for compliant motion of a three-dimensional rigid body (three degrees of translation and three degrees of rotation).

Mason [1985] analyzes the in-plane pushing of a rigid slider with in-plane forces, by a pusher that is assumed to move along a predetermined path; and with spatially uniform Coulomb friction at all points of contact. Given the non-determinacy of the exact support pressure distribution between the slider and the supporting surface, Mason formulates theorems to predict qualitatively the sense of rotation or pure translation of the slider, for planning robotic manipulation strategies. His theorems are based on the knowledge of the center of pressure and of the geometry of the slider, the path of the pusher and the coefficient of friction between the two.

Following up on his work Peshkin [1986] determines quantitative bounds on the possible motions for all possible support distributions between the above slider and supporting plane, at any given instant of the pusher's motion. He obtains the boundary of the locus of all possible CORs for a given pushing geometry, by scanning a circular region enclosing the support area with two point supports (one placed infinitesimally close to the center of pressure and the other on the outer bound on the opposite side of the center of pressure), and finding the COR which minimizes the energy dissipated to friction.

Alexander and Maddocks [1987] analyze the kinematics and control of robots which contact the supporting surface through wheels (which can be driven and steered for mobility of the robot) and castors, with Coulomb friction. They derive the kinematic constraint equation for each wheel to be in a state of pure rolling (without slip). For motions of these robots which involve slippage of the wheels, they state that the overall motion of the robot is that which minimizes the friction functional (the power dissipated to friction forces during slip) for the given rotation rates of the wheels, although this friction functional is not explained clearly.

1.7.7 Summary And Contributions Of Present Work

From the surveyed literature directly applicable to the present study, it may be summarized that the analogy between plasticity and friction is well known. Work exists on the application of convexity and normality to simple friction laws. The dynamics of slip of planar rigid bodies in the presence of dry contact friction have been formulated in mathematical terms; some problems in their solutions identified; and certain results presented

about the free motions of some classes of objects. The characterization of the friction force in terms of the moment function is known.

In view of the above, the main contributions of this work seem to be:

1. The development of the three dimensional limit surface description for the frictional load-motion relation of a planar slider, based on friction laws that obey convexity and normality.
2. Formulation of methods for constructing these limit surfaces.
3. Identification of the correspondence between the non-uniquenesses in the frictional load motion relation and the geometry of the limit surface.
4. Relating moment surfaces to limit surfaces.
5. Application of the limit surface description to obtain results about uniqueness of motion at forced incipient slip, and existence of certain final motions during free sliding of arbitrary planar sliders.

1.8 Layout Of Document

The order for the material presented in the rest of the document is as follows.

- Chapter 2: The geometry of three-dimensional motion space is defined and related to the set of CORs (Center Of Rotation) in the plane. Frictional load for a planar slider is defined and related in a general way to its motion.
- Chapter 3: The friction laws considered in this paper are defined in terms of admissible limit curves (i.e. force-translation relation for individual points of contact) and the maximum work inequality.
- Chapter 4: The overall load motion relation of the slider stemming from these friction laws is examined. The concepts of the limit surface and the moment surface are developed and their inter-relationships shown.
- Chapter 5: Methods for the construction of limit surfaces are developed.
- Chapter 6: Methods for the construction of moment surfaces for isotropic friction are shown.
- Chapter 7: Several examples of simple normal pressure distributions with their corresponding limit surfaces and moment surfaces (where relevant) are presented.
- Chapter 8: Dynamics of simple objects with dry friction are analyzed with particular attention being paid to the starting problem and the problem of free sliding.
- Chapter 9: The load-motion inequality is interpreted as a statement of extremum principles for frictional slip.
- Chapter 10: Some possible frictional models of velocity dependent behaviour are presented.
- Chapter 11: The main conclusions are stated with some possible directions for future work.

Chapter 2

Basic Relations, Definitions And Notation

In this section we present basic definitions, relations and notation, needed in the rest of the document. Bold letters (e. g. $\mathbf{P}, \mathbf{Q}$) stand for vectors (lists of numbers), non-bold (e. g. q_x, q_y, ω) for scalars or components. Components of vectors are enclosed within square brackets (e. g. $\mathbf{V} = [V_x, V_y]$). Components with the subscripts x (e. g. q_x), y (e. g. q_y) and ω (e. g. q_ω) are components along the X, Y and ω coordinate axes respectively. Matrices (e. g. $\underline{\mathbf{I}}$) are represented with underlined bold letters. All variables are non-dimensional. Non-dimensionalization is achieved through division or multiplication (as appropriate) by a reference mass m_r, a reference length l_r and a reference time t_r.

2.1 Description Of Motion Of Slider

Since we shall be using rate independent friction laws, we only need the motion direction (and not its magnitude) at each point of frictional contact to calculate the friction force. For the planar slider of fig. 1, its instantaneous motion direction can be represented as either:

1. A pure rotation about an instantaneous center of rotation (COR) C in the plane. One must specify the position of C and the sense of rotation (clockwise or counter-clockwise) of the slider. Pure translation of the slider can be conceived of as a pure rotation about a COR at an infinite distance from the slider.
2. A point on a unit sphere. With $\mathbf{V} = [V_x, V_y]$ as the linear velocity of the slider and ω its angular velocity, $\mathbf{Q} = [V_x, V_y, \omega]$ specifies the complete velocity of the slider. Then its motion direction is given by the 'motion vector' $\mathbf{q} = \mathbf{Q}/|\mathbf{Q}| = [q_x, q_y, q_\omega]$, or the 'versor' in the language of Zmitrowicz [1981].

The set of all possible motion vectors q for the slider is the set of unit vectors in $\Re^3$, i. e. points on a unit sphere centered at the origin of the three dimensional motion space ($[V_x, V_y, \omega]$ space), as shown in fig. 2.

2.1.1 Geometric Relation Between The Motion Vector And The COR

Mason [1985] noted the one-to-one correspondence between signed CORs and points on a unit sphere. The following construction shows that the sphere can be the unit motion sphere centered at the origin of three dimensional motion space and representing the set of all possible motion vectors at O. Fig. 2 shows two copies (one for each rotation sense) of the plane of rotation centers, placed at the 'north and south pole' of the unit sphere, with the origins of their coordinate systems coinciding with the poles of the sphere. The ω axis is perpendicular to these planes, and the coordinate systems for the upper plane and the bottom plane are rotated 180° (about the ω axis) with respect to each other so that the positive Y_c axis of the upper plane is parallel to the positive V_x axis of the motion space.

The COR corresponding to a motion vector $\mathbf{q}$ (coordinates $[q_x, q_y, q_\omega]$ on the unit sphere), is found by extending the ray $\mathbf{q}$ until it intersects the plane of CORs at the point 'C', with position $\mathbf{r_c} = [\mathbf{x_c}, \mathbf{y_c}]$ in the plane of CORs. The upper hemisphere of the unit sphere projects onto the upper plane of CORs with associated positive angular velocities and similarly the lower hemisphere projects onto the lower plane of CORs with associated negative angular velocities. The equator (corresponding to pure translation of the slider) maps into a single circle at infinity. The projection we have explained describes the one-to-one correspondence between the set of all possible motion vectors and the set of all possible signed CORs, including the circle consisting of the CORs at infinity. This projection is justified in detail in appendix A.1.

2.2 Description Of Frictional Load

Frictional load is defined as the net frictional force $\mathbf{F}=[F_x, F_y]$ and frictional moment M (about a vertical axis passing through the reference point 'O') that a rigid planar slider of arbitrary shape and pressure distribution exerts on the flat supporting surface on which it slides. It is expressed as the 'generalized friction force vector', $\mathbf{P}=[F_x, F_y, M]$. If inertial forces were neglected, $\mathbf{P}$ would be equal to the total external in plane load that must be applied to the sliding object to overcome friction. It is negative of that which would appear in a free body diagram of the sliding object as representing the total frictional forces and frictional moments acting on the object. Alternatively one can imagine the contact surface, including an infinitesimally thin (massless) layer of the rigid solid, as a separate mechanical system. The distributed forces $-f_x$ and $-f_y$ act on it from the support plane. The generalized load $\mathbf{P}=[F_x, F_y, M]$ is the resultant of the forces from the rigid body on to that thin layer (whether or not inertial terms are important in the slider dynamics), as shown in fig. 3.

2.2.1 Summation (or Integration) of Forces And Moments

Consider the planar slider of fig. 4 with 'C' (its instantaneous COR) at $\mathbf{r_c}= [r_{cx}, r_{cy}]$. We take elemental areas da of the slider at $\mathbf{r_a}=[r_{ax}, r_{ay}]$ where the frictional force is given by $\mathbf{f_a}=[f_{ax}, f_{ay}]$. Summing forces and moments over the area A of the slider gives:

$$F_x = \int_A f_{ax}\,da, \quad F_y = \int_A f_{ay}\,da, \quad M = \int_A (r_{ax} f_{ay} - r_{ay} f_{ax})\,da \tag{2.1}$$

We can also calculate the moment of the frictional forces M_c about a vertical axis passing through C as:

$$M_c = M + \mathbf{r_c} \times \mathbf{F} = \int_A ((x_a - x_c) f_{ay} - (y_a - y_c) f_{ax}) da \tag{2.2}$$

The integrands in the above equations can sometimes be written in terms of the motion vector q, once the pressure distribution is known and the directional dependence of friction specified. For isotropic Coulomb friction $\mathbf{f_a}$ will be parallel to the direction of the slip velocity $\mathbf{v_a}$ at da, independent of the speed but directly proportional to the normal force at da. If points of support are involved, the integrands contain delta functions (or equivalently are replaced by sums).

2.2.2 Indeterminacy Of P For COR At Finite Support

If the slider has finite support points and one of these points is also the instantaneous COR, there is for the friction laws considered here, an indeterminacy in the friction force at that point (having no relative velocity with the supporting surface), and the integrals in equations 2.1 and 2.2 cannot be evaluated. This indeterminacy corresponds to a flat facet on the limit surface, as will be discussed. If the COR is at a point of distributed support, the indeterminacy of the finite integrands at that point does not affect the value of the integrals, so the friction force is usually then determined by the equations of motion.

2.3 Important Points On Slider

Certain points on the sliding object are now identified. The 'center of mass' (CM) of the planar object is the centroid of its mass distribution. The 'center of pressure' (CP) is the centroid of the contact pressure distribution between the sliding object and the supporting surface. With all externally applied loads being in the plane of the slider (except gravity), and with either *a*) negligible acceleration or *b*) center of mass on the plane, then its CP is the same as its CM.

The 'center of twist' (CT) is that COR for which the generalized load is a pure moment. Or in other words, the CT is that point about which the planar slider begins to rotate, if a pure moment load is applied to it. Zhukovskii [1948] calls the center of twist the 'pole of friction'. The CT is not necessarily unique. As an example, for a symmetric thin bar supported symmetrically at its ends with Coulomb friction, all points on the bar are centers of twist. For isotropic friction, the CT lies within the convex hull of the support distribution, as can be shown [Zhukovskii 1948]. But this is not necessarily true for anisotropic friction. For example, for the same thin symmetric bar as above, supported symmetrically at its ends with ideal wheels (to be defined) with their axes perpendicular to the bar, all points in the strip shaped region contained between the two parallel lines drawn at the ends of the bar (and perpendicular to it), are centers of twist.

The centroid of the frictional forces during pure translation is called the 'center of friction' (CF) [MacMillan 1936, Mason 1985]. Assuming isotropic Coulomb friction, the CF is unique, and it lies within the convex hull of the support distribution.

For uniform isotropic friction and in-plane loads (for example all the pressure distributions considered by Zhukovskii [1948]), CP=CF. Additionally, if the pressure distribution has certain symmetries, then all the above points (CM, CP, CT, CF) coincide. For all of

the friction laws we consider, the magnitude of the friction force turns out to be maximum during pure translation of the slider, and for isotropic friction, its line of action is through the CF.

2.4 Equations Of Motion

The motion of a planar slider is governed by the equation:

$$\mathbf{P^e} - \mathbf{P} = \underline{\mathbf{I}}\frac{d\mathbf{Q}}{dt} \tag{2.3}$$

where $\mathbf{P^e} = [F_x^e, F_y^e, M^e]$ is the externally applied load at the center of mass (CM) of the slider, $\mathbf{P}$ is the frictional load at the CM,

$$d\mathbf{Q}/dt = [dV_x/dt, dV_y/dt, d\omega/dt]$$

is the generalized acceleration of the CM of the slider and $\underline{\mathbf{I}}$ is the generalized inertia matrix given as:

$$\underline{\mathbf{I}} = \begin{bmatrix} m & 0 & 0 \\ 0 & m & 0 \\ 0 & 0 & J \end{bmatrix}$$

Here m is the mass of the slider, $J = m\rho_g^2$ is the mass moment of inertia of the slider about a vertical axis passing through the CM and ρ_g is its radius of gyration.

If equation 2.3 is non-dimensionalized by choosing the reference mass $m_r = m$ and the reference length $l_r = \rho_g$, the governing equation of motion for the slider becomes:

$$\mathbf{P^e} - \mathbf{P} = \frac{d\mathbf{Q}}{dt} \tag{2.4}$$

Chapter 3

Friction Law At One Point

The frictional behaviour at the interface of two solids that are sliding against each other is a complex thermomechanical and chemical phenomenon dependent on a multitude of factors [e. g. Tabor 1981], and no single constitutive law has been able to encompass them all [Oden and Martins 1984]. The friction laws we choose neglect the constitution of the interface, the dependence on the relative rate of slip between the surfaces and the history of contact.

We consider only the direction of slip and the normal force (or pressure) at each point (or elemental area) of contact; a further simplification for our problem assumes that the normal force distribution is known and is fixed. For most of the presentation we also exclude the possibility of a single point having a resisting frictional torque (resistance to rotation), something that might be included to model a small but finite region of support like a 'soft finger'. The presentation below for each point of frictional contact applies also to elemental areas of contact (da) in regions of distributed support.

3.1 Limit Curves And Maximum Work Inequality

At each point of frictional contact with a fixed normal force, the friction law is assumed to be expressed by the specification of:

1. A closed curve in force space ($[f_x, f_y]$ space), called the limit curve (LC), on which lie the frictional forces corresponding to all possible directions of slip at the point of contact. The LC encloses the origin.
2. The maximum work inequality which can be stated as :

$$(\mathbf{f} - \mathbf{f}^*) \cdot \mathbf{v} \geq 0 \tag{3.1}$$

where $\mathbf{f}$ and $\mathbf{v}$ are the frictional force and the slip velocity respectively, related by the friction law with $\mathbf{f}$ lying on the LC, and $\mathbf{f}^*$ is any other friction force lying within the LC.

A schematic of such a friction law is illustrated in fig. 5. Inequality 3.1 [Hill 1950 and 1967, Drucker 1951, Rice 1970] provides our basic link with classical plasticity. By classical arguments [Drucker 1951] and geometric reasoning [Moreau 1974, 1979], the maximum work inequality implies that the LC must be convex, and that any $\mathbf{f}$ and $\mathbf{v}$ related by the

friction law are such that the direction of $\mathbf{v}$ is given by the normal to the LC at $\mathbf{f}$, where the LC is smooth. Hence the LC can be used to specify a unique relation between $\mathbf{f}$ and the direction of $\mathbf{v}$, in all smoothly curving parts of the curve.

At a vertex on the LC, within the constraints implied by inequality 3.1, the motion direction $\mathbf{v}$ is not unique for the given friction force $\mathbf{f}$, and a whole range of motion directions are associated with $\mathbf{f}$. Similarly on a straight segment of the LC, within the constraints implied by inequality 3.1, the friction force $\mathbf{f}$ is not unique for the given motion direction $\mathbf{v}$, and a whole range of friction forces are associated with the motion direction $\mathbf{v}$.

3.2 Friction Models That Satisfy The Maximum Work Inequality

The following friction laws can be specified in the manner described above, since they all obey the maximum work inequality.

3.2.1 Coulomb Friction

If the friction law governing the frictional interaction at the point of contact 'a' is isotropic Coulomb friction, then it can be specified by a LC which is a circle of radius $|\mathbf{f_a}|$ and the maximum work inequality, as shown in fig. 6. Here $\mathbf{f_a}$ is the friction force associated with a slip direction $\mathbf{v_a}$ at 'a' and also it is parallel to $\mathbf{v_a}$.

3.2.2 Frictional Contact With Wheels

When the frictional interaction between the slider and the supporting surface occurs through perfectly rigid and massless wheels, with the friction law between the wheel base and the contacting surface being isotropic friction; then the frictional behaviour depicted between the slider and the supporting surface by ignoring the wheels, exhibits *anisotropy* [Moreau 1974, 1979]. Fig. 7(a) shows a planar slider with a small embedded wheel that rolls or skids on a horizontal supporting surface. The shape of the LC for the friction law between the slider and the supporting surface depends on whether the axle of the wheel is completely frictionless, has bearing friction or is ratcheted, as shown below.

1. Completely ideal wheel (or skate): If the wheel is completely ideal (i.e. no friction at the axle), which is also equivalent to the slider having an ideal skate instead of the wheel, then the only frictional resistance to the sliding of the slider on the supporting surface is felt when the wheel between them skids along its axis. Hence the LC is given by the straight line segment (parallel to the axis of the wheel) shown in fig. 7(b). This is a highly singular LC with respect to the $\mathbf{f}, \mathbf{v}$ relationship. It shows non-uniqueness in the $\mathbf{f}, \mathbf{v}$ relationship from the presence of both vertices and straight segments. The straight segment passing through the origin corresponds to rolling forward and backward of the wheel (without slipping), and its ends correspond to skidding sideways of the wheel.
2. Wheel with bearing friction: If there is bearing friction at the axle of the wheel which is less than the frictional resistance at the base of the wheel during

sideways skidding, then the LC is given by the convex curve shown in fig. 7(c). The straight segments on the LC correspond to pure forward and backward rolling of the wheel and the circular arcs correspond to skidding. Note that if the bearing friction is either equal to, or greater than the frictional resistance to skidding, then the wheel does not roll and the LC is the circle of isotropic Coulomb friction.

3. Wheel with ratchet: If the axle has a ratchet so that the wheel is allowed to roll freely only in one direction and it locks in the other direction, then the LC is the closed semicircle of fig. 7(d). The straight segment passing through the origin corresponds to the rolling of the wheel in the preferred direction and the semicircle corresponds to skidding along the other directions.

3.2.3 Other Friction Laws

Ziemba [1952] specifies a law of anisotropic friction that obeys the maximum work inequality and whose LC is an ellipse. Moszynski [1951] in Michalowski and Mroz [1978] presents some other anisotropic friction laws that obey the maximum work inequality.

3.3 Friction Laws That Do Not Obey The Maximum Work Inequality

The requirement that acceptable friction laws satisfy the maximum work inequality is a definite restriction because there is no a priori reason to expect that all friction laws should obey it. It is easy to imagine friction laws that violate inequality 3.1, although their thermodynamic validity may be disputed [Ziegler 1981].

A variation on Coulomb friction with the friction force not being parallel to the slip direction but making a non-zero angle with it, has a LC which is convex, but does not obey inequality 3.1, as shown in fig. 9(a). A contact between a slider and the supporting surface mediated by the infinitesimally small (massless and perfectly rigid) castor wheel shown in fig. 8(a) manifests this not-normal friction law. The castor consists of a massless rigid 'L' shaped structure (in a plane parallel to the slider), one end of which is pivoted to the slider, and the other end has a wheel with bearing friction mounted on it. The castor pivots about the vertical axis in a frictionless bearing at its point of attachment to the slider. For any given slip velocity of the slider at the castor pivot point, the castor is given time to relax to an equilibrium orientation through rotation about the pivot. The equilibrium orientation of the castor wheel for a given slip direction $\mathbf{v}$ would be one for which the line of action of the corresponding friction force $\mathbf{f}$ passes through the pivot point, as shown in fig. 8(b). The LC for such a frictional contact is as shown in fig. 9(a). So although the instantaneous force velocity relation for the castor seems to obey convexity and normality, if it is given the time to attain an equilibrium orientation, then the resulting friction law for the slider does not obey normality.

A simple model of anisotropy, with the friction force always parallel to the slip direction and magnitude dependent on direction, also does not obey inequality 3.1, as shown in fig. 9(b).

The microscopic model for friction of Michalowski and Mroz [1978] describing anisotropy due to wedge asperities, also does not satisfy inequality 3.1. The orthotropic friction tensor

of Zmitrowicz [1981] describes a friction law that does not obey inequality 3.1. For the remainder of the paper we concentrate on friction laws that do obey the maximum work inequality.

Chapter 4

Overall Load Motion Relation

We now proceed towards the overall frictional load and motion relation for rigid planar sliders based on the friction laws described previously.

4.1 Possible Descriptions And Problems

One expects that the full characterization of the relation between load and motion for a slider of the type being considered here would involve, say, the ability to determine the friction load (two force components and a moment) for any possible motion. For a given contact pressure distribution and friction law, this involves (when it is possible) the evaluation of three integrals (equation 2.1) for every possible motion. Since the friction laws we use are rate independent, one need only consider all sets of signed CORs or all points on the unit motion sphere for possible motions.

Thus the frictional behaviour is characterized by three real valued functions $[F_x, F_y, M]$ over the two planes of CORs or over the unit motion sphere. Only in special cases can the integrals in equation 2.1 be evaluated analytically. Further, depending on the friction law and the support distribution, these integrals may have indeterminate values, such as when the COR is a point of finite support. If one arbitrarily specifies the motion, there is low probability of the implied COR coinciding with a support point, and the indeterminacy associated with this situation may not seem to be a problem. However, for specified load directions, it turns out that such motion is quite likely.

If one does not know the contact pressure distribution or the friction law, then alternatively, one can characterize the object's sliding behaviour experimentally, and one has the experimental task of finding three functions of two variables. For a given friction law, all information can be derived from the contact pressure distribution (just one function of two variables), evaluated over the region of contact. However, finding this pressure from the given load motion information involves solving the integral equations 2.1. To use the information about frictional forces during slip, the integrals in equation 2.1 need to be evaluated again, for all motion directions.

With the limit surface (LS) description that is described below, an object's frictional behaviour is characterized by one closed, convex surface in three dimensional load space (equivalent to one function of two variables) instead of three functions of two variables. Indeterminacies in the load motion relation have clear representations in terms of the shape of the LS. Fortunately, the LS gives a somewhat simplified and complete description of the given object's sliding behaviour and additionally, it helps clarify (though not completely

remove) some indeterminacies, like those associated with rotation about finite support points.

4.2 Limit Surface And The Load Motion Inequality For The Slider

The limit curve (LC) in the $[f_x, f_y]$ plane, when used with the maximum work inequality, fully describes the rate independent frictional properties of a point of contact. The LC can be replaced by an equipollent limit curve in load space ($[F_x, F_y, M]$ space) with its origin at 'O'. This equipollent LC and its interior in three dimensional load space is called as the 'individual limit surface' for the point of contact and it can be considered as a closed (flat) surface. The friction force (or traction) at each point of contact contributes to the total frictional load $\mathbf{P} = [F_x, F_y, M]$ at 'O', through the sums in equation 2.1. Hence the overall LS for the slider, which completely characterizes its frictional behaviour, can be obtained by appropriate summation of points from the individual limit surfaces.

The formal construction of overall limit surfaces in load space ($[F_x, F_y, M]$ space) follows directly from inequality 3.1 for each point of support and the principle of virtual work (PVW), which may be expressed as:

$$\mathbf{P} \cdot \mathbf{Q} = \sum \mathbf{f} \cdot \mathbf{v} \tag{4.1}$$

where $\mathbf{P}$ and $\mathbf{f}$ are any generalized load and force distribution respectively, related by the equilibrium equation 2.1; and $\mathbf{Q} = [V_x, V_y, \omega]$ and $\mathbf{v}$ (slip velocity at point located at $\mathbf{r}$) are any generalized motion vector and velocity distribution respectively, related by the compatibility equation:

$$\mathbf{v} = (v_x, v_y) = (\mathbf{V} - \omega \times \mathbf{r}) = (V_x - \omega r_y, V_y + \omega r_x)$$

Now suppose that both $\mathbf{f}$ and $\mathbf{f}^*$ are frictional force distributions that do not violate the slip condition anywhere ($\mathbf{f}$ and $\mathbf{f}^*$ are on or inside their limit curves) and they correspond respectively to $\mathbf{P}$ and $\mathbf{P}^*$ through equation 2.1. Further, $\mathbf{f}$ is also consistent with the friction law for the motion $\mathbf{Q}$. Applying the PVW (equation 4.1) and inequality 3.1 to each of the two cases ($(\mathbf{P}, \mathbf{f})$ and $(\mathbf{P}^*, \mathbf{f}^*)$), and then subtracting, gives:

$$(\mathbf{P} - \mathbf{P}^*) \cdot \mathbf{q} \geq 0 \tag{4.2}$$

So $\mathbf{P}$ is the load vector at O during slip associated with a motion vector $\mathbf{q} = \mathbf{Q}/|\mathbf{Q}|$, and $\mathbf{P}^*$ is any other load vector at O during no slip or during slip with a motion vector different from $\mathbf{q}$. If the constitutive law for frictional interaction between the two sliding surfaces obeys inequality 3.1 at each microscopic contacting element, then inequality 4.2 is the macroscopic load motion inequality that is obeyed by slip loads and associated motions for the slider at O.

4.2.1 Convexity And Normality Of LS

The structure of the load motion inequality 4.2 is identical to the maximum work inequality, and by classical arguments [Drucker 1951], it leads us to the LS description: The load $\mathbf{P}$ and the associated motion vector $\mathbf{q}$ for the slider are related to each other by means of a

closed, convex surface (the limit surface) in three-dimensional load space. When the state of load is inside the LS, no motion occurs, and when motion occurs, the load $\mathbf{P}$ is on the limit surface. If the LS is smooth at $\mathbf{P}$, the slider slips with a motion vector $\mathbf{q}$ which is the normal to the LS at $\mathbf{P}$.

Analogous to the friction law at each point of contact, the constitutive law for frictional slip for the slider can now be expressed by the specification of:

1. A closed surface in load space ($[F_x, F_y, M]$ space), enclosing the origin, called the LS, on which lie the frictional loads corresponding to all possible motions of the slider.
2. The load motion inequality, $(\mathbf{P} - \mathbf{P}^*) \cdot \mathbf{q} \geq 0$.

Limit surfaces are usually specified at the reference point 'O' coinciding with either the CP, or the CF, or a CT of the slider.

Convexity of the limit surface is defined as follows: given any two points $\mathbf{P_1}$ and $\mathbf{P_2}$ in load space that are on or inside the surface, the line segment $\mathbf{P_1P_2}$ is inside or on the region contained by the surface. An equivalent definition of convexity is that at any point on the surface, a plane exists (the tangent plane) that divides the space into two half spaces such that one of the half spaces has no point of the surface interior. For a strictly convex surface the plane would include only one point of the surface boundary. In either case inequality 4.2 is the mathematical statement of convexity and normality of the LS.

When the LS is specified with reference to a CT of the slider, then the maximum moment of the frictional forces is seen at the point when the LS intersects the M axis, a fact that is true due to the convexity and normality of the LS, and a result which agrees with that of Zhukovskii [1948].

4.2.2 Non-Uniquenesses In The Load Motion Relation

At a vertex or an edge of the LS (non-smooth region of the LS), within the constraints implied by inequality 4.2, the motion direction $\mathbf{q}$ is not unique for the given load $\mathbf{P}$, and a whole range of motions are associated with $\mathbf{P}$. Similarly on a flat region or a straight segment of the LS (regions of constant slope on the LS), within the constraints implied by inequality 4.2, the load $\mathbf{P}$ associated with the given motion $\mathbf{q}$ is not unique, and a whole range of loads are associated with the same $\mathbf{q}$.

For isotropic friction, vertices occur on the limit surface only for sliders that have all support points on one line. In this case whole sets of CORs (and hence whole sets of motion vectors) lying on this line but outside the region of support, give the same total frictional load. Because each of the CORs belonging to this set give the same direction of velocity at the support points, this implies the same frictional force at these points, and the same total load on the slider. If the supports are not all collinear and friction is isotropic, then the limit surface is smooth everywhere. However, for anisotropic friction, non-collinear support does not guarantee smoothness of the LS, as shown later.

Also for isotropic friction, flat regions occur only for sliders that have discrete points of support. When the motion is such that one of these discrete points of support is the COR (i.e this point of support is not moving), then the frictional force at that point and hence for the whole body is not uniquely determined. In fact for sliders with discrete supports, every point of support, leads to two parallel flat facets on the limit surface of the slider.

For sliders with distributed support, the LS has no flat regions. Again, this last statement is not necessarily true for anisotropic friction, as shown later.

For models of anisotropic friction that we consider, the non-uniqueness in the load motion relation is a bit more complex because the individual limit surfaces for each point of support have straight edges; and these straight edges show both the non-uniqueness characteristics of vertices and flat regions. As can be visualized, a straight edge on the three dimensional LS not only has a whole range **q** of motion vectors for any candidate load lying on this edge, but corresponding to this range **q** of motion vectors, we have the whole range **P** of loads lying on the edge, so that there is indeterminacy both ways.

4.2.3 Symmetries Of Limit Surfaces For Isotropic Friction

The limit surfaces of sliders with isotropic friction, have certain easily understood symmetries which are highlighted below. If load P (associated with motion **q**) is on the LS for the slider, then load $-$P (associated with motion $-$**q**) is also on its LS. Because reversal of the motion **q** of the slider leads to reversal of the slip direction at each point of support. This leads to a reversal of the friction forces at each point of support and hence a reversal of the load **P**. The section of the LS on the force $[F_x, F_y]$ plane is always a circle. If the LS is drawn at the reference point O coinciding with the CF for the slider, pure force loads have pure translation as one of the possible motions. Also then normality and convexity imply that any load in the positive M half-space corresponds to a positive sense of rotation and any load in the negative M half space corresponds to a negative sense of rotation.

The LS presents a more visual interpretation to Mason's theorems [1985] for predicting the sense of rotation or a state of pure translation of the slider by determining the moment of the frictional forces about the CF, for both displacement and force boundary conditions on the slider. For a clockwise moment, they predict clockwise rotation, for an anti-clockwise moment they predict anti-clockwise rotation, and for zero moment, a state of pure translation of the slider.

For sliders with symmetries in the pressure distributions and uniform, isotropic coefficients of friction, and equivalent symmetries in the limit curves of individual points of support, additional symmetries of the LS drawn at the CT exist, allowing a simpler geometric description of the LS. For example, the LS for a bar supported at its ends (illustrated later) can be obtained completely if its shape in one octant in load space is known. The limit surfaces for objects with axially symmetric support distributions, like uniformly supported annuli and circular discs, are surfaces of revolution about the M axis. An object with a three-fold rotational symmetry has a three-fold symmetric limit surface (not necessarily a surface of revolution), etc..

4.2.4 Evolution Of LS Due To Motion Of Slider

A given LS specified at a certain reference point completely characterizes the load motion relationship only for the given contact configuration of the slider and the supporting surface, and fixed normal pressure distribution. We assume that the contact pressure distribution remains fixed and known in a slider fixed coordinate system, throughout the slider's motion. Then depending on the nature of the contacting surfaces and their geometries and the friction law specifying the frictional interaction, the contact geometry

between the slider and the supporting surface may change due to the motion of the slider. And this may lead to a change in the shape of the LS, a fact that we now investigate.

If the supporting surface is completely isotropic and homogenous (in frictional properties), then the LS for the slider (irrespective of whether the slider is frictionally isotropic or anisotropic) has a fixed shape which rotates in load space about the M-axis, as the slider rotates in physical space (about an axis perpendicular to the supporting plane). The rotational velocity for both the LS and the slider is the same. That is, the LS rotates with the slider and is most conveniently defined in a slider fixed axis system. An example would be a slider that makes contact with a completely smooth horizontal surface through wheels attached to the slider. Additionally, if the LS is a surface of revolution about the M-axis, then it does not change at all. An example would be a thin ring supported uniformly with wheels (having their axes aligned tangentially to the ring) sliding on a smooth horizontal surface.

If the slider is completely isotropic and axisymmetric with regard to both support distribution and frictional properties, then the LS for this slider (irrespective of the anisotropy of the supporting surface) has a fixed shape and orientation in load space that does not rotate in load space, as the slider rotates in physical space. An example would be a smooth circular disk sliding on a bed of parallel wheels.

If both the slider and the supporting surface are anisotropic, then the LS for the slider rotates and changes shape in load space, as the slider moves in physical space and a single LS cannot characterize the sliding behaviour of the given slider as it moves.

For all the above cases, during the final stages of the slider's motion before it comes to a halt, when the velocities of the slider are infinitesimal; the changes in the contact geometry, support distribution and frictional properties due to the motion of the slider, all approach zero, and the LS has a fixed shape and orientation in load space. This fact is used to get an important result about the final motions from the asymptotic analysis of free sliding sliders.

4.3 Dissipation Function

It can be observed that the most important quantity that appears in inequality 4.2, and that which governs the load motion relationship of a sliding object in the presence of dry friction is $\mathbf{P} \cdot \mathbf{q}$ or the power dissipated by friction, and aptly termed the dissipation function; as mentioned in Moreau [1974, 1979], Michalowski and Mroz [1978], Ziegler [1981] and Curnier [1984]. For friction laws that obey the maximum work inequality, the dissipation function D serves as the inverse to the limit surface description. In our case the dissipation function is $D = \mathbf{P} \cdot \mathbf{Q}$ and should be thought of as a function of $\mathbf{Q}$. Surfaces of constant dissipation, i.e. D=constant, in motion space ($\mathbf{Q} = [V_x, V_y, \omega]$ space), are closed and convex. The normal to the surface of constant dissipation D, for a given $\mathbf{Q}$ in motion space can be shown, using the chain rule and normality of the LS, to be equal to the load $\mathbf{P}$. Namely, where D is differentiable:

$$\mathbf{P} = \frac{\partial D}{\partial \mathbf{Q}} \equiv \left[\frac{\partial D}{\partial V_x}, \frac{\partial D}{\partial V_y}, \frac{\partial D}{\partial \omega} \right] \tag{4.3}$$

4.4 The Moment Surface For Isotropic Friction

For sliders with isotropic friction and known normal force distributions, the total moment M_c of the frictional forces about a vertical axis passing through the COR can be plotted as a surface in $[x_c, y_c, M_c]$ space, because M_c is a real valued function of the two variables of the position $\mathbf{r_c} = [x_c, y_c]$ of the COR [Zhukovskii 1948]. The M_c function does not have any uniqueness problems (as does the friction force $\mathbf{f}$) associated with rotation about points of support. We call this surface the 'moment surface' (MS) and like the LS, it completely characterizes the frictional load motion behaviour of the slider, as shown below.

4.4.1 Moment Surfaces And Limit Surfaces

Returning to the slider of fig. 4, we consider an elemental area da at $\mathbf{r_a} = [r_{ax}, r_{ay}]$, having a coefficient of friction μ_a and normal force N_a. If the COR is at $\mathbf{r_c} = [x_c, y_c]$, then the frictional force $\mathbf{F} = [F_x, F_y]$ over the area A of the slider is given by:

$$F_x = \int_A f_{ax} da = -\int_A \mu_a N_a \frac{r_{ay} - y_c}{|\mathbf{r_a} - \mathbf{r_c}|} da$$

$$F_y = \int_A f_{ay} da = \int_A \mu_a N_a \frac{r_{ax} - x_c}{|\mathbf{r_a} - \mathbf{r_c}|} da$$

The M_c function for the slider is given as:

$$M_c = \int_A (\mathbf{r_a} - \mathbf{r_c}) \times \mathbf{f_a} da = \int_A \mu_a N_a |\mathbf{r_a} - \mathbf{r_c}| da$$

By differentiating $M_c(x_c, y_c)$ with respect to x_c and y_c, we obtain:

$$\frac{\partial M_c}{\partial x_c} = \int_A \mu_a N_a \frac{r_{ax} - x_c}{|\mathbf{r_a} - \mathbf{r_c}|} da = -F_y$$

$$\frac{\partial M_c}{\partial y_c} = -\int_A \mu_a N_a \frac{r_{ay} - y_c}{|\mathbf{r_a} - \mathbf{r_c}|} da = F_x$$

$$M = M_c + \mathbf{r_c} \times \mathbf{F}$$

Condensing the above results we get:

$$F_x = \frac{\partial M_c}{\partial y_c}, \quad F_y = -\frac{\partial M_c}{\partial x_c}, \quad M = M_c - \mathbf{r_c} \cdot \nabla \mathbf{M_c} \tag{4.4}$$

where

$$\nabla = [\frac{\partial}{\partial x_c}, \frac{\partial}{\partial y_c}]$$

Equation 4.4 shows that for sliders with isotropic friction and known support distribution, the components of the frictional load $[F_x, F_y, M]$ or the LS can be obtained analytically through differentiation of its $M_c(x_c, y_c)$ function, where it is differentiable. Hence the MS effectively parameterizes the LS, with the parameters being the coordinates (x_c, y_c) of the COR in the plane.

We show in the appendix A.2 that the unit normal to the LS at a point $\mathbf{P}(x_c, y_c) = [F_x(x_c, y_c), F_x(x_c, y_c), M(x_c, y_c)]$, is indeed the motion vector $\mathbf{q}$ associated with $\mathbf{P}(x_c, y_c)$. This connection between the MS and the LS allows us to understand the limitations on the geometric characteristics of the MS and the relation between the singularities (vertices and flat regions) on the LS and the MS. Equation 4.4 implies that:

1. A vertex (a slope discontinuity) on the MS at a point $M_c(x_c, y_c)$ corresponds to a flat region on the LS for the motion vector $\mathbf{q}$ associated with the COR at (x_c, y_c). Conversely, a flat region on the LS corresponds to a vertex on the MS.
2. A flat region (region of constant slope) on the MS corresponds to a vertex on the LS and conversely, a vertex on the LS corresponds to a flat region on the MS.

4.4.2 Some Properties Of Moment Surfaces

The minimum of the MS occurs at the CORs which are the CTs for the slider because at a minima, we have (equation 4.4) $F_x = F_y = 0$, or a state of pure torque, and except for sliders with a single point of support, this torque $M = M_c \neq 0$. Moment surfaces are convex surfaces that do not have straight edges because limit surfaces for isotropic friction do not have straight edges. It will be shown in a later section that limit surfaces for isotropic friction do not have straight edges. $M_c \geq 0$ for $\omega \geq 0$ and $M_c \leq 0$ for $\omega \leq 0$. In regions far removed from the contact region, the MS closely approximates a circular cone.

4.5 MS And LS For A Bar Supported At Its Ends

As an illustration, we consider the MS and the LS for a one dimensional bar, supported at its two ends with Coulomb friction, each a unit distance away from its center at O (fig. 10). The total frictional load F_x and F_y and a moment M are also shown. We assume a unit coefficient of friction and unit normal force at each support point; f_{ax}, f_{ay} and f_{bx}, f_{by} are the components of the frictional forces acting on the supporting surface due to frictional interaction with the slider at the support points 'a' and 'b' respectively.

Fig. 11 shows a part of the MS for the bar, which along with its reflection about the $[x_c, y_c]$ plane (for $\omega < 0$), forms the complete MS for the bar. It is convex and smooth everywhere except for two vertices. Its minimum lies along CORs corresponding to rotations of the bar about points lying on it, which implies that all points on the bar are CTs. At regions far away from the bar, the MS approaches a circular cone in shape. Fig. 12 shows the limit surface for the bar, which is a closed and convex surface (loosely describable as an ovaloid with four flattened elliptical facets) smooth at all points except at four vertices lying on the $[F_x, M]$ plane. It also has four planar elliptical faces, which correspond to the vertices on the MS; corresponding to the rotations of the bar about the points of support. The vertices on the LS correspond to the straight lines on the MS; which correspond to the rotation of the bar about points on the y-axis, except the points of support. The sections of the LS on both the $[F_x, F_y]$ plane and the $[F_y, M]$ plane are circles, and the section on the $[F_x, M]$ plane is a square. It has reflection symmetry about each of the coordinate planes, i.e. the $[F_x, F_y]$ plane, the $[F_y, M]$ plane and the $[M, F_x]$ plane. In fact, the complete shape of the LS can be determined, if its shape is known in just one octant in load space. The construction of these surfaces will be discussed in later sections.

To examine the consequences of normality for this LS, we look at its section on the $[F_x, M]$ plane, which, as just stated is a square, fig. 13. For any load vector $\mathbf{P} = [F_x, 0, M]$ in the first quadrant, the resulting motion vector $\mathbf{q}$ for O is given by the normal to the LS

at P, as shown, and it corresponds to instantaneous counter-clockwise rotation of the bar about support point 'b'. For a 'pure force' load vector i.e. say for P lying on the vertex of the LS on the positive F_x axis, there is no unique normal, but all motion vectors in the circular arc outlined in the figure are possible motions. This implies that if the bar were only acted upon by a force in the direction of the x-axis, it would either rotate counter-clockwise about any point on the positive y-axis except the interior of the bar or rotate clockwise about any point on the negative y-axis except the interior of the bar. Similarly for a 'pure moment' load vector with positive moment, lack of uniqueness of the motion vector and the set of possible motion vectors as outlined in the figure imply that the bar can rotate counter-clockwise about any point on the bar between 'a' and 'b'. Incidentally, this object and these motions are discussed by Prescott [1923], but without limit surfaces.

Chapter 5

Construction Of Limit Surfaces

Given the normal pressure distribution and the friction law everywhere over the contacting surfaces, the overall LS for the slider can be obtained either by the Minkowsky summation of the individual limit surfaces, or by differentiation of the MS, or analytically by direct integration. The individual LS in $[F_x, F_y, M]$ space for any point of contact can be obtained from its LC; the case of isotropic friction is described in detail below.

5.1 LS For A Point Of Isotropic Contact

The LC for a point of isotropic support 'a' at $\mathbf{r_a}$ from the reference point 'O', is a circle of radius $|\mathbf{f_a}|$ centered at 'a' (fig. 6). Each of the friction forces $\mathbf{f_a} = [f_{ax}, f_{ay}]$ at 'a' can be replaced by equipollent generalized load vectors $\mathbf{p_a}$ at O, given by:

$$\mathbf{p_a} = [f_{ax}, f_{ay}, \mathbf{r_a} \times \mathbf{f_a}] = [f_{ax}, f_{ay}, r_a f_a \sin\theta]$$

where θ is the angle specifying the orientation of $\mathbf{f_a}$ with reference to $\mathbf{r_a}$.

These $\mathbf{p_a}$ are then the applied loads at O during slip at 'a' with any possible direction of slip velocity $\mathbf{v_a}$ at 'a'. The locus of all these $\mathbf{p_a}$ in load space is an ellipse (appendix A.3). This ellipse and its interior are the limit surface for the slider at O due to frictional contact at the point 'a', as shown in fig. 14. Each point $\mathbf{p_a}$ on this limit surface corresponds to the load at O during slip at 'a', with a motion vector $\mathbf{q}$ at O that is the normal to this LS at $\mathbf{p_a}$. The projection of this limit surface on the $[F_x, F_y]$ plane is a circle of radius f_a, because a physical interpretation for the construction of this LS is that the LC for the point of contact 'a' is translated to the reference point O and then to each force on this LC is added an altitude corresponding to the moment of that friction force about O.

Forces whose lines of action pass through O, i.e. $\mathbf{f_a} \parallel \mathbf{r_a}$, have no moment about O and the LS intersects the $[F_x, F_y]$ plane along the direction of $\mathbf{r_a}$. Friction forces that are perpendicular to $\mathbf{r_a}$, i.e. $\mathbf{f_a} \perp \mathbf{r_a}$, have the maximum moment about O. The minor axis of this ellipse is f_a, major axis is $f_a(1+r_a^2)^{\frac{1}{2}}$ and the angle β which it makes with the $[F_x, F_y]$ plane is given by $\tan\beta = |\mathbf{r_a}|$. The origin of load space is on the LS.

Since this LS is a planar ellipse, it has a flat region, the normal to which corresponds to a state of instantaneous rotation of the slider about the support point 'a'. It also has a curved edge (the one defining the ellipse) that has no unique normal. The LS at O due to contact at some other point or elemental area with some other LC, can also be derived similarly.

5.2 Overall Limit Surface Of The Slider By Minkowsky Summation

The envelope of the Minkowsky sum of the individual limit surfaces for the points (and elemental areas) of contact of the slider, is the overall LS for the slider; the Minkowsky sum of two sets being the addition of each point of one set to every other point of the other set. The load vector **P** obtained for some motion vector **q** at O, after summing the frictional forces and moments arising at points and areas of frictional contact, can also be obtained by vectorial summation of the load vectors $\mathbf{p_a}$ on the individual limit *surfaces* (all obtained at the same reference point O) corresponding to the motion vector **q** at O for all points and areas of frictional contact.

Consider points **P** and **P*** in the Minkowsky sum of the individual limit surfaces for the slider, given as:

$$\mathbf{P} = \sum \mathbf{p}, \quad \mathbf{P^*} = \sum \mathbf{p^*}$$

where loads **p** are loads associated with the motion **q** on the individual limit surfaces and loads **p*** are any other loads lying within or on the individual limit surfaces. Since inequality 4.2 is satisfied at each individual LS, we have:

$$(\mathbf{p} - \mathbf{p^*}) \cdot \mathbf{q} \geq 0 \tag{5.1}$$

And summation of inequalities 5.1 gives:

$$(\mathbf{P} - \mathbf{P^*}) \cdot \mathbf{q} \geq 0$$

So load **P** in the Minkowsky sum, obtained as a summation of loads **p** from individual limit surfaces that have an associated motion vector **q**, satisfies the load motion inequality with respect to any other load **P*** in the Minkowsky sum. This implies that:

1. **P** lies on the boundary i.e. on the envelope of the Minkowsky sum, since **P*** can be any other point in the Minkowsky sum, including its envelope.
2. The envelope is closed and convex, and every load **P** lying on it obeys normality.
3. **P** is the total load on the slider at O during slip with an associated motion vector **q**.

This demonstrates that the envelope of the Minkowsky sum of the individual limit surfaces yields the overall LS of the slider.

A way of visualizing the Minkowsky summation operation is by understanding that all it accomplishes is the process of 'convolution' of the individual limit surfaces. An individual LS is chosen and keeping it fixed, the origin of another individual LS (while keeping its orientation fixed) is slid on the boundary of the fixed LS, and the envelope of the volume thus swept out, obtained. Then successively the remaining individual limit surfaces are slid with fixed orientations over the envelopes obtained as a result of the previous convolution. The overall LS is then the outer boundary of the region swept out after all the convolutions. For example, the LS shown in fig. 12 for the slider supported at its two ends, has been obtained by the convolution of one planar ellipse (individual LS for one point of support) over another (individual LS for the other point of support) while keeping their orientations fixed.

5.2.1 Uniqueness Of Decomposition Of Overall Load For Isotropic Friction

For sliders with a known support pressure distribution and isotropic friction, it can now be shown that the vectorial decomposition of a given load $\mathbf{P}$ on the overall LS of the slider (obtained as the Minkowsky sum of individual limit surfaces), in terms of loads $\mathbf{p}$ lying on individual limit surfaces, is unique. Suppose that load $\mathbf{P}$ (with an associated motion vector $\mathbf{q}$) has two alternate decompositions:

$$\mathbf{P} = \sum \mathbf{p} = \sum \mathbf{p}^* \tag{5.2}$$

such that $\mathbf{p} \neq \mathbf{p}^*$ on at least two individual limit surfaces. Equation 5.2 implies that:

$$\sum((\mathbf{p} - \mathbf{p}^*) \cdot \mathbf{q}) = 0 \tag{5.3}$$

Since inequality 5.1 is satisfied at each individual LS, equation 5.3 implies that:

$$(\mathbf{p} - \mathbf{p}^*) \cdot \mathbf{q} = 0 \tag{5.4}$$

for all individual limit surfaces. Equations 5.4 can be true only if:

1. $\mathbf{p} = \mathbf{p}^*$ for all individual limit surfaces which contradicts our assumption that $\mathbf{p} \neq \mathbf{p}^*$ on at least two individual limit surfaces.
2. $\mathbf{q}$ corresponds to the motion vector associated with the flat regions of at least two individual limit surfaces. But this would mean that the slider is rotating about two distinct points of support simultaneously, which is impossible, and hence $\mathbf{p} = \mathbf{p}^*$ on all individual limit surfaces.

So we arrive to the conclusion that for isotropic friction, the terms in the summation from the individual limit surfaces, leading to the load $\mathbf{P}$ on the envelope of the Minkowsky sum, are unique. This uniqueness property is not necessarily true for the models of anisotropic friction considered here, because $\mathbf{q}$ could correspond to loads on the straight edges of at least two different individual limit surfaces (as stated in condition 2 above) without implying simultaneous rotation about two distinct points of support.

5.2.2 Non-Uniqueness In The Load Motion Relation Through Minkowsky Sum

We now investigate the pressure distribution leading to vertices and flat regions on the LS through the Minkowsky sum.

1. Vertex: Consider a load $\mathbf{P}$ (with associated motions $\mathbf{q}$ and $\mathbf{q}'$) on the vertex of the LS, given by:
$$\mathbf{P} = \sum \mathbf{p} = \sum \mathbf{p}' \tag{5.5}$$
where $\mathbf{p}$ and $\mathbf{p}'$ are loads on the individual limit surfaces, with associated motion vectors $\mathbf{q}$ and $\mathbf{q}'$ respectively. The fact that with isotropic friction the terms in the summation leading to $\mathbf{P}$ are unique and equation 5.5 imply that $\mathbf{p} = \mathbf{p}'$ on all the individual limit surfaces. So $\mathbf{p} = \mathbf{p}'$ must lie on a vertex on every individual limit surface, with associated motions $\mathbf{q}$ and $\mathbf{q}'$.

In summary we can say that for sliders with isotropic friction, a certain range of motions are associated with a vertex on the overall LS, only if they are associated with a vertex on every individual limit surface for the points of support of the slider. Reasoning from the orientational properties of individual limit surfaces for isotropic points of support, we see that such a situation can only occur if all the support lay along a line. So for isotropic friction, a finite slider has vertices on its LS only if all its support is confined to a line.

Similarly, for anisotropic friction, there exist vertices on the overall LS of the slider, if there exist a range of motions that are associated with a vertex on every individual limit surface, corresponding to each point (or elemental area) of support. But unlike isotropic friction, due to straight edges on individual limit surfaces for anisotropic friction, equation 5.5 can also be satisfied for cases where, $\mathbf{p} = \mathbf{p}'$ for at least two different individual limit surfaces (non-uniqueness of decomposition of the sum). Hence, here non-collinearity of support does not guarantee the lack of vertices on the overall LS for the slider. A four wheeled cart is an example.

2. Flat Regions: Two different summations $\sum \mathbf{p}$ and $\sum \mathbf{p}''$ of loads from individual limit surfaces, all associated with the motion vector $\mathbf{q}$, with $\mathbf{p} \neq \mathbf{p}''$ for at least one individual LS and hence lying on a flat region (with associated motion $\mathbf{q}$) for that individual LS; would lead to two different loads $\mathbf{P}$ and $\mathbf{P}''$ respectively, both associated with the motion vector $\mathbf{q}$ on the LS of the slider.

$$\mathbf{P} = \sum \mathbf{p}, \quad \mathbf{P}'' = \sum \mathbf{p}'', \quad \mathbf{P} \neq \mathbf{P}''$$

Hence $\mathbf{P}$ and $\mathbf{P}''$ are on a flat region of the LS with motion $\mathbf{q}$.

For sliders with isotropic friction and point supports, the individual LS for each point of support has a flat region associated with the motion $\mathbf{q}$ (and so too the motion $-\mathbf{q}$), corresponding to rotation of the slider about the point of support itself. Hence, each point of support contributes two flat facets, equal in size and parallel to the individual LS corresponding to this point of support, on the overall LS of the slider. But if the slider has distributed support, then howsoever small an elemental area *da* that we consider, its individual LS would be such that it has no flat regions. This is because for rotation of the slider about any point within *da*, the magnitude of the frictional resistance at that point would be zero, which is determinate, and the frictional resistance over the rest of *da* would be uniquely determinate. So for sliders with isotropic friction, we can summarize that flat regions only occur on the overall LS, if the slider has point supports.

Similar reasoning for anisotropic friction shows that, point supports lead to flat regions on the overall LS. But the presence of only distributed support does not guarantee the lack of flat regions, again due to straight edges on the individual limit surfaces. A uniformly supported disk with ideal wheels with their axes radial to the disk, is an example.

3. Straight Edges: As an extension of the arguments given above for the appearance of vertices and flat regions on the overall LS through the Minkowsky sum, it can be shown that straight edges appear on the three-dimensional LS only if: (*a*) at least one of the individual LS has a straight edge and (*b*) the set of

motions q corresponding to this straight edge is associated with a vertex on every other individual LS.

This implies directly that limit surfaces for isotropic friction do not have straight edges because the individual LS corresponding to a point of isotropic support does not have straight edges.

5.3 Limit Surfaces Derived From Moment Surfaces

As a direct consequence of equation 4.4, it follows that for sliders with isotropic friction, their LS can be derived from their MS by differentiation, as shown in examples later.

5.4 Limit Surfaces By Direct Integration (Or Summation)

The LS for a slider can also be obtained by direct integration (or summation) of the frictional forces over the contact region for all possible motions, if the pressure distribution and the friction law allow analytical evaluation of the integrals in equation 2.1, as will be seen in some examples later.

Chapter 6

Construction Of Moment Surfaces For Isotropic Friction

From equation 2.2, it can be seen that the MS for a slider with isotropic friction can be obtained by summing the moments of the friction forces about the COR, for all possible CORs. For pressure distributions that do not allow easy analytical evaluation of the integral in equation 2.2, the overall MS can also be obtained by summation of the individual moment surfaces for each point of support, as shown below.

6.1 MS For Each Point Of Isotropic Support

For each individual point of support 'a', with friction coefficient μ_a and normal force N_a, the MS plots as an infinite cone in $[X_c, Y_c, M_c]$ space, centered at 'a' and its generators making an angle γ given by $\tan\gamma = \mu_a N_a$, with the $[x_c, y_c]$ plane (fig. 15). The cone with positive m_c corresponds to $\omega \geq 0$ for the slider and a similar cone obtained as its reflection about the $[x_c, y_c]$ plane is the $m_c(x_c, y_c)$ function for $\omega \leq 0$ of the slider.

6.2 Overall MS For The Slider

The overall MS for the slider can be obtained by simple summation of superposed individual moment surfaces corresponding to each point (or elemental area) of support, just as the overall moment is obtained as the summation of individual moments from each point of support. The value of the $M_c(x_c, y_c)$ function on the overall MS for the slider, at some point (x_c, y_c) in the plane of CORs, is the summation of the values of individual $m_c(x_c, y_c)$ functions at each point of support, all evaluated at (x_c, y_c).

$$M_c(x_c, y_c) = \sum m_c(x_c, y_c) \tag{6.1}$$

For sliders with distributed support, the above summation is replaced by an integration.

6.2.1 Vertices And Flat Regions On Moment Surfaces

We now investigate pressure distributions with isotropic friction, that lead to vertices and flat regions on moment surfaces.

1. Vertex: From equation 6.1 we have that:

$$\nabla M_c(x_c, y_c) = \sum \nabla m_c(x_c, y_c) \tag{6.2}$$

where $\nabla m_c(x_c, y_c)$ is the gradient of the individual MS, evaluated at the point (x_c, y_c).This implies that a non-uniqueness of the gradient on the overall MS at (x_c, y_c) will only occur, if there is a non-uniqueness of the gradient on at least one of the individual moment surfaces at (x_c, y_c). Observation of the infinite cones, which are the individual moment surfaces corresponding to each point (or elemental area) of support, shows that a slope discontinuity on the individual MS occurs only for the motion of the slider corresponding to a rotation about the corresponding point of support.

For distributed support, however, the individual MS for any point within the region of support contributes no singularity to the overall limit load, because the normal force N associated with that point is zero. Again we are led to our previously known result, that for isotropic friction, rotation about a point of support corresponds to a vertex on the MS (and a flat region on the LS), and distributed support guarantees a lack of vertices on the MS.

2. Flat region: Equation 6.2 also implies that a constant gradient ∇M_c for a range of CORs occurs on the MS, only when ∇m_c is constant for the same range of CORs, for each individual MS. From the geometry of the individual moment surfaces (the cones), we see that a region of constant gradient occurs only along their generators. Hence a region of constant ∇M_c would occur in situations where the generators of the individual moment surfaces, lay superposed over one another. And this can only happen, if all the support for the slider were to lie along a line. So we conclude that for sliders with isotropic friction, non-collinearity of support guarantees a lack of flat regions on the MS (vertices on the LS).

Chapter 7

Examples Of Limit Surfaces And Moment Surfaces

We consider below a few simple contact pressure distributions and derive the equations of their corresponding limit surfaces and moment surfaces (wherever applicable). For simplicity, the coefficient of friction is assumed to be unity everywhere.

7.1 One Point Of Isotropic Support

For a point of isotropic support with unit normal force located at $\mathbf{r_a} = [r_{ax}, r_{ay}]$, the moment function and the frictional loads corresponding to a COR at (x_c, y_c), are given as:

$$M_c(x_c, y_c) = \sqrt{(x_c - r_{ax})^2 + (y_c - r_{ay})^2} \tag{7.1}$$

$$F_x = \frac{y_c - r_{ay}}{\sqrt{(x_c - r_{ax})^2 + (y_c - r_{ay})^2}}, \quad F_y = -\frac{x_c - r_{ax}}{\sqrt{(x_c - r_{ax})^2 + (y_c - r_{ay})^2}},$$

$$M = \frac{r_{ax}(r_{ax} - x_c) + r_{ay}(r_{ay} - y_c)}{\sqrt{(x_c - r_{ax})^2 + (y_c - r_{ay})^2}} \tag{7.2}$$

For $-\infty \leq x_c, y_c \leq \infty$, equation 7.1 parameterizes the MS for the point of support, i. e. the cone of fig. 15 and equation 7.2 parameterizes its LS, which is the ellipse of fig. 14 (appendix A.3).

7.2 Two Points Of Isotropic Support

For the unidimensional bar of fig. 10, the M_c function and the frictional loads are given as:

$$M_c = \sqrt{x_c^2 + (y_c + 1)^2} + \sqrt{x_c^2 + (y_c - 1)^2} \tag{7.3}$$

$$F_x = \frac{y_c + 1}{\sqrt{x_c^2 + (y_c + 1)^2}} + \frac{y_c - 1}{\sqrt{x_c^2 + (y_c - 1)^2}},$$

$$F_y = -\frac{x_c}{\sqrt{x_c^2 + (y_c + 1)^2}} - \frac{x_c}{\sqrt{x_c^2 + (y_c - 1)^2}},$$

$$M = \frac{y_c + 1}{\sqrt{x_c^2 + (y_c + 1)^2}} - \frac{y_c + 1}{\sqrt{x_c^2 + (y_c - 1)^2}} \tag{7.4}$$

For $-\infty \leq x_c, y_c \leq \infty$, equation 7.3 parameterizes the MS for the bar (fig. 11) and equation 7.4 parameterizes the LS for the bar (fig. 12).

The MS for a slider with n points of support can be obtained in a similar manner by the addition of the cones corresponding to each point of support. The LS for the slider can then be obtained by differentiation of the equation for the MS obtained above.

7.3 Two Points Of Asymmetric Isotropic Support

Consider another unidimensional bar as in fig. 10, with its CM at $(0,0)$, and supported by normal forces of magnitude 2 and 1 at $(0,1)$ and $(0,-2)$ respectively. For this asymmetric normal force distribution, the M_c function and the frictional loads at the CM are given as:

$$M_c = \sqrt{x_c^2 + (y_c + 2)^2} + 2\sqrt{x_c^2 + (y_c - 1)^2} \tag{7.5}$$

$$F_x = \frac{y_c + 2}{\sqrt{x_c^2 + (y_c + 2)^2}} + 2\frac{y_c - 1}{\sqrt{x_c^2 + (y_c - 1)^2}},$$

$$F_y = -\frac{x_c}{\sqrt{x_c^2 + (y_c + 2)^2}} - 2\frac{x_c}{\sqrt{x_c^2 + (y_c - 1)^2}},$$

$$M = \frac{2(2 + y_c)}{\sqrt{x_c^2 + (y_c + 2)^2}} + \frac{2(1 - y_c)}{\sqrt{x_c^2 + (y_c - 1)^2}} \tag{7.6}$$

For $-\infty \leq x_c, y_c \leq \infty$, equation 7.5 parameterizes the MS for the asymmetric bar and equation 7.6 parameterizes its LS.

It is interesting to note that although the LS has all the general symmetries and properties of isotropic friction (like both loads **P** and $-\mathbf{P}$ being on the LS, and a pure force load having pure translation as one of the associated motions), the CF and the CT do not coincide. The CF coincides with the CM of the bar at the origin. The CT is unique and it coincides with the support point at $(0,1)$. Also, as shown in fig. 16, which shows the section of the LS on the $[F_x, M]$ plane, the pure moment load (corresponding to rotation about the CT) is less than the maximum moment of the frictional forces.

7.4 Axisymmetric Pressure Distributions

We now consider some examples of axisymmetric pressure distributions (axisymmetric about a vertical axis passing through the CM of the slider and no point supports) that lead to limit surfaces that are axisymmetric about the M-axis in load space.

7.4.1 Ring Of Isotropic Support

We consider a uniformly supported thin ring of unit radius (fig. 17) with unit normal force. Since the pressure distribution is axisymmetric and the friction isotropic leading to

axisymmetric MS and LS, we only need look at frictional loads corresponding to CORs located at r_c along the X-axis, for $0 \leq r_c \leq \infty$. The $M_c(r_c)$ function is then given as:

$$M_c(r_c) = \frac{1}{2\Pi}\int_0^{2\Pi}\sqrt{1+r_c^2-2r_c\cos\theta}\,d\theta = \frac{1}{\Pi}\int_0^{\Pi}\sqrt{1+r_c^2-2r_c\cos\theta}\,d\theta \tag{7.7}$$

$$F_y(r_c) = -\frac{\partial M_c}{\partial r_c} = \frac{1}{\Pi}\int_0^{\Pi}\frac{\cos\theta - r_c}{\sqrt{1+r_c^2-2r_c\cos\theta}}d\theta,$$

$$M(r_c) = \frac{1}{\Pi}\int_0^{\Pi}\frac{1-r_c\cos\theta}{\sqrt{1+r_c^2-2r_c\cos\theta}}d\theta \tag{7.8}$$

Equation 7.7 parameterizes the generating curve for the MS for the ring, a part of which is shown in fig. 18. Equation 7.8 parameterizes the generating curve for the LS for the ring of isotropic support and is shown in fig. 19. There are no vertices or flat regions on either of the surfaces.

For $0 \leq r_c \leq \infty$, equation 7.8 parameterizes the section of the LS for the ring on the $[-F_y, M]$ quadrant of the $[F_y, M]$ plane. Manipulation of equation 7.8 reveals that this curve has the symmetry noted by Ishlinskii et al. [1981] and Voyenli and Eriksen [1985]:

$$F_y(\frac{1}{r_c}) = -M(r_c), \quad M(\frac{1}{r_c}) = -F_y(r_c) \tag{7.9}$$

Hence the complete generating curve for the LS for the ring can be obtained by only considering values of r_c within $0 \leq r_c \leq 1$; fig. 19 shows that the generating curve in each quadrant is symmetric about the line bisecting the quadrant which intersects the curve at $r_c = 1$. As shown in appendix A.4, the integrals in equation 7.8 can be obtained as elliptic integrals.

7.4.2 Disk Of Isotropic Support

Now we consider a uniformly supported disk of unit radius (fig. 20) with unit normal force. Summing up frictional forces and moments at elemental areas $rd\theta dr$ over the whole disk, for CORs located at r_c along the X-axis, we get:

$$M_c(r_c) = \frac{2}{\Pi}\int_0^1\int_0^{\Pi} r\sqrt{r^2+r_c^2-2rr_c\cos\theta}\,d\theta dr \tag{7.10}$$

$$F_y(r_c) = \frac{2}{\Pi}\int_0^1\int_0^{\Pi}\frac{r(r\cos\theta - r_c)}{\sqrt{r^2+r_c^2-2rr_c\cos\theta}}d\theta dr,$$

$$M(r_c) = \frac{2}{\Pi}\int_0^1\int_0^{\Pi}\frac{r^2(r-r_c\cos\theta)}{\sqrt{r^2+r_c^2-2rr_c\cos\theta}}d\theta dr \tag{7.11}$$

Equation 7.10 parameterizes the generating curve for the MS for the disk, a part of which is shown in fig. 21. Equation 7.11 parameterizes the generating curve for the LS for the uniformly supported disk and is shown in fig. 22. For nondimensionalizing the curve of fig. 22, the reference length is chosen to be $l_r = 1/\sqrt{2} = \rho_g$, if mass is uniformly distributed in contact region. As shown in appendix A.5, the integrals in equation 7.11 can be obtained as elliptic integrals.

7.4.3 Ring Of Radial Wheels

We consider a thin ring that is supported uniformly with ideal wheels which have their axes radial to the ring, and unit normal force. From the LC for ideal wheels (fig. 7(b)), we have that the individual LS for each elemental area of contact is then a straight line in the $[F_x, F_y]$ plane passing through the origin, along the radial direction passing through the elemental area. The Minkowsky summation of all these individual limit surfaces yields the overall LS of the slider which is a circle (and its interior) in the $[F_x, F_y]$ plane of radius $2/\Pi$. Despite distributed non-collinear support of wheels, the LS still has vertices and flat regions.

Note that this LS is the same as that obtained for a point of isotropic support at the center of the ring with normal force $2/\Pi$. Hence *the limit surfaces for all sliders with isotropic support can be obtained by a suitable and equivalent arrangement of ideal wheel supports.*

7.4.4 Ring Of Tangential Wheels

Now we consider a thin ring of unit radius supported uniformly with ideal wheels with their axes tangential to the ring, and unit normal force. Since the LS is axisymmetric, we only need consider frictional loads corresponding to CORs located at r_c along the X-axis. For any instantaneous COR (with a positive sense of rotation) lying within or on the ring ($0 \leq r_c \leq 1$), the total frictional load sums up to be a pure moment given as $\mathbf{P} = [0, 0, 1]$. This leads to a vertex on the LS for the slider at its intersection with the M-axis (fig. 24), even though it has non-collinear support.

For a typical r_c satisfying $r_c > 1$, the distribution of frictional forces is shown schematically in fig. 23, and their summation leads to:

$$F_y(r_c) = -\frac{4}{2\Pi}\int_0^{\phi} \cos\theta d\theta = -\frac{2\sin\phi}{\Pi} = -\frac{2\sqrt{r_c^2 - 1}}{\Pi r_c} \tag{7.12}$$

$$M(r_c) = \frac{4}{2\Pi}\int_{\phi}^{\Pi/2} d\theta = \frac{2}{\Pi}\left(\frac{\Pi}{2} - \cos^{-1}(\frac{1}{r_c})\right) \tag{7.13}$$

where $\cos\phi = 1/r_c$. From the symmetry of the distribution, it can also be seen that $F_x = 0$. For $r_c > 1$, equations 7.12 and 7.13 parameterize the generating curve for the uniformly supported ring with radial ideal wheels, shown in fig. 24.

7.4.5 Ring Of Tangential Wheels With Ratchets

Consider again the uniformly supported ring of unit radius and unit normal force with ratcheted wheels with their axes tangential to the ring, so that the wheel at each elemental area of contact jams when its relative slip direction is away from the center of the ring. For a typical r_c between $0 \leq r_c \leq 1$, the distribution of frictional forces is shown in fig. 25, and their summation leads to:

$$F_x(r_c) = -\frac{2}{2\Pi}\int_0^{\Pi/2} \sin\theta d\theta - \frac{1}{2\Pi}\int_{\Pi}^{2\Pi} \frac{\sin\theta}{\sqrt{1 + r_c^2 - 2r_c\cos\theta}} d\theta$$

$$\Rightarrow F_x(r_c) = -\frac{1}{\Pi} + \frac{1}{\Pi} = 0$$

$$F_y(r_c) = \frac{1}{2\Pi}\int_{\Pi}^{2\Pi} \frac{\cos\theta - r_c}{\sqrt{1 + r_c^2 - 2r_c\cos\theta}} d\theta$$

$$\Rightarrow F_y(r_c) = -\frac{1}{2\Pi}\int_{0}^{\Pi} \frac{\cos\theta + r_c}{\sqrt{1 + r_c^2 + 2r_c\cos\theta}} d\theta = -\frac{1}{\Pi r_c}(E(r_c) + (r_c^2 - 1)K(r_c)) \qquad (7.14)$$

$$M(r_c) = \frac{1}{2\Pi}\int_{0}^{\Pi} d\theta + \frac{1}{2\Pi}\int_{\Pi}^{2\Pi} \frac{1 - r_c\cos\theta}{\sqrt{1 + r_c^2 - 2r_c\cos\theta}} d\theta$$

$$\Rightarrow M(r_c) = \frac{1}{2} + \frac{1}{2\Pi}\int_{0}^{\Pi} \frac{1 + r_c\cos\theta}{\sqrt{1 + r_c^2 + 2r_c\cos\theta}} d\theta = \frac{1}{2} + \frac{E(r_c)}{\Pi} \qquad (7.15)$$

Equations 7.14 and 7.15 parameterize the generating curve for the LS of the slider for $0 \leq r_c < 1$, where K and E are complete elliptic integrals of the first and second kind respectively. For a typical r_c satisfying $r_c \geq 1$, the distribution of frictional forces is shown in fig. 26, and their summation leads to:

$$F_x(r_c) = -\frac{2}{2\Pi}\int_{\phi}^{\Pi/2} \sin\theta d\theta - \frac{1}{2\Pi}\int_{\Pi}^{2\Pi} \frac{\sin\theta}{\sqrt{1 + r_c^2 - 2r_c\cos\theta}} d\theta$$

$$\Rightarrow F_x(r_c) = -\frac{1}{\Pi r_c} + \frac{1}{\Pi r_c} = 0$$

$$F_y(r_c) = -\frac{2}{2\Pi}\int_{0}^{\phi} \cos\theta d\theta + \frac{1}{2\Pi}\int_{\Pi}^{2\Pi} \frac{\cos\theta - r_c}{\sqrt{1 + r_c^2 - 2r_c\cos\theta}} d\theta$$

$$\Rightarrow F_y(r_c) = -\frac{\sqrt{r_c^2 - 1}}{\Pi r_c} - \frac{1}{2\Pi}\int_{0}^{\Pi} \frac{\cos\theta + r_c}{\sqrt{1 + r_c^2 + 2r_c\cos\theta}} d\theta$$

$$\Rightarrow F_y(r_c) = -\frac{\sqrt{r_c^2 - 1}}{\Pi r_c} - \frac{1}{\Pi}E(\frac{1}{r_c}) \qquad (7.16)$$

$$M(r_c) = \frac{2}{2\Pi}\int_{\phi}^{\Pi/2} d\theta + \frac{1}{2\Pi}\int_{\Pi}^{2\Pi} \frac{1 - r_c\cos\theta}{\sqrt{1 + r_c^2 - 2r_c\cos\theta}} d\theta$$

$$\Rightarrow M(r_c) = \frac{1}{2} - \frac{1}{\Pi}\cos^{-1}(\frac{1}{r_c}) + \frac{1}{2\Pi}\int_{0}^{\Pi} \frac{1 + r_c\cos\theta}{\sqrt{1 + r_c^2 + 2r_c\cos\theta}} d\theta$$

$$\Rightarrow M(r_c) = \frac{1}{2} - \frac{1}{\Pi}\cos^{-1}(\frac{1}{r_c}) + \frac{r_c}{\Pi}\left(E(\frac{1}{r_c}) + (\frac{1}{r_c^2} - 1)K(\frac{1}{r_c})\right) \qquad (7.17)$$

Equations 7.16 and 7.17 parameterize the generating curve for the LS for the slider for r_c satisfying $r_c \geq 1$. The complete generating curve for the LS for the ring supported uniformly by tangential ratcheted wheels is shown in fig. 27. There are no vertices or flat regions on this LS.

7.4.6 Ring Of Radial Wheels With Ratchets

This time the uniformly supported ring of unit radius and unit normal force has ratcheted wheels with their axes radial to the ring, so that the wheels jam when the ring rotates with a positive sense of rotation. For all r_c lying between $0 \leq r_c \leq 1$, and $\omega > 0$, the slider behaves like a ring of isotropic support and hence the generating curve for the LS is parameterized as:

$$F_y(r_c) = \frac{1}{\Pi}\int_0^{\Pi} \frac{\cos\theta - r_c}{\sqrt{1 + r_c^2 - 2r_c\cos\theta}} d\theta = \frac{2}{\Pi r_c}((1 - r_c^2)K(r_c) - E(r_c)) \tag{7.18}$$

$$M(r_c) = \frac{1}{\Pi}\int_0^{\Pi} \frac{1 - r_c\cos\theta}{\sqrt{1 + r_c^2 - 2r_c\cos\theta}} d\theta = \frac{2}{\Pi}E(r_c) \tag{7.19}$$

For values of r_c satisfying $r_c \geq 1$ and $\omega > 0$, the slider behaves partially like a ring of isotropic support and partially like a ring supported with ideal radial wheels, as shown in fig. 28. Summing the frictional loads gives:

$$F_y(r_c) = -\frac{2}{2\Pi}\int_0^{\phi} \sin\theta d\theta + \frac{2}{2\Pi}\int_{\phi}^{\Pi} \frac{\cos\theta - r_c}{\sqrt{1 + r_c^2 - 2r_c\cos\theta}} d\theta$$

$$\Rightarrow F_y(r_c) = -\frac{r_c - 1}{\Pi r_c} + \frac{1}{\Pi}\int_{\phi}^{\Pi} \frac{\cos\theta - r_c}{\sqrt{1 + r_c^2 - 2r_c\cos\theta}} d\theta \tag{7.20}$$

$$M(r_c) = \frac{1}{\Pi}\int_{\phi}^{\Pi} \frac{1 - r_c\cos\theta}{\sqrt{1 + r_c^2 - 2r_c\cos\theta}} d\theta \tag{7.21}$$

where $\cos\phi = 1/r_c$. Equations 7.20 and 7.21 parameterize the generating curve for the LS for the slider for $r_c \geq 1$ and $\omega > 0$.

For values of r_c satisfying $r_c \geq 1$ and $\omega < 0$, the slider again behaves like a mixture of isotropic support and radial ideal wheels, but opposite to that with $\omega > 0$. Here summation of frictional loads gives:

$$F_y(r_c) = \frac{2}{2\Pi}\int_{\phi}^{\Pi} \sin\theta d\theta - \frac{2}{2\Pi}\int_0^{\phi} \frac{\cos\theta - r_c}{\sqrt{1 + r_c^2 - 2r_c\cos\theta}} d\theta$$

$$\Rightarrow F_y(r_c) = \frac{r_c + 1}{\Pi r_c} - \frac{1}{\Pi}\int_0^{\phi} \frac{\cos\theta - r_c}{\sqrt{1 + r_c^2 - 2r_c\cos\theta}} d\theta \tag{7.22}$$

$$M(r_c) = -\frac{1}{\Pi}\int_0^{\phi} \frac{1 - r_c\cos\theta}{\sqrt{1 + r_c^2 - 2r_c\cos\theta}} d\theta \tag{7.23}$$

Equations 7.22 and 7.23 parameterize the generating curve for the LS for the slider for $r_c \geq 1$ and $\omega < 0$. For $0 \leq r_c < 1$ and $\omega < 0$, the slider behaves like a ring of radial ideal wheels. The complete generating curve for the LS for the ring with radial ratcheted wheels is shown in fig. 29.

The notable features of this LS are that it has no points in the negative M half space, and also that the slider requires a moment and a force for pure translation. It also has vertices and flat regions.

7.4.7 Infinite Disk With Tangential Wheels

Imagine an infinite disk supported with ideal wheels with their axes tangential to the disk and a radially varying (hence axisymmetric) support pressure distribution $p(r)$ (pressure $p(r)$ at a radial distance r from the center of disk) given by the special relation:

$$p(r) = \frac{1}{\Pi r(1+r^2)^2} \tag{7.24}$$

The total normal force on the infinite disk with the above pressure distribution is finite because:

$$\lim_{\epsilon \to 0} \int_{\epsilon}^{1/\epsilon} p(r) 2\Pi r dr = \lim_{\epsilon \to 0} \int_{\epsilon}^{1/\epsilon} \frac{2}{(1+r^2)^2} dr = \frac{\Pi}{2}$$

This infinite disk can be thought of as composed of an infinite number of concentric rings, each uniformly supported by tangential ideal wheels. Then for a COR located at r_c along the X axis, only the rings with $r > r_c$ contribute net non-zero frictional forces, but all rings contribute frictional torques. Summing up these frictional loads, as for a single ring, gives us:

$$F_y(r_c) = -4 \int_0^{r_c} \int_0^{\phi} p(r) \cos\theta r d\theta dr, \quad \cos\phi = \frac{r}{r_c}$$

$$\Rightarrow F_y(r_c) = -\frac{4}{\Pi r_c} \int_0^{r_c} \frac{\sqrt{r_c^2 - r^2}}{(1+r^2)^2} dr \tag{7.25}$$

$$M(r_c) = 4 \int_0^{r_c} \int_{\phi}^{\Pi/2} r p(r) r d\theta dr + \int_{r_c}^{\infty} \int_0^{2\Pi} r p(r) r d\theta dr$$

$$\Rightarrow M(r_c) = 1 - \frac{4}{\Pi} \int_0^{r_c} \frac{r}{(1+r^2)^2} \cos(\frac{r}{r_c}) dr \tag{7.26}$$

For $0 \leq r_c \leq \infty$, the generating curve obtained from the parametric equations 7.25 and 7.26 is a semicircle (as shown in appendix A.6), which implies that the LS for this infinite disk is a sphere of unit radius! This LS is the three dimensional analog of the circular LC for isotropic friction; the frictional load **P** is constant in magnitude and in the direction of the motion **q**.

Chapter 8

Dynamics Of Planar Sliders With Dry Friction

We now proceed towards the application of our knowledge of the overall frictional load and motion relation and its LS description to equations 2.3 and 2.4, which govern the dynamics of planar sliders. Within the framework of the limitations imposed on the load motion behaviour of the slider due to the load motion inequality, we specifically address the following two issues: 1) The starting problem, 2) Frictional effects during free sliding.

8.1 Starting Problem

The starting problem deals with finding the motion $\mathbf{q}$ associated with a given applied load $\mathbf{P^e}$, or finding the associated load with a given motion, at first slip. There are two separate contexts to this problem: quasi-static slipping, and slipping with combined inertial and frictional loads.

8.1.1 Quasi-Static Slipping

If the velocity of the slider is considered to be low enough so that inertial forces are negligible and frictional loads dominate, then one assumes that the slider is in static equilibrium at slip, so that the externally applied load $\mathbf{P^e} = \mathbf{P}$, the frictional load. With the LS description, this implies that $\mathbf{P^e}$ is on the LS. If the LS for the slider is known (i.e. given friction law that satisfies inequality 3.1, and the normal pressure distribution everywhere over the contacting surface), then the $\mathbf{q}$ associated with this $\mathbf{P^e}$ that does not violate the slip condition, can be found. Conversely, under the same circumstances, we can calculate the load on the LS associated with any desired motion $\mathbf{q}$ of the slider.

A unique solution to the starting problem cannot be found if $\mathbf{P^e}$ lies on a vertex of the LS for the slider, for which there is no unique associated $\mathbf{q}$. Similarly for a desired $\mathbf{q}$ that lies on a flat region of the LS, an associated unique $\mathbf{P^e}$ cannot be calculated.

8.1.2 Slipping With Combined Inertial And Frictional Loads

If inertial forces are included, then a unique solution to the starting problem can always be found [as Mason 1985 states without proof], as shown below. At slip under the action of the load $\mathbf{P^e}$, the resulting motion $\mathbf{Q}$ of the slider is in the direction of its acceleration

$d\mathbf{Q}/dt$, if $d\mathbf{Q}/dt$ is bounded and continuous, as shown in appendix A.7. So the acceleration at slip can be expressed as:

$$\frac{d\mathbf{Q}}{dt} = \left|\frac{d\mathbf{Q}}{dt}\right| \mathbf{q}$$

Assume that for a given $\mathbf{P^e}$ that violates the slip condition, there exist two motions $\mathbf{Q_1}$ and $\mathbf{Q_2}$ for the slider (with associated frictional loads $\mathbf{P_1}$ and $\mathbf{P_2}$ respectively), both of which satisfy dynamic equilibrium (equation 2.4) implying:

$$\mathbf{P^e} - \mathbf{P_1} = \frac{d\mathbf{Q_1}}{dt}, \quad \mathbf{P^e} - \mathbf{P_2} = \frac{d\mathbf{Q_2}}{dt}$$

Subtracting one equation from the other gives:

$$\mathbf{P_1} - \mathbf{P_2} = \left(\frac{d\mathbf{Q_2}}{dt} - \frac{d\mathbf{Q_1}}{dt}\right) \tag{8.1}$$

$\mathbf{P_1}$ and $\mathbf{P_2}$ lie on the LS for the slider and obey inequality 4.2; $d\mathbf{Q_1}/dt$ and $d\mathbf{Q_2}/dt$ are in the direction of $\mathbf{q_1}$ and $\mathbf{q_2}$ respectively; and equation 8.1 imply that:

$$(\mathbf{P_1} - \mathbf{P_2}) \cdot \frac{d\mathbf{Q_1}}{dt} = \frac{d\mathbf{Q_1}}{dt} \cdot \left(\frac{d\mathbf{Q_2}}{dt} - \frac{d\mathbf{Q_1}}{dt}\right) \geq 0 \tag{8.2}$$

$$(\mathbf{P_2} - \mathbf{P_1}) \cdot \frac{d\mathbf{Q_2}}{dt} = \frac{d\mathbf{Q_2}}{dt} \cdot \left(\frac{d\mathbf{Q_1}}{dt} - \frac{d\mathbf{Q_2}}{dt}\right) \geq 0 \tag{8.3}$$

Adding equations 8.2 and 8.3 gives us:

$$\left(\frac{d\mathbf{Q_2}}{dt} - \frac{d\mathbf{Q_1}}{dt}\right) \cdot \left(\frac{d\mathbf{Q_2}}{dt} - \frac{d\mathbf{Q_1}}{dt}\right) \leq 0 \tag{8.4}$$

Equation 8.4 can only be true if:

$$\frac{d\mathbf{Q_1}}{dt} = \frac{d\mathbf{Q_2}}{dt} \Rightarrow \mathbf{P_1} = \mathbf{P_2} \Rightarrow \mathbf{Q_1} = \mathbf{Q_2} \Rightarrow \mathbf{q_1} = \mathbf{q_2} \tag{8.5}$$

Equation 8.5 shows that at initiation of slip, with combined frictional and inertial loads, there is always a unique frictional load and motion relation for the slider, implying a unique solution to the starting problem.

8.2 Frictional Effects During Free Sliding

Free sliding of a slider is the motion of the slider under the retarding action of frictional forces only. We now investigate the nature of this motion as the slider comes to rest. With $\mathbf{P_e} = 0$, equation 2.4 becomes:

$$\frac{d\mathbf{Q}}{dt} = -\mathbf{P} \tag{8.6}$$

which states that the deacceleration of the slider is in the direction of the frictional load. For simplicity we assume that the supporting surface is completely isotropic and homogenous, so that the LS of the slider rotates with an angular velocity ω in load space as the slider rotates with an angular velocity ω in physical space.

8.2.1 Eigen Directions As Final Motions

To analyze the evolution of the absolute velocity $\mathbf{Q}$ of the deaccelerating slider with time, we observe the evolution of $\mathbf{Q_b}$ (the velocity $\mathbf{Q}$ of the slider as seen in a reference frame that rotates with the slider). Then $d\mathbf{Q}/dt$ and $d\mathbf{Q_b}/dt$ are related by:

$$\frac{d\mathbf{Q}}{dt} = \frac{d\mathbf{Q_b}}{dt} + \omega \times \mathbf{Q_b} \tag{8.7}$$

The governing equation for the evolution of $\mathbf{Q_b}$ is given as (from equations 8.6 and 8.7):

$$\frac{d\mathbf{Q_b}}{dt} = -\mathbf{P} - \omega \times \mathbf{Q_b} \tag{8.8}$$

As the slider comes to a rest, both ω and $\mathbf{Q_b}$ become very small in magnitude so that their product is even smaller and can be ignored as compared to $-\mathbf{P}$ (for non-zero friction). So asymptotically as the slider speed approaches zero, the difference between $d\mathbf{Q}/dt$ and $d\mathbf{Q_b}/dt$ and their governing equations disappears, and we have:

$$\frac{d\mathbf{Q}}{dt} = \frac{d\mathbf{Q_b}}{dt} = -\mathbf{P} \tag{8.9}$$

From appendix A.7 we have that for any slider with bounded and smooth enough acceleration, the acceleration and velocity are parallel as it comes to rest. Applying this fact to equation 8.9 leads us to an important result that *when the slider comes to rest during free sliding, its motion* $\mathbf{Q}$ *is parallel to the frictional load* $\mathbf{P}$. This implies that the velocity vector $\mathbf{Q}$ comes to rest at only those special points on the LS for the slider (during its evolution in free sliding) where the direction of $\mathbf{P}$ is parallel to the normal $\mathbf{q}$ at that point. A more mathematical reasoning is given in appendix A.8. We call these special directions in load space eigen directions; they include all extrema of the LS loads.

The simplifying assumption about the isotropy and homogeneity of the supporting surface was used to relate the rate of change of the slider's velocity in an inertial system $d\mathbf{Q}/dt$ and in a slider fixed coordinate system $d\mathbf{Q_b}/dt$, through equation 8.7. This assumption can be relaxed to generalize our result about final motions resting at eigen directions, for all free sliding planar sliders covered by the LS description in this paper. As for the slider considered above, the changes in the shape and orientation of the LS due to the motion of the slider over the anisotropic supporting surface, approach zero asymptotically as the slider comes to rest (i.e. when the velocities become very small in magnitude). Hence their final motion is governed by equation 8.9, which implies that it is an eigen direction on the final LS which characterizes the frictional load motion behaviour of the slider.

8.2.2 Stability Criterion For Eigen Directions

The stability of an eigen direction on the LS is determined by whether free motions of the slider of very small magnitude in the vicinity of the eigen direction are attracted to, repelled by, or not affected by it. It is found that the behaviour of small perturbed motions in the neighbourhood of an eigen direction on the LS and hence the stability of the eigen direction are governed by the principal radii of curvature of the LS and the frictional load $\mathbf{P}$ at the eigen direction.

For sliders with an axisymmetric pressure distribution and hence an axisymmetric LS, the determination of the effect of an eigen direction on perturbed motions in its vicinity, on

the three-dimensional LS reduces to the determination of its effect on perturbed motions in its vicinity on its planar generating curve. At an eigen direction **P** on the generating curve of an axisymmetric LS, the *parallel* principal radius of curvature (in the plane M = *constant*) is $|\mathbf{P}|$ [O'Neill 1966], and let the *meridional* principal radius of curvature (in the plane of the generating curve passing through **P**) be ρ_c. Since the *parallel* principal radius of curvature equals the load magnitude $|\mathbf{P}|$ at the eigen direction, perturbations of motion along the *parallel* principal direction are neutrally stable (neither attracted or repelled by the eigen direction), but this aspect of the motion is not very important for axisymmetric sliders; this will be clear later on. As shown in appendix A.9, for small perturbations of motion near **P** we find that:

1. $\rho_c > |\mathbf{P}|$ implies that the perturbed motion is attracted to the eigen direction, and it is a stable or attracting eigen direction.
2. $\rho_c < |\mathbf{P}|$ implies that the perturbed motion is repelled away from the eigen direction, and it is an unstable or repelling eigen direction.
3. $\rho_c = |\mathbf{P}|$ implies that the perturbed motion is not affected by the eigen direction, and it is a neutrally stable eigen direction.

It can easily be seen that the eigen direction corresponding to a vertex on the generating curve is always a repeller and the one lying on a straight segment is always an attractor. Since the generating curve starts and ends on the M axis, is convex and contains the origin, it has to have at least two loads that are eigen directions, the minimum and the maximum load respectively. Also, the minimum load is either a stable or a neutrally stable eigen direction, as shown in appendix A.10.

Proceeding similarly for limit surfaces in three dimensional load space in appendix A.11, by analyzing the trajectories of motions of small magnitude in the neighbourhood of an eigen direction **P**, with associated principal radii of curvature ρ_1 and ρ_2 (in load space), we find that:

1. $\rho_1, \rho_2 > |\mathbf{P}|$ implies that $|\mathbf{P}|$ is a stable eigen direction.
2. ρ_1 or $\rho_2 < |\mathbf{P}|$ implies that $|\mathbf{P}|$ is an unstable eigen direction.
3. $\rho_1 = \rho_2 = |\mathbf{P}|$ implies that $|\mathbf{P}|$ is a neutrally stable eigen direction.

Again, the fact that the LS is closed, convex and encloses the origin, implies that it has to have at least two eigen directions, the minimum and the maximum load respectively. The minimum load is either a stable or a neutrally stable eigen direction. Similarly, the maximum load is either an unstable or a neutrally stable eigen direction.

8.2.3 Stability Criterion At Non-Zero Velocities During Free Sliding

It is to be stressed here that the above analysis and criterion for determining the stability of an eigen direction (based on the governing equation of motion 8.9) depending on the principal radii of curvature of the LS and the magnitude of the frictional load, are only valid for the free sliding of the slider with almost zero velocity magnitudes. At finite non-zero velocities, equation 8.8 is the appropriate governing equation of motion. For non-axisymmetric bodies, the incorporation of the extra $\omega \times \mathbf{Q_b}$ term can change the stability of an eigen direction from its zero velocity state.

8.2.4 Effect Of Change Of Radius Of Gyration On Eigen Directions

If the radius of gyration ρ_g of the slider is changed by altering its mass distribution and the support pressure distribution is left unaffected, then the LS for the given slider changes in shape; an understandable concept when one remembers that we use $l_r = \rho_g$ for non-dimensionalizing the length for studying the dynamics of the system. Effectively, the LS is stretched along the M axis by reducing the value of ρ_g (concentrating the mass closer to the CM) and it is contracted along the M axis by increasing the value of ρ_g (concentrating the mass further away from the CM). This in turn changes the eigen directions on the new LS for the slider and also their stability properties.

In fact, as shown for the examples of the uniformly supported ring and the disk, the final motion (the stable eigen direction) can be varied, by changing the mass distribution, without changing the support pressure distribution. Also, finite inner and outer bounds exist for ρ_g beyond which the final motion is a pure translation and a pure rotation about the CM, respectively.

8.3 Examples Of Free Sliding

As illustrations, we find the final motions of freely sliding uniformly supported rings and disks and the bar supported symmetrically at its ends. These examples have also been considered by Ishlinskii et. al [1981]. The uniformly supported ring and disk are subsets of sliders with axisymmetric pressure distributions and limit surfaces, and are considered by Voyenli and Eriksen [1985].

8.3.1 Uniformly Supported Ring

For the uniformly supported ring with isotropic friction, unit radius and $\rho_g = 1$, from analysis of equations 7.8 and fig. 19, we can conclude the following behaviour for the freely sliding ring.

1. The frictional load corresponding to a pure rotation of the ring about its center is an unstable eigen direction. This implies that if the ring is set in pure rotation about its center, it continues to do so until it comes to rest; no other initial motion of the ring ends with this motion.
2. Loads corresponding to pure translation of the ring are unstable eigen directions. This implies that if the ring is set in pure translation in a certain direction, then it continues to translate along the same direction until it comes to rest; no other initial motion of the ring ends with pure translation along this direction.
3. Loads corresponding to an instantaneous rotation of the ring about any point on it, are stable eigen directions; one such stable eigen direction with $\mathrm{P} = [0, 2/\Pi, 2/\Pi]$ (associated $\mathrm{q} = [0, 1/\sqrt{2}, 1/\sqrt{2}]$) is shown in fig. 19. This implies that all initial motions of the freely sliding ring, except pure translation and rotation about its center, end up as rotation about a point on the ring. Hence the final attracting motion is a pure 'rolling like' motion of the ring along a tangent line.

These results agree with those of Ishlinskii et. al [1981] and Voyenli and Eriksen [1985].

Also, from the calculations of appendix A.12, we can infer that any desired motion can be made to be the final attracting motion for the uniformly supported ring, by varying its radius of gyration ρ_g between $1/\sqrt{2}$ and $\sqrt{2}$, while keeping its support pressure distribution unaltered. In fact, we may summarize that:

1. For $\rho_g < 1/\sqrt{2}$, all initial motions of the freely sliding ring end as pure translations.
2. For $\rho_g > \sqrt{2}$, all initial motions of the ring end as pure rotations about its center.
3. For $1/\sqrt{2} \leq \rho_g \leq \sqrt{2}$, the final attracting motion depends on the value of ρ_g, and they range from rotations about the center to pure translations.

Due to the axisymmetry of the LS, the contribution of the $\omega \times \mathbf{Q_b}$ term in the free sliding analysis of the ring with non-zero velocities, does not change the stability criterion of the final attracting motion, and all the above results are still valid.

8.3.2 Uniformly Supported Disk

From a similar analysis of equations 7.11 and fig. 22 for the uniformly supported disk with isotropic friction (unit radius and original $\rho_g = 1/\sqrt{2}$), we conclude that for the freely sliding disk:

1. The frictional load corresponding to a pure rotation of the disk about its center is an unstable eigen direction, which implies that if the disk is set in pure rotation about its center, it continues to do so until it comes to rest; no other initial motion of the disk ends with this motion.
2. Loads corresponding to pure translation of the disk are unstable eigen directions, which implies that if the disk is set in pure translation in a certain direction, then it continues to translate along the same direction until it comes to rest; no other initial motion of the disk ends with pure translation along this direction.
3. Loads corresponding to an instantaneous rotation of the disk about any point on a circle centered at its center and radius $\simeq 0.653$, are stable eigen directions; one such stable eigen direction with $\mathbf{P} =\simeq [0, 0.616, 0.667]$ (associated $\mathbf{q} \simeq [0, 0.678, 0.735]$) is shown in fig. 22. This implies that all initial motions of the freely sliding disk, except pure translation and rotation about its center, end up as rotation about a point on a circle of radius $\simeq 0.653$ drawn on the ring.

These results agree with those of Voyenli and Eriksen [1985] and differ slightly from the final radius $\simeq 0.707$, reported by Ishlinskii et. al [1981].

From the calculations of appendix A.13, we can infer that any desired motion can be made to be the final attracting motion for the uniformly supported disk, by varying its radius of gyration ρ_g between $1/2$ and $\sqrt{2/3}$, while keeping its support pressure distribution unaltered. In fact, we may summarize that:

1. For $\rho_g < 1/2$, all initial motions of the freely sliding disk end as pure translations.

2. For $\rho_g > \sqrt{2/3}$, all initial motions of the disk end as pure rotations about its center.
3. For $1/2 \leq \rho_g \leq \sqrt{2/3}$, the final attracting motion depends on the value of ρ_g, and they range from rotations about the center to pure translations.

Generally speaking, for sliders with axisymmetric pressure distributions and limit surfaces, the final attracting motion for all initial motions during free sliding, is a pure rolling like motion along a tangent line to a circle (with its center coinciding with the center of the slider) of some radius. Also due to the axisymmetry of their LS about the M axis (the rotation axis), the contribution of the $\omega \times \mathbf{Q_b}$ term during free sliding due to higher velocities, does not affect the stability analysis done for eigen directions with almost zero velocity, and the stability results are unaltered. Note that for the infinite disk with tangential wheels, whose LS is a sphere, every load is a neutrally stable eigen direction, so that all initial motions continue without changing, until the disk comes to rest.

8.3.3 Bar Supported Symmetrically At Its Ends

As an illustration of a slider with a LS that is not axisymmetric, we investigate the freely sliding behaviour of the bar uniform bar supported at its ends, shown in fig. 10, a motion investigated numerically by Ishlinskii et. al [1981]. From the analysis of equations 7.4 and also the LS drawn in fig. 12, we can conclude that:

1. The load corresponding to a rotation of the bar about its center is an unstable eigen direction. The bar stops with pure rotation about its center only if it were set in that motion.
2. Similarly, loads corresponding to pure translations of the bar are unstable eigen directions too. So the bar stops with pure translation along a given direction only if it were set in pure translation along that direction.
3. Loads corresponding to instantaneous rotations of the bar about its points of support are stable eigen directions. So all initial motions of the bar, except pure translations and rotations about its center, end as rotations about points of support. In addition, these final motions about a point of support are sustainable for a finite amount of time [Wittenburg 1970], due to the flat region corresponding to this motion on the LS.

To verify the above conclusions, numerical simulations were done of the evolution of the motion of the freely sliding bar as it comes to rest, given various initial motions, and some of their results depicted on the unit motion sphere of fig. 30. The figure shows the evolution of motion as seen in a slider fixed axes system. An implicit assumption while formulating the simulation was that the frictional load $\mathbf{P}$ varies smoothly (without jumps) during the simulation. The light curves on the unit motion sphere depict the flow field, along which various motions of almost zero magnitude approach the stable eigen direction. The dark line shows the trajectory of evolution of a finite non-zero motion of the bar as it comes to rest along the stable eigen direction $\mathbf{P} = [1, 0, 1]$ and associated $\mathbf{q} = [1/\sqrt{2}, 0, 1/\sqrt{2}]$.

It can be noticed that not only do all initial motions come to rest along a stable eigen direction, but also their direction of final approach towards this $\mathbf{q}$ is nearly unique. It corresponds to a slight translation along the bar superposed on the rotation about one

point. Its apparent physical origin is the centripetal pull of the last moving point on the point which is about to be the center of rotation. Observe also that although loads on the $[F_y, M]$ plane are eigen directions, no motions (except a pure translation or a rotation about the center) ever come to rest on these, because the inherent q_ω component is enough to repel the motions away (equation 8.8).

Once again due to the symmetry of the support distribution and the relative symmetries of the limit curves for each point of support, the above results are not changed for free sliding of the bar starting with non-zero velocities.

8.3.4 Bar Supported Asymmetrically At Its Ends

To give another interesting example of an asymmetric pressure distribution, consider a unidimensional bar as in fig. 10 with its CM at $(0,0)$, supported by normal forces of magnitude 2 and 1 at $(0,1)$ and $(0,-2)$ respectively, with mass distribution such that its radius of gyration $\rho_g = 4$. Then the section of its LS on the $[F_x, M]$ plane, non-dimensionalized by choosing $l_r = \rho_g = 4$, is given by fig. 31. As can be seen in this figure, the only attracting motion for the bar is rotation about the heavier point of support at $(0,1)$. Rotation about the other point of support at $(0,-2)$ is no more an eigen direction. Loads corresponding to pure translations of the bar are still unstable eigen directions.

8.4 Propensity To Rotate About Points Of Support

It has been observed by various investigators including Jellett [1872], Prescott [1923] and MacMillan [1936] that sliders with isotropic friction have a propensity towards rotating about points of support. Based on our understanding of the overall load motion relation through limit surfaces, we can explain this phenomenon roughly as follows.

Point supports on sliders with isotropic friction lead to flat regions on their LS that might occupy a substantial area of the total surface of the LS. Hence, given a certain applied load that violates slip, there is higher probability that the corresponding motion of the slider will be a rotation about a point of support.

Also, for the same reason and the added fact that the principal radii of curvature ρ_1 and ρ_2 of the LS at the flat region are $\rho_1 = \rho_2 = \infty$, there is higher probability that one of the loads on it is a stable eigen direction, that attracts other free motions of the slider. This is observed in the motion of the bar supported at its ends, which stops with rotations about its points of support. However, all flat regions need not have an attracting eigen direction as can be seen in the example presented in the previous section where rotation about the lighter point of support is not an attracting motion.

Chapter 9

Extremum Principles For Frictional Load Motion Behaviour

Similar to the statements of Moreau [1979] and in analogy with plasticity [Drucker 1954, Kalker 1971], we now interpret the load motion inequality 4.2 as an expression of extremum principles for frictional slip. The inequality can also be written as:

$$\mathbf{P} \cdot \mathbf{q} \geq \mathbf{P}^* \cdot \mathbf{q} \tag{9.1}$$

The three vectors that appear in the above inequality are: the motion vector $\mathbf{q}$, an associated frictional load $\mathbf{P}$, and any other load $\mathbf{P}^*$ lying within or on the LS. Another meaningful interpretation that can be given to $\mathbf{P}^*$ is that it is a candidate applied load which does not violate the slip condition and is not constrained to satisfy equilibrium *a priori*. Then $\mathbf{P}^* \cdot \mathbf{q}$ (the right hand side of inequality 9.1) represents the 'power released' into the system by the candidate load and $\mathbf{P} \cdot \mathbf{q}$ (the left hand side of inequality 9.1) represents the power absorbed by the frictional resistance to the slider's motion. Then inequality 9.1 can be viewed as effectively stating that:

(power absorbed by frictional resistance for a certain motion $\mathbf{q}$ *of the slider)* $\geq$ *(power released by any candidate applied load that does not violate the slip condition, for the same* $\mathbf{q}$*)*

During slip, with motion $\mathbf{q}$ of the slider, the candidate applied load $\mathbf{P}^*$ must satisfy equilibrium, $\mathbf{P}^* = \mathbf{P}$. In doing so, $\mathbf{P}^*$ automatically satisfies power balance, 'power absorbed' = 'power released', or $\mathbf{P} \cdot \mathbf{q} = \mathbf{P}^* \cdot \mathbf{q}$. The ramifications of this can be stated in the form of the following two bound theorems that are complementary to one another. The first one is analogous to the statement of the 'principle of maximum plastic work' (upper bound theorem) and the second one is analogous to the statement of the 'principle of path of least resistance' (lower bound theorem).

Theorem 1 *For a given motion* $\mathbf{q}$ *of the slider, the load* $\mathbf{P}^*$ *satisfies equilibrium only if it is such that the scalar product* $\mathbf{P}^* \cdot \mathbf{q}$ *is maximized over all candidate* $\mathbf{P}^*$ *on or inside the LS.*

Theorem 2 *For a given direction* $\mathbf{n}$ *in load space, the motion vector* $\mathbf{q}$ *that satisfies the constitutive law is that, such that the magnitude of the quantity* $(\mathbf{P} \cdot \mathbf{q})/(\mathbf{n} \cdot \mathbf{q})$ *is minimized, over all possible candidate motions* $\mathbf{q}$*, and* $\mathbf{P}$ *being an associated load with the candidate motion* $\mathbf{q}$*.*

The quantity $P^* = (\mathbf{P} \cdot \mathbf{q})/(\mathbf{n} \cdot \mathbf{q})$ that is being minimized is the load that would be calculated by balance of power, where $P^*\mathbf{n} \cdot \mathbf{q}$= power supplied, and $\mathbf{P} \cdot \mathbf{q}$= power absorbed.

Chapter 10

Velocity Dependent Behaviour Arising From Rate Independent Friction

In an effort to relax the restriction of rate independence that we have imposed on all the friction laws considered so far, in the following presentation, we construct and introduce frictional models that show dependence of friction forces on the slip rate between the slider and the supporting surface, arising from rate independent friction. Some of the models that we introduce can in fact, be used as basic building blocks for obtaining sliders with frictional models depicting the rate independent behaviour that we have considered so far.

10.1 Driven Wheels

For simplicity, we start with a uni-dimensional model of 'driven wheels' with dry friction. Assume that the slider is a line (with a fixed orientation on the supporting surface), for which the only allowable motion is sliding along its length. Also, that it makes contact with the supporting surface through completely ideal wheels fixed with their axes perpendicular to this line slider. These ideal wheels are driven independently by motors (or some other rotary motion source) at all possible speeds V_w, such that $-\infty \leq V_w \leq \infty$.

The normal pressure distribution between the slider and the supporting surface is given as a function $P(V_w)$ of the driven wheel velocities V_w, rather than the location of the wheels, since in this uni-dimensional case the location of the wheels is irrelevant in summing up the frictional force. Also, there is no frictional torque. We can have both point supports (specified as delta functions for $P(V_w)$ and distributed support.

As an illustration, we consider the support pressure distribution $P(V_w)$ between the slider with driven wheels and supporting surface, shown in fig. 32. The coefficient of friction $\mu = 1$, everywhere over the slider. Then the friction force $F(V)$ associated with any speed V of the slider is given as:

$$F(V) = \int_{-\infty}^{V} P(V_w) dV_w - \int_{V}^{\infty} P(V_w) dV_w \tag{10.1}$$

This is because all the driven wheels on the slider, except for the ones with $V_w = V$, are rolling with slip and hence the dry friction force at their point of contact with the supporting surface is known. Also, the driven wheels with $V_w < V$ slip in one direction

while the driven wheels with $V_w > V$ slip in the opposite direction. Hence the total friction forces from both these categories of driven wheels oppose each other.

Applying equation 10.1 to the pressure distribution of fig. 32 gives us that the friction force $F(V)$, as a function of the slider speed V, is the curve of fig. 33. It can be observed that the $F(V)$ is rate dependent and also that it is monotonic.

Now we look at the total power $D(V)$, dissipated to dry frictional forces between the slider and the supporting surface.

$$D(V) = \int_{-\infty}^{V} (V - V_w) P(V_w) dV_w + \int_{V}^{\infty} (V_w - V) P(V_w) dV_w \tag{10.2}$$

$$\begin{aligned} D(V) &= V \int_{-\infty}^{V} P(V_w) dV_w - V \int_{V}^{\infty} P(V_w) dV_w \\ &\quad - \int_{-\infty}^{V} V_w P(V_w) dV_w + \int_{V}^{\infty} V_w P(V_w) dV_w \end{aligned}$$

$$\Rightarrow D(V) = F(V)V - \int_{-\infty}^{V} V_w P(V_w) dV_w + \int_{V}^{\infty} V_w P(V_w) dV_w \tag{10.3}$$

In equation 10.3, the first term on the right represents the power dissipated to the friction force $F(V)$ for moving the slider at speed V; the second term represents the power dissipated by the driving motors that are aided by the dry friction forces; and the third term represents the power dissipated by the driving motors that work against the dry friction forces.

Differentiating equation 10.2 with respect to V (using Leibnitz's rule), we get:

$$\frac{\partial D(V)}{\partial V} = \int_{-\infty}^{V} \frac{\partial (V - V_w) P(V_w)}{\partial V} dV_w + \int_{V}^{\infty} \frac{\partial (V_w - V) P(V_w)}{\partial V} dV_w$$

$$\Rightarrow \frac{\partial D(V)}{\partial V} = F(V) \tag{10.4}$$

Equation 10.4 states that the gradient of the dissipation function gives the friction force, analogous to the normality property of the limit surface. For the pressure distribution of fig. 32, the dissipation function $D(V)$ is given by the curve of fig. 34. Observe that D(V) is a convex curve, which is kind of analogous to the convexity of the limit surface.

10.2 Driven Wheels With Continuous Distribution Of Mounted Ideal Wheels On Their Rim

To add dimensionality to the above model, and to give orientational properties to driven wheels (through which the slider makes contact with the supporting surface), we add to these wheels a continuous distribution of massless ideal wheels (not driven) mounted on their rims as shown schematically in fig. 35. For motion along the axis of this driven wheel, the mounted ideal wheels begin to roll and hence there is zero corresponding friction force. These wheels form the building blocks, from which all sliders with ideal wheels considered earlier, can be replicated.

10.3 Driven Wheels With Continuous Distribution Of Mounted Ratcheted Wheels On Their Rim

This model is similar to the one described above, except that the driven wheel now has a continuous distribution of massless ratcheted wheels (not driven) mounted on their rims as shown in fig. 35. All the mounted ratcheted wheels roll freely along one direction of lateral motion of the driven wheel (on which they are mounted) and lock for lateral motion along the opposite direction.

Chapter 11

Conclusions

Some of the main conclusions of this work are enumerated as follows:

1. For sliders whose microscopic frictional interaction with the supporting surface is governed by the maximum work inequality 3.1 (which generalizes Coulomb friction to include contact with wheels and skates), their frictional load and the associated motion relationship is completely characterized by a closed, convex surface in load space, called the limit surface. The LS gives us a geometrical tool for visualizing and reasoning about the overall frictional load and motion relation for the slider.
2. For isotropic friction, the LS can be completely characterized by the moment surface (moment of the frictional forces about the COR, plotted on the plane of CORs).
3. The limit surfaces for sliders with a known friction law and normal pressure distribution can be constructed through simple methods.
4. For sliders with isotropic friction, their moment surfaces can be constructed through simple means too.
5. Vertices (non-unique motion associated with the load on the vertex) and flat regions (non-unique load associated with the corresponding motion) on the overall LS for the slider, stem from vertices and flat regions on the individual limit surfaces for each point of support for the slider.
6. Limit surfaces for sliders with isotropic friction have certain symmetries. In addition, flat regions appear on them only due to point supports and vertices are caused only by collinear support. These singularities on the LS correspond to singularities on the MS. A vertex on the LS corresponds to a flat region on the MS and a flat region on the LS corresponds to a vertex on the MS.
7. The motion of the slider at onset of slip due to an externally applied load is unique if both inertial and frictional loads are considered (a direct consequence of the load motion inequality 4.2).
8. The final motion of the sliders during free sliding is always along special directions called eigen directions; the stability of these eigen directions depends on the principal radii of curvature of the LS at that point.
9. The stability of an eigen direction as determined from the near zero velocity analysis during free sliding may be altered, by finite velocities.

10. The eigen directions for a given slider can be altered by changing its radius of gyration (changing the mass distribution), while leaving the given normal pressure distribution unaffected.
11. For sliders with axisymmetric pressure distributions and limit surfaces, the final motion is a pure 'rolling like' motion on a tangent line to a circle (with its center at the center of the slider) of some radius. Inner and outer bounds exist on the radius of gyration of these sliders beyond which their final motion is a pure translation or a rotation about their center, respectively.
12. Sliders with isotropic friction have a propensity to rotate about points of support.

11.1 Possible Directions For Future Work

The basic framework developed so far for looking at the overall frictional load motion relationship could be extended to address many more issues, some of which are stated below.

1. Understanding the load motion relationship for cases where some components of load are prescribed and some of motion, in terms of the load motion inequality 4.2.
2. Formulating the load motion relation and limit surfaces for sliders moving in contact (hinged to one another or slipping against each other). This would relate directly to manipulation problems in robotics.
3. Allowing the normal loads to vary.
4. Incorporating rate dependent friction models such as those of driven wheels.
5. Experimental verification of results.

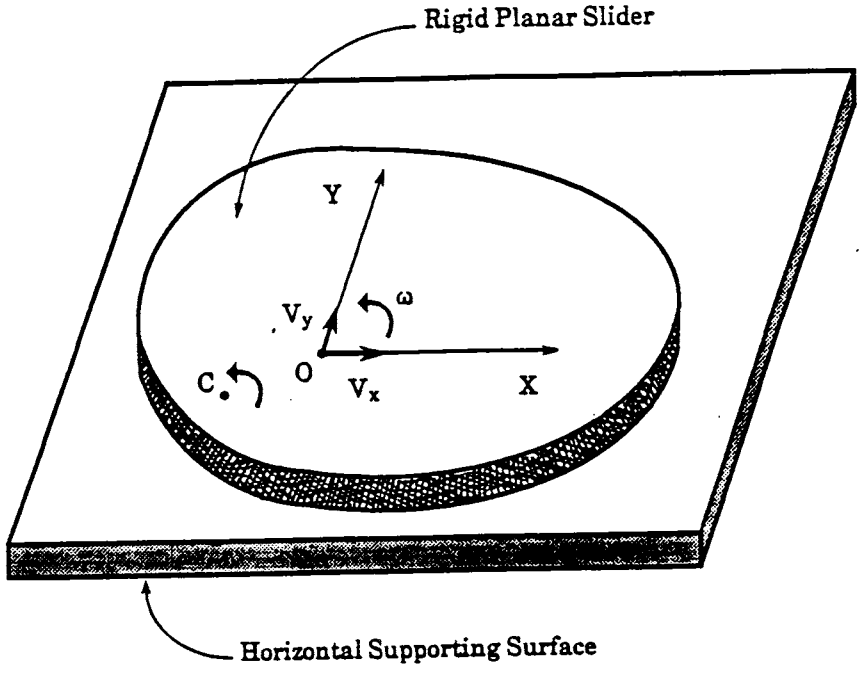

Figure 1: Pictorial View of a Rigid Planar Slider on a Supporting Surface, With Slider Fixed Axes

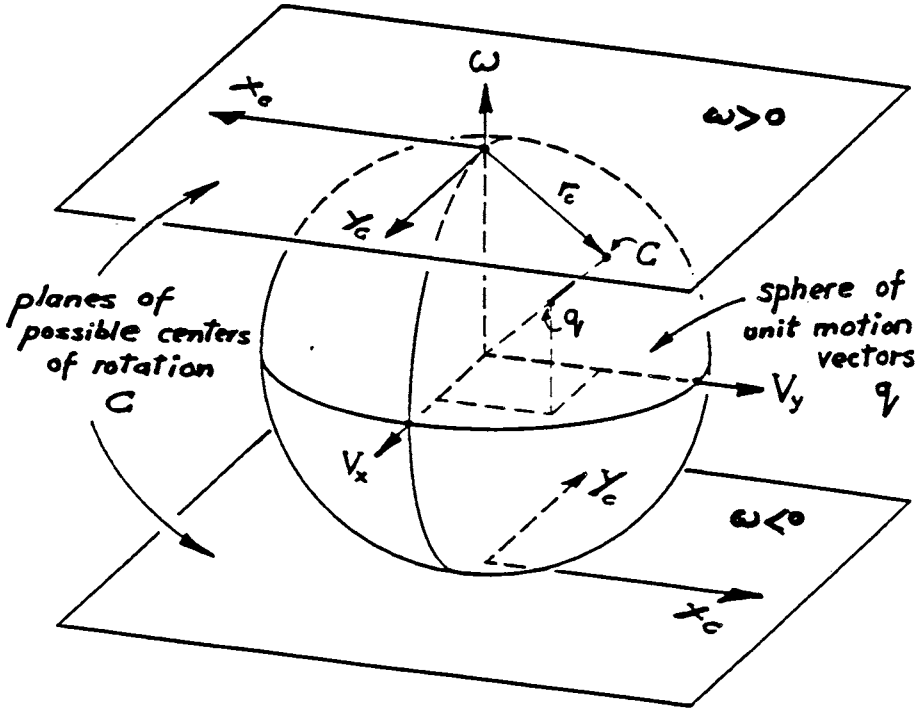

Figure 2: Geometrical Projection Relating Motion Space And The Plane of CORs

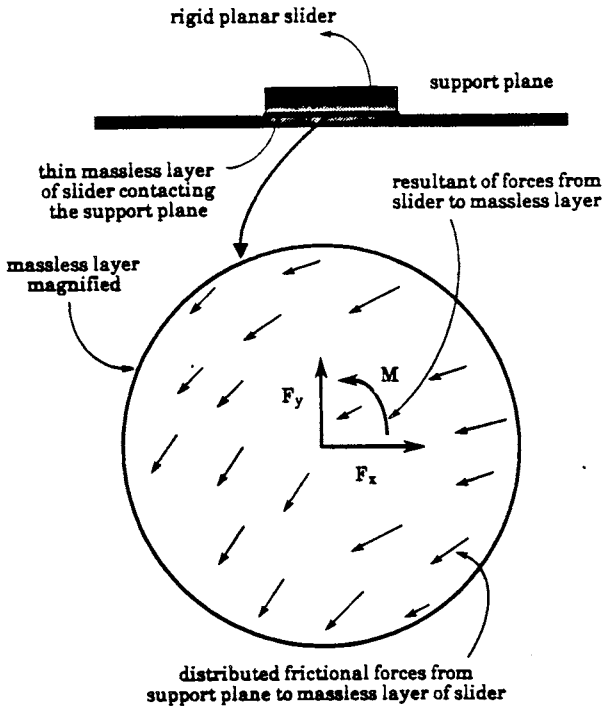

Figure 3: Massless Layer at Interface of Rigid Slider And Supporting Surface

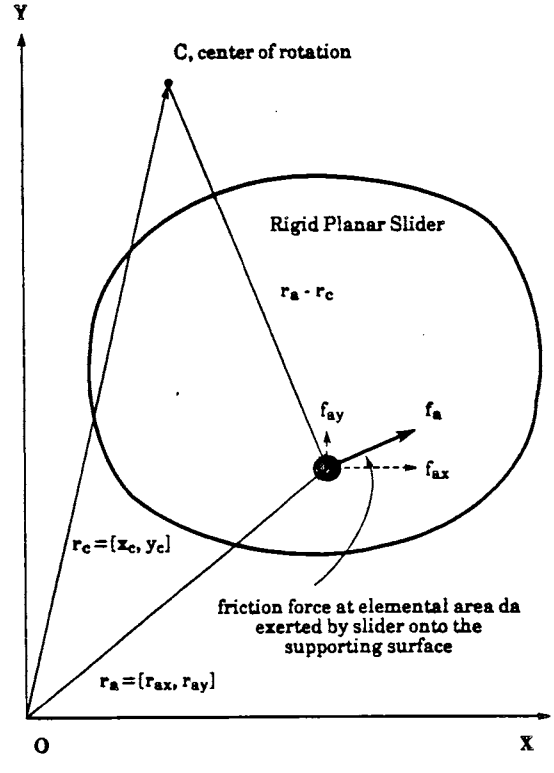

Figure 4: Elemental Frictional Forces on a Rigid Slider

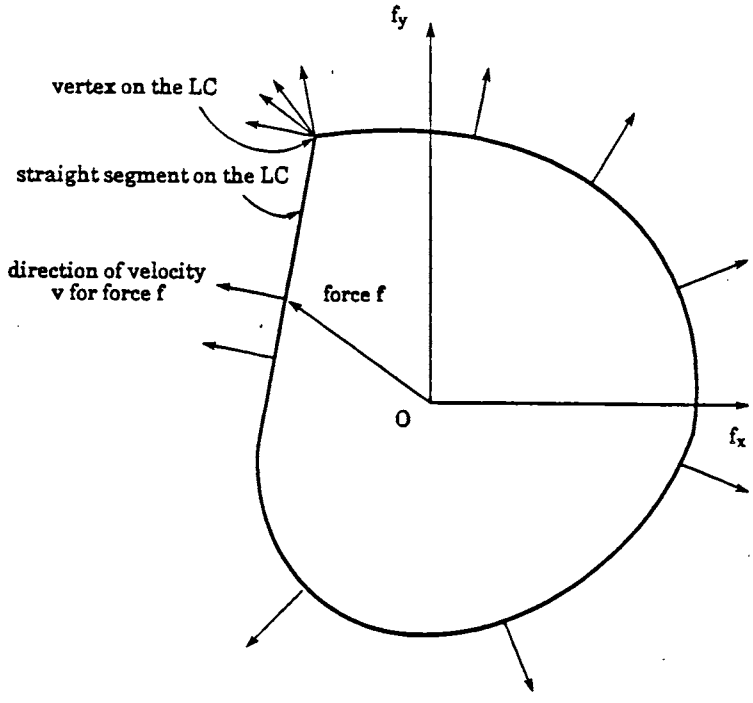

Figure 5: Schematic Of An Acceptable Friction Law

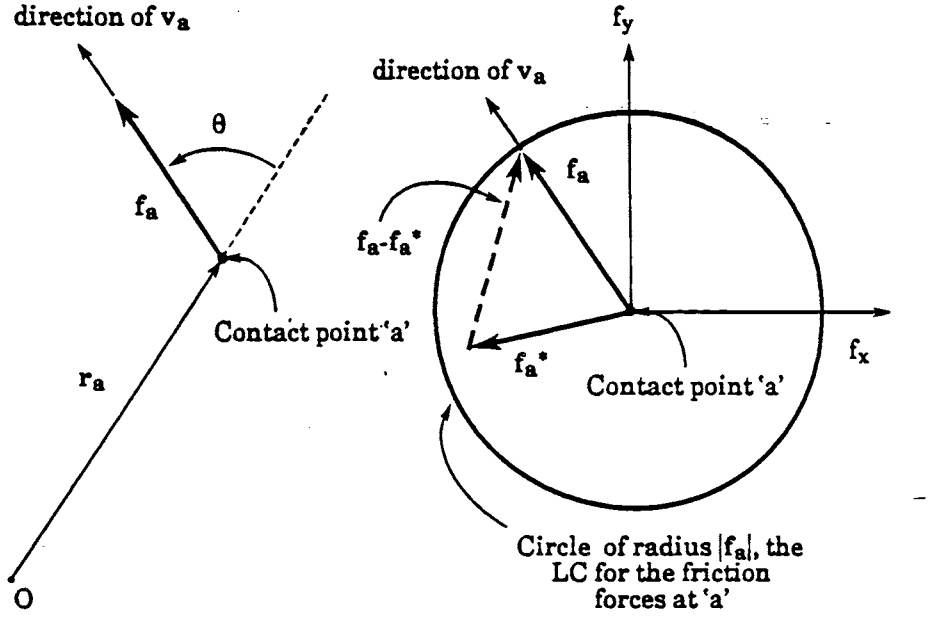

Figure 6: LC For Coulomb Friction

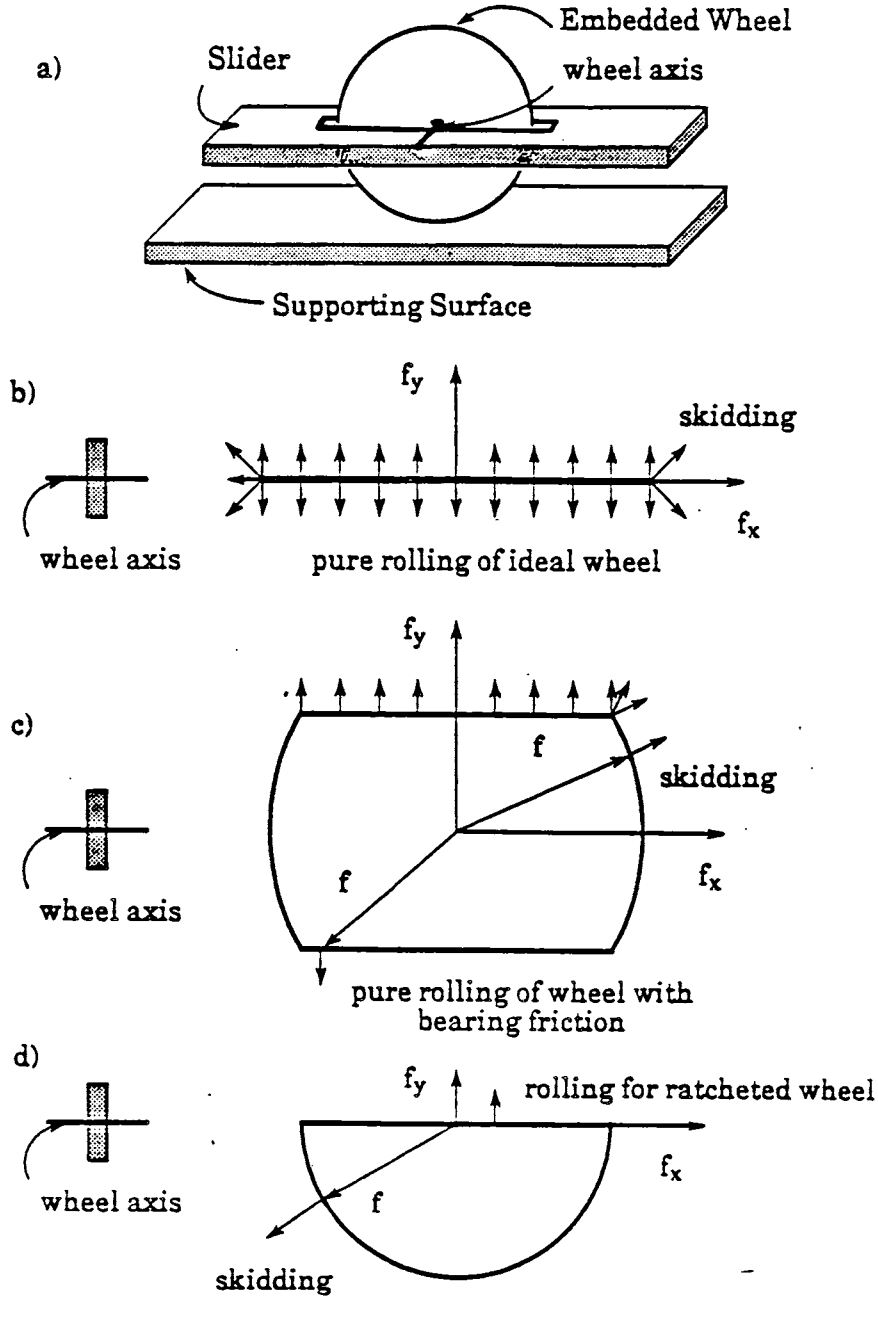

Figure 7: Rigid Slider With Embedded Wheel And Corresponding Limit Curves

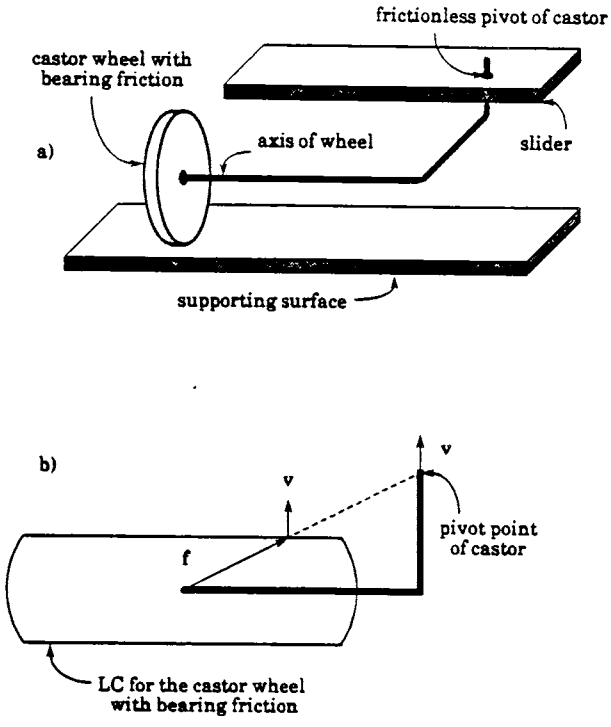

Figure 8: Frictional Contact Between Slider And Supporting Surface Mediated By Castor Wheels, That Does Not Obey Normality

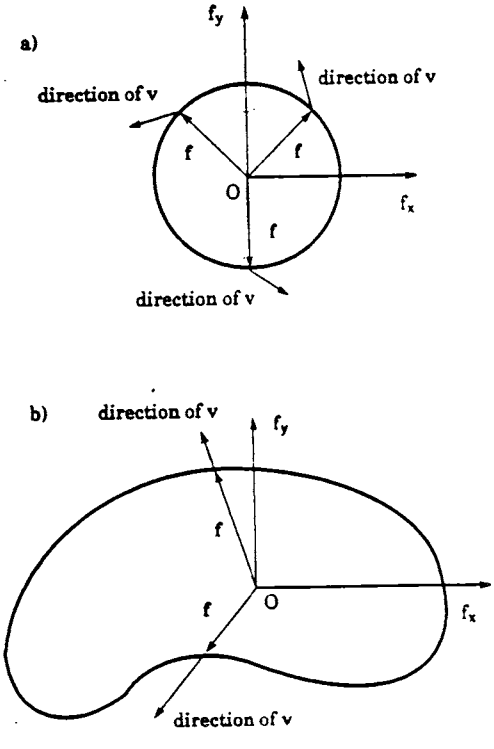

Figure 9: Friction Laws That Do Not Obey The 'Maximum Work Inequality'

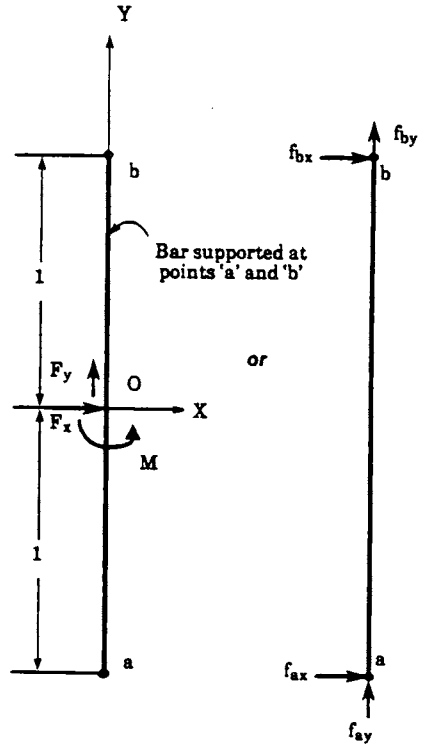

Figure 10: Unidimensional Bar Supported At Its Ends

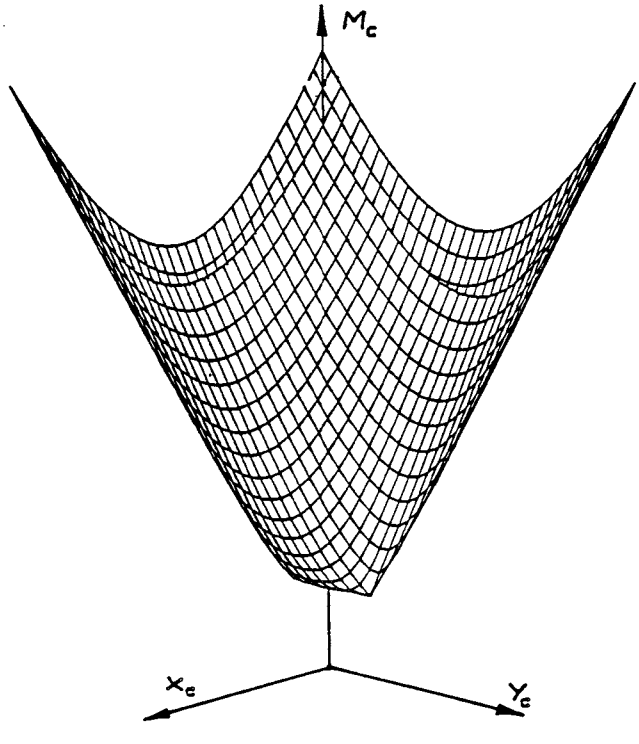

Figure 11: MS For Bar Supported Symmetrically With Coulomb Friction At Its Ends

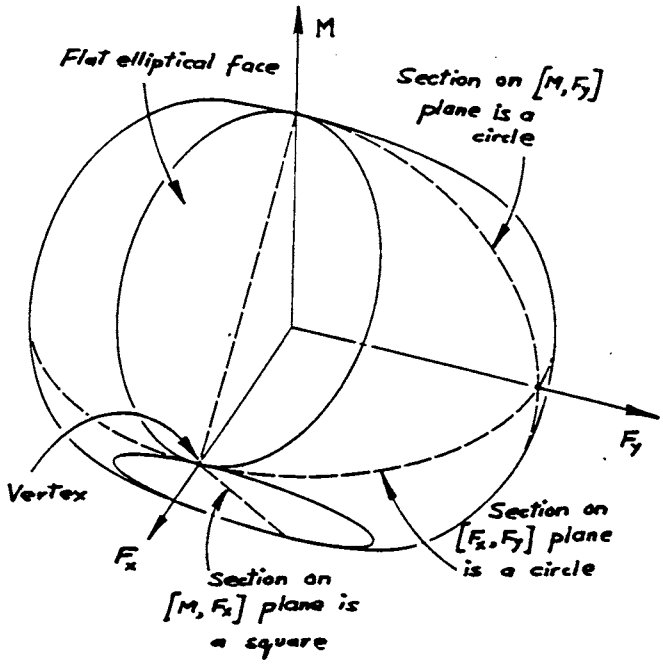

Figure 12: LS For Bar Supported Symmetrically With Coulomb Friction At Its Ends

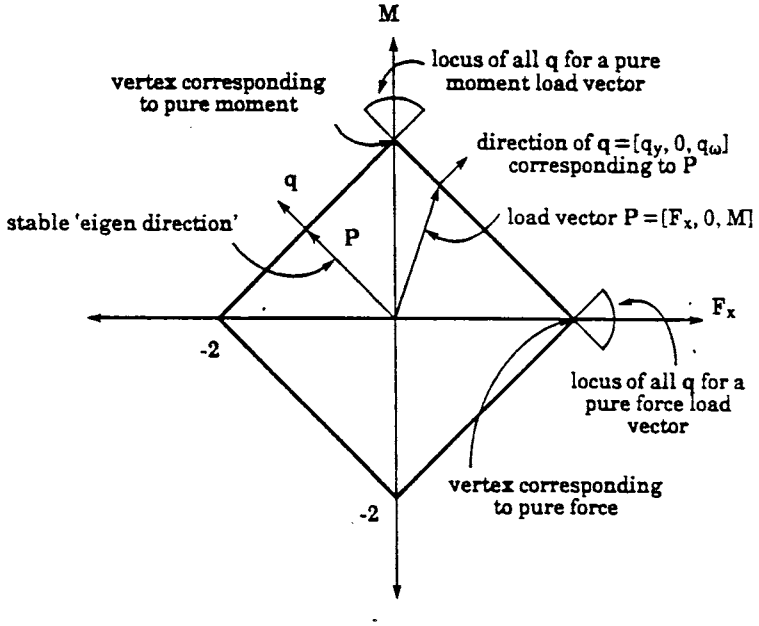

Figure 13: Section Of LS For The Bar Supported Symmetrically With Coulomb Friction At Its Ends On The $[F_x, M]$ Plane

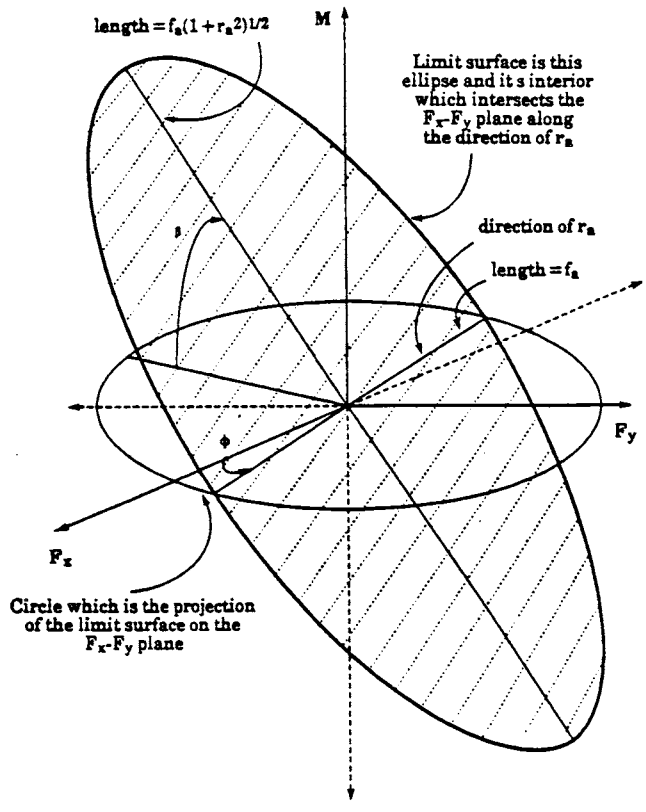

Figure 14: Individual LS (Planar Ellipse) For One Point Of Isotropic Support

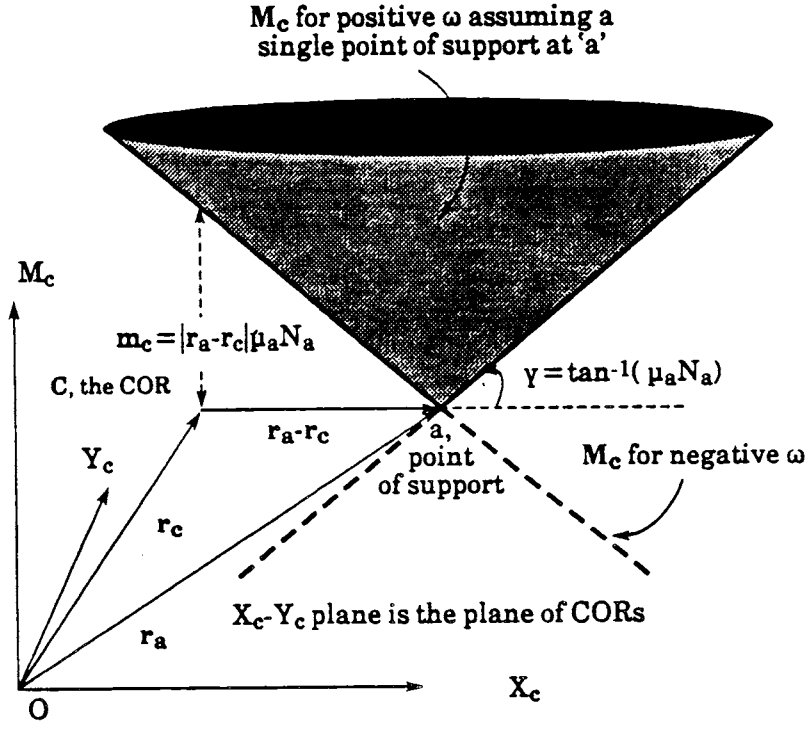

Figure 15: MS For One Point Of Isotropic Support

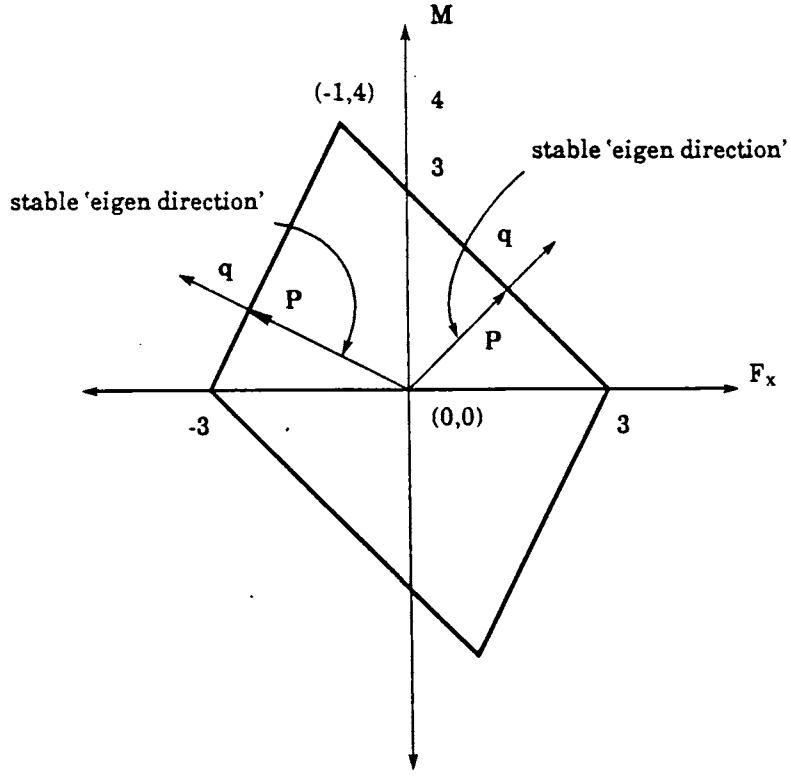

Figure 16: Section Of LS For Bar Supported Asymmetrically With Coulomb Friction At Its Ends, On The $[F_x, M]$ Plane

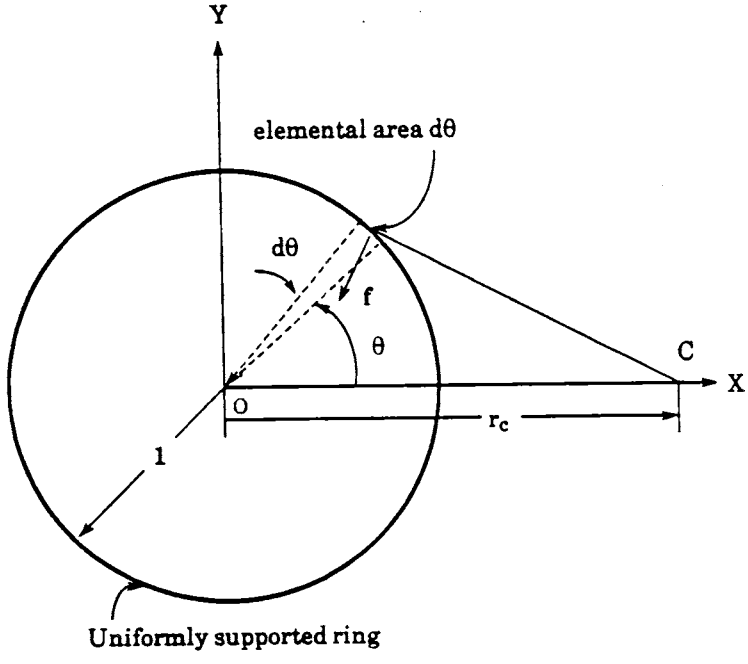

Figure 17: Elemental Friction Forces On Uniformly Supported Thin Ring (Unit Radius) With Isotropic Friction

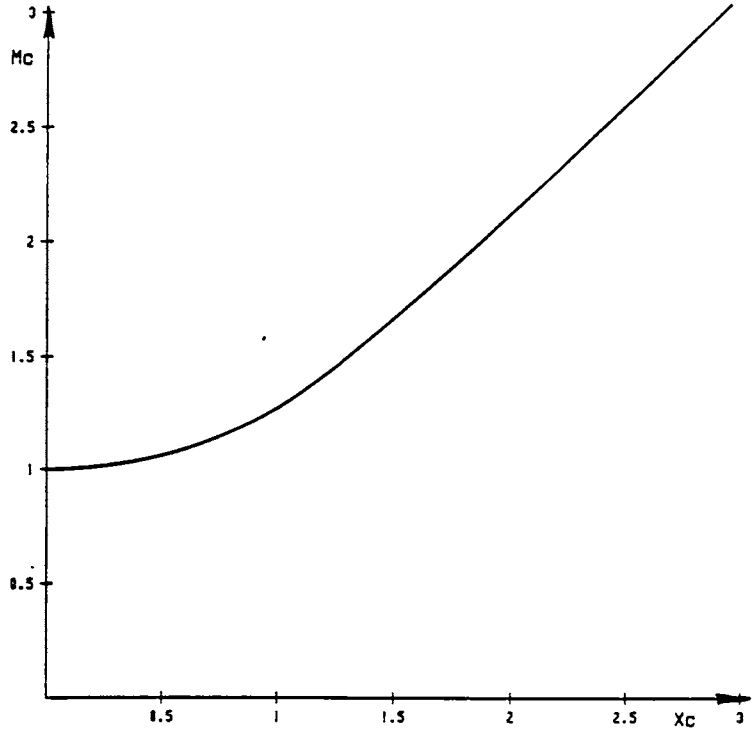

Figure 18: Partial Generating Curve For MS For Thin Ring Of Isotropic Friction

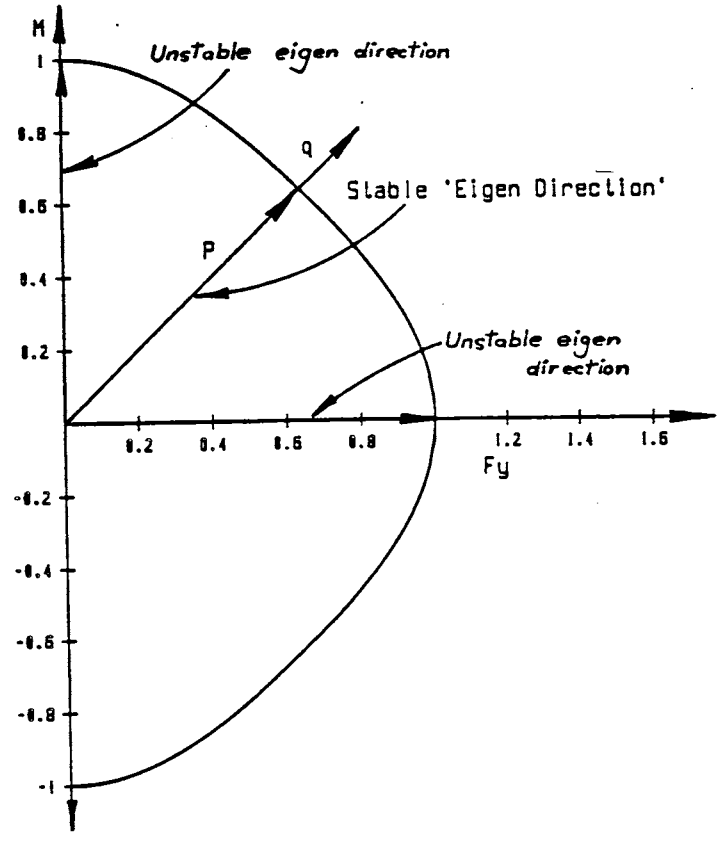

Figure 19: Generating Curve For LS For Thin Ring Of Isotropic Friction

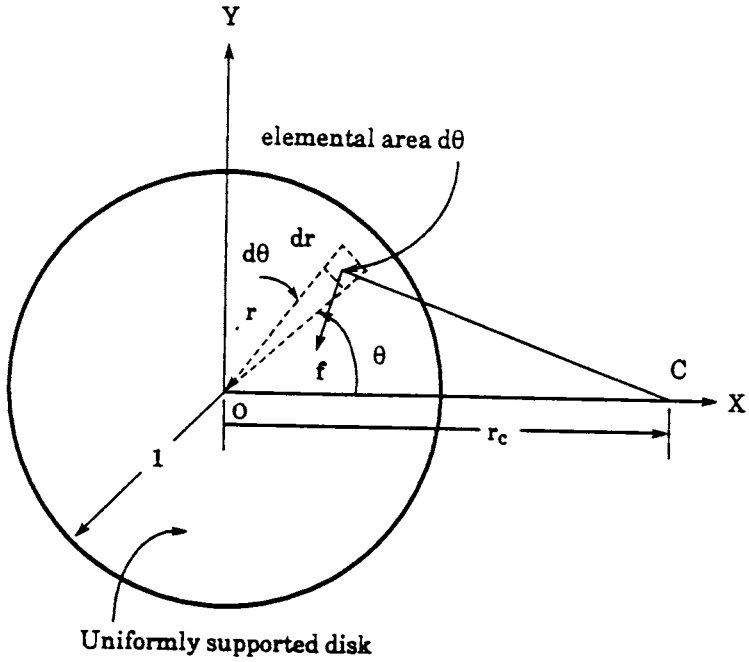

Figure 20: Elemental Friction Forces On Uniformly Supported Disk (Unit Radius) With Isotropic Friction

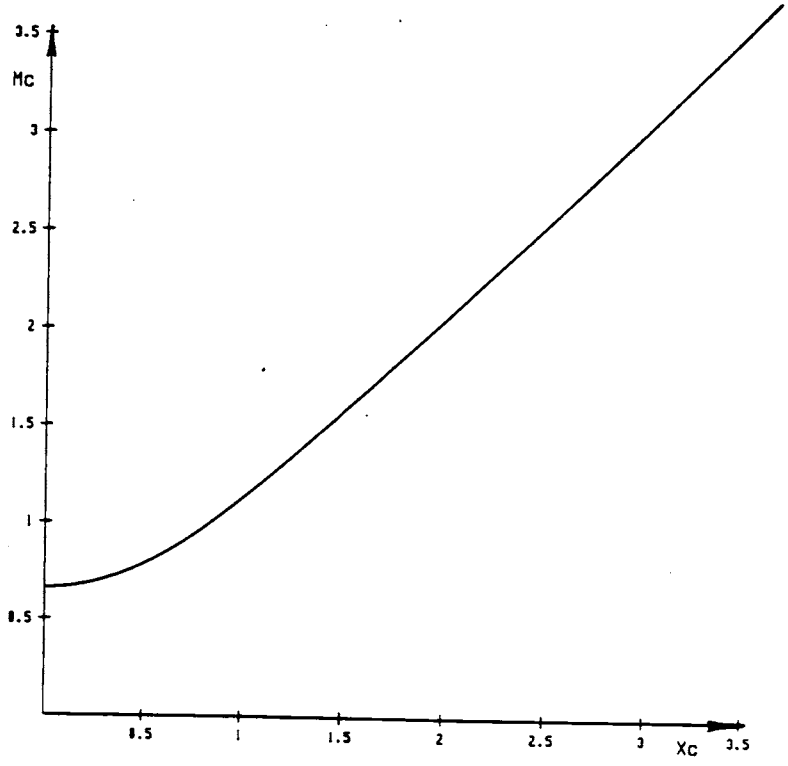

Figure 21: Partial Generating Curve For MS For Disk Of Isotropic Friction

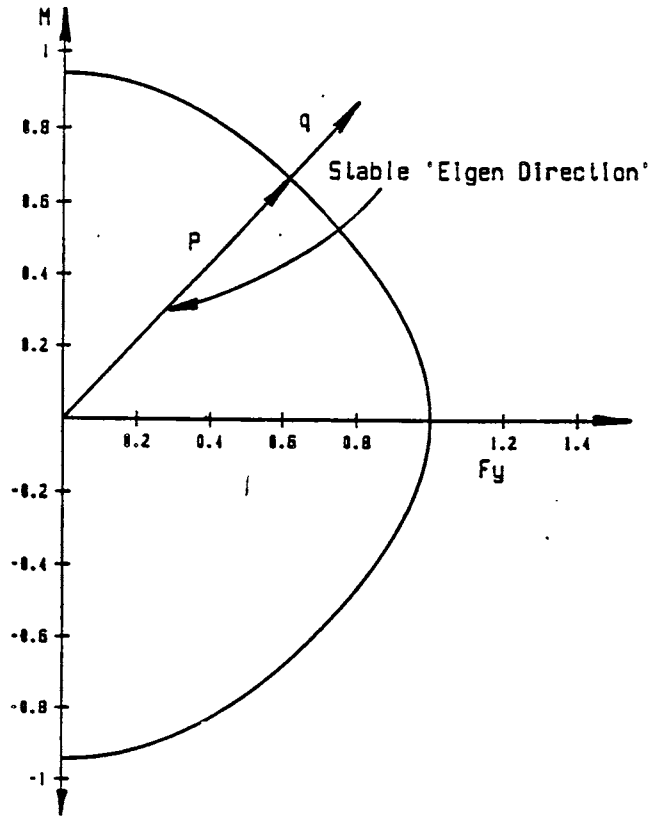

Figure 22: Generating Curve For LS For Disk Of Isotropic Friction

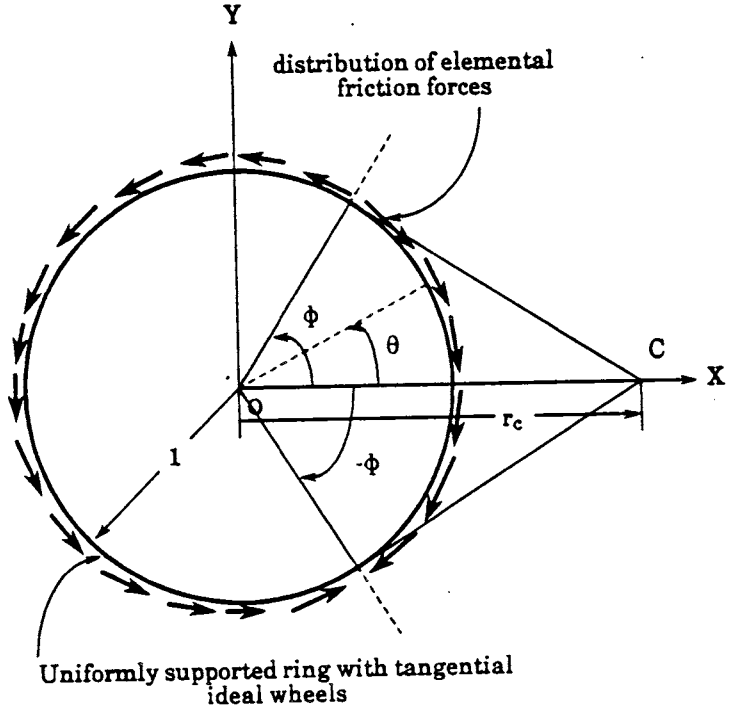

Figure 23: Distribution Of Elemental Frictional Forces For Uniformly Supported Ring With Tangential Ideal Wheels For $r_c > 1$

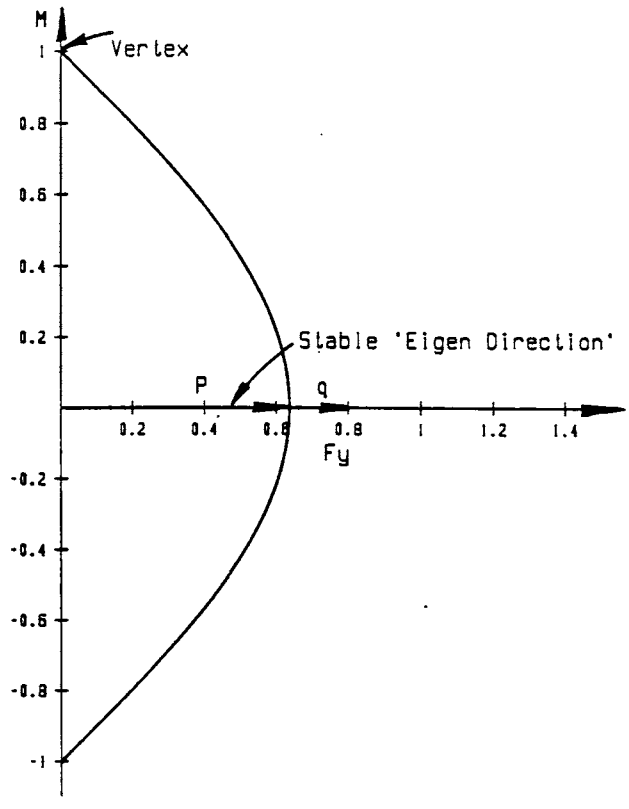

Figure 24: LS For Uniformly Supported Ring With Tangential Ideal Wheels

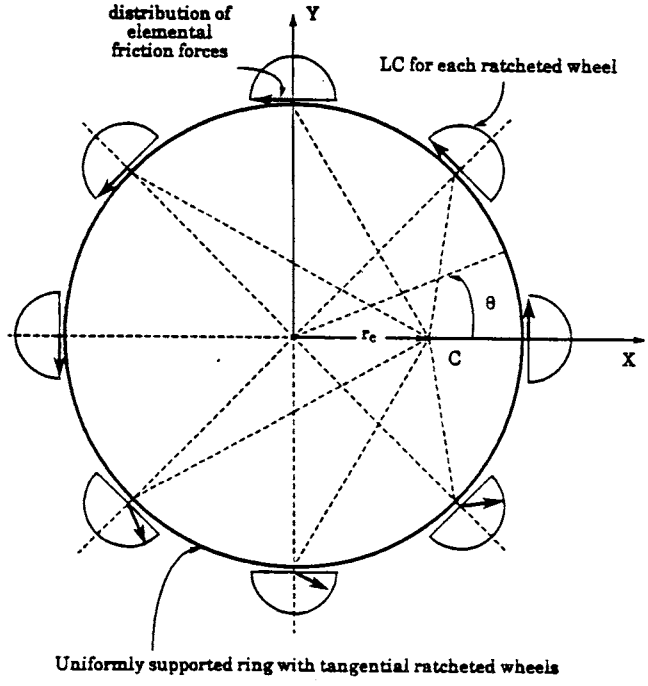

Figure 25: Distribution Of Elemental Frictional Forces For Uniformly Supported Ring With Tangential Ratcheted Wheels For $0 \leq r_c < 1$

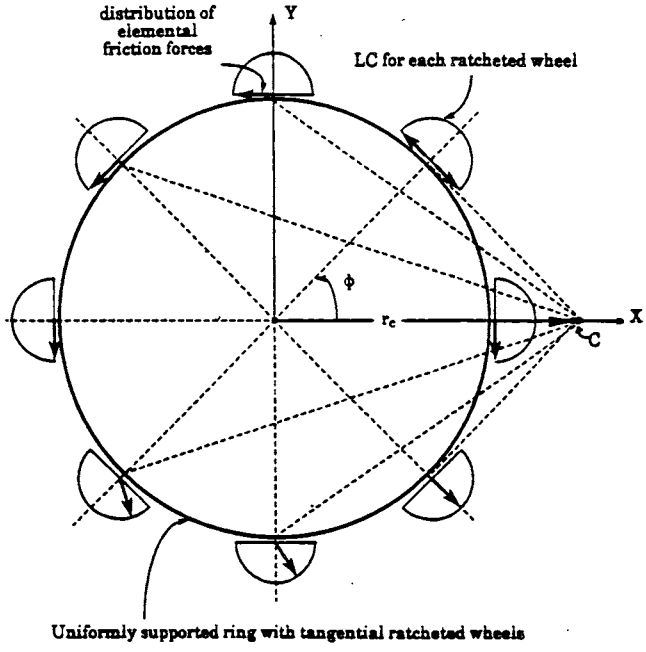

Figure 26: Distribution Of Elemental Frictional Forces For Uniformly Supported Ring With Tangential Ratcheted Wheels For $r_c \geq 1$

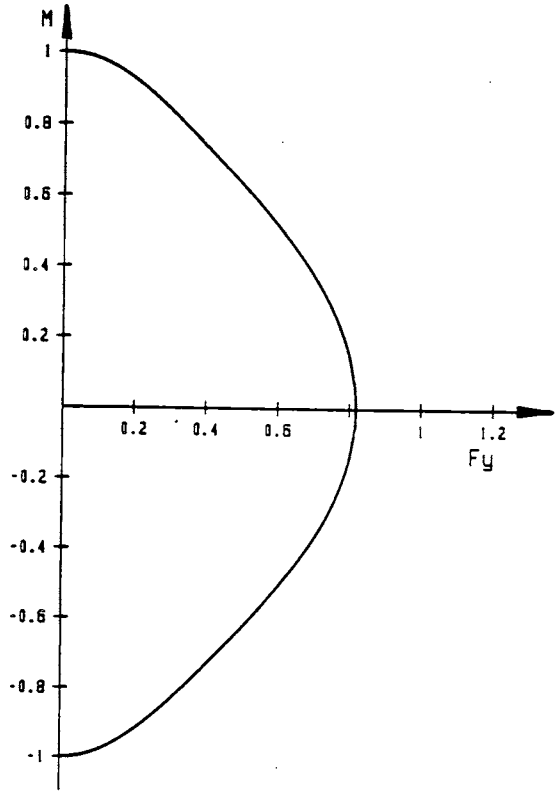

Figure 27: LS For Uniformly Supported Ring With Tangential Ratcheted Wheels

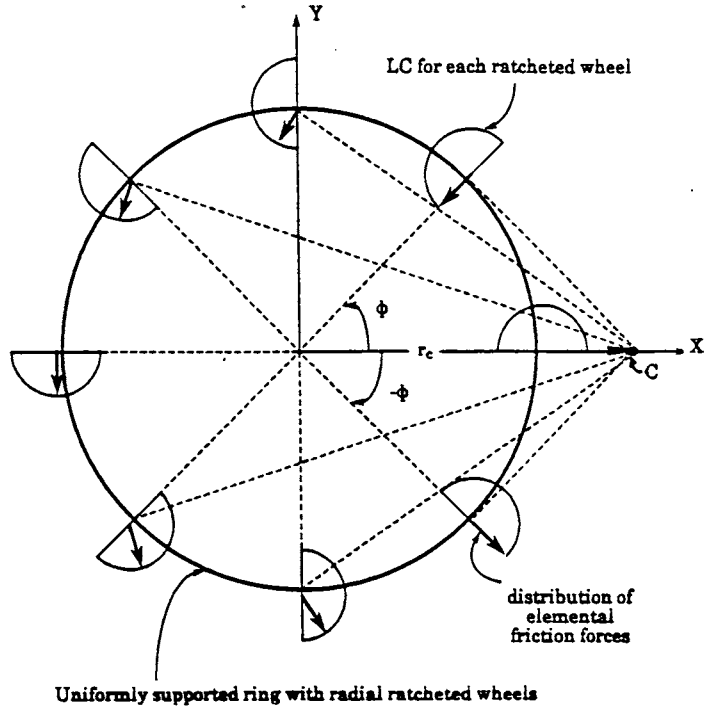

Figure 28: Distribution Of Elemental Frictional Forces For Uniformly Supported Ring With Radial Ratcheted Wheels For $r_c \geq 1$ and $\omega > 0$

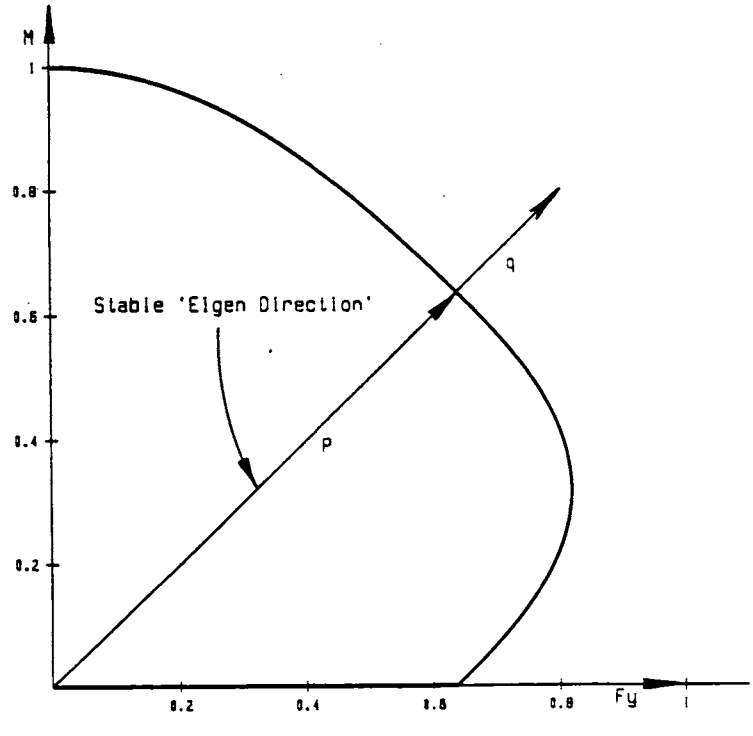

Figure 29: LS For Uniformly Supported Ring With Radial Ratcheted Wheels

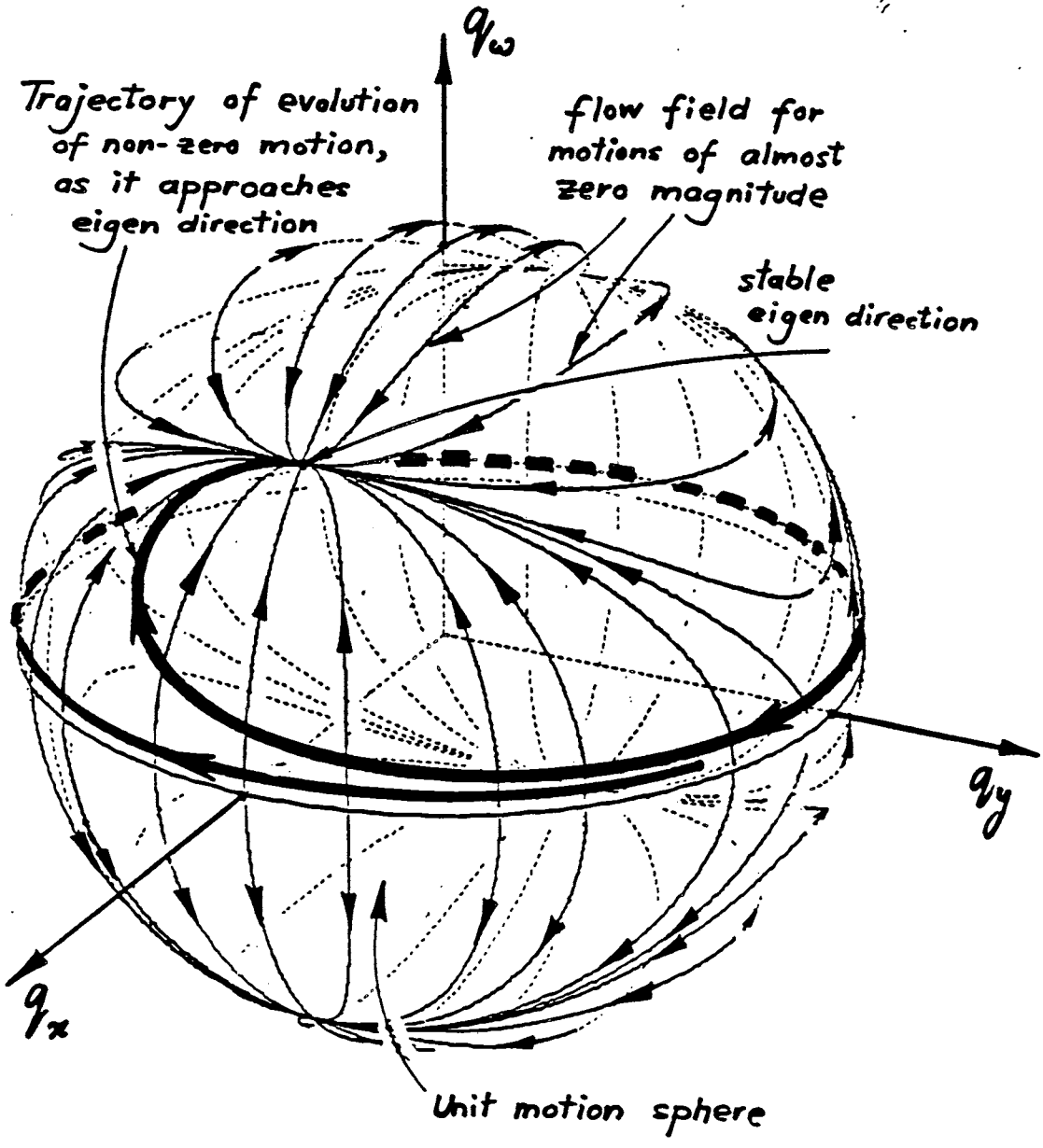

Figure 30: Results Of Numerical Simulation Of 'Free Sliding' Of Bar Supported Symmetrically At Its Ends with Coulomb Friction, As Depicted On The Unit Motion Sphere (Slider Fixed Axes System)

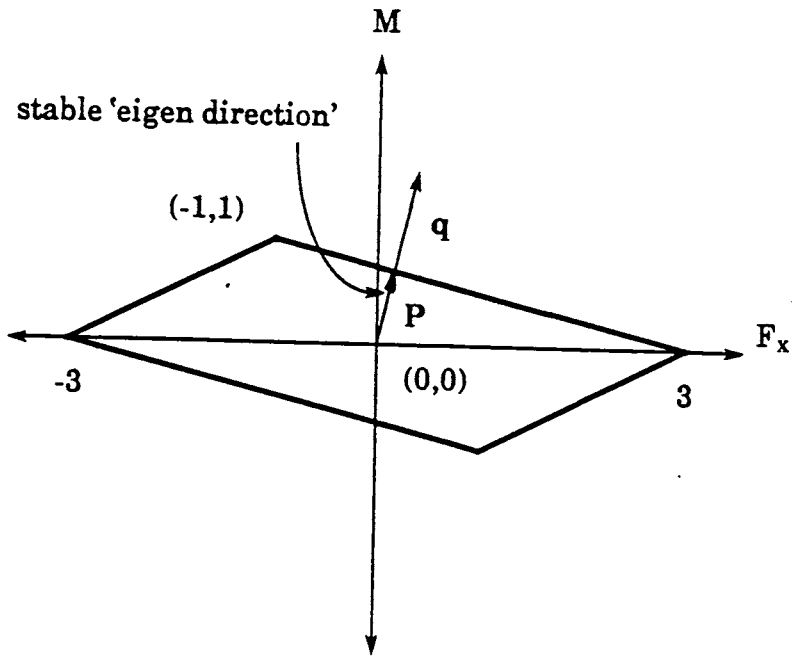

Figure 31: Section Of LS On $[F_x, M]$ Plane For The Bar Supported Asymmetrically At Its Ends And $\rho_g = 4$.

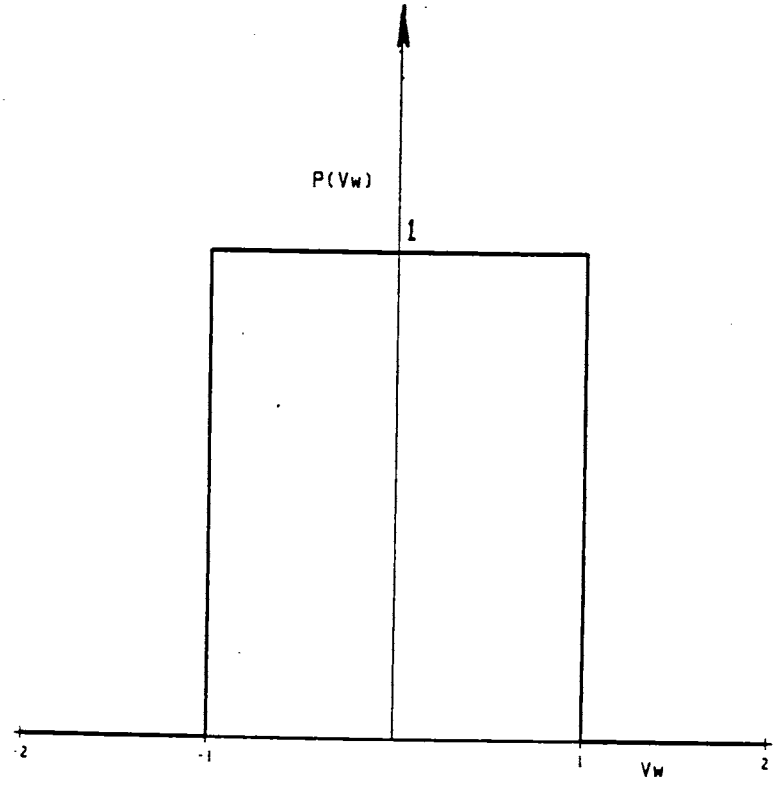

Figure 32: Normal Pressure Distribution Between Uni-Dimensional Slider With Driven Wheels, And Supporting Surface

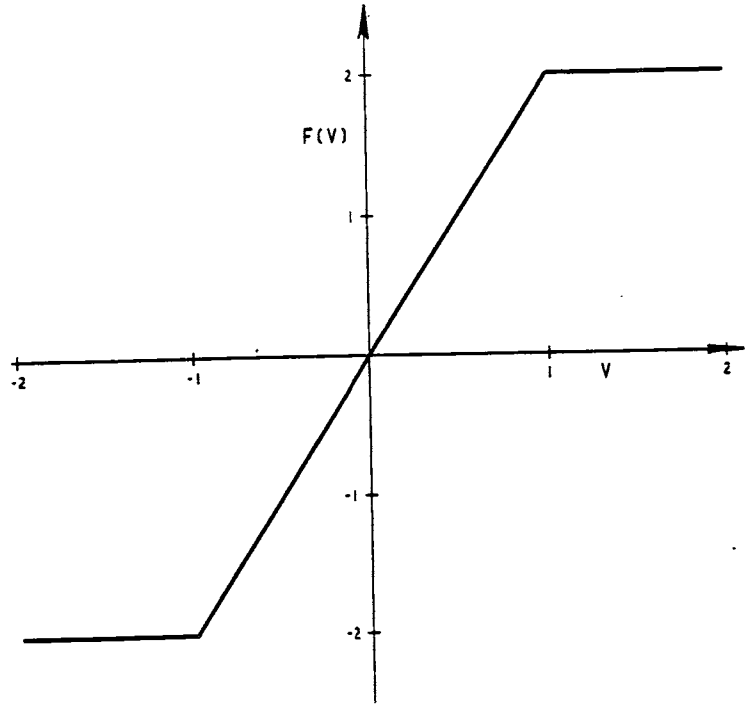

Figure 33: Friction Force As A Function Of Slider Speed For Uni-Dimensional Slider With Driven Wheels

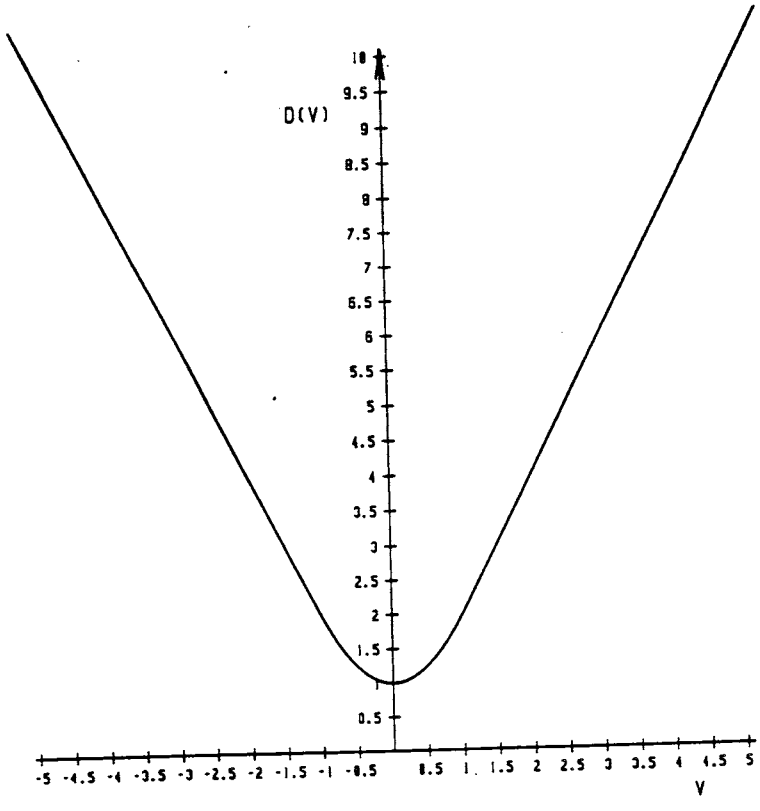

Figure 34: Dissipation Function For The Given Uni-Dimensional Slider With Driven Wheels

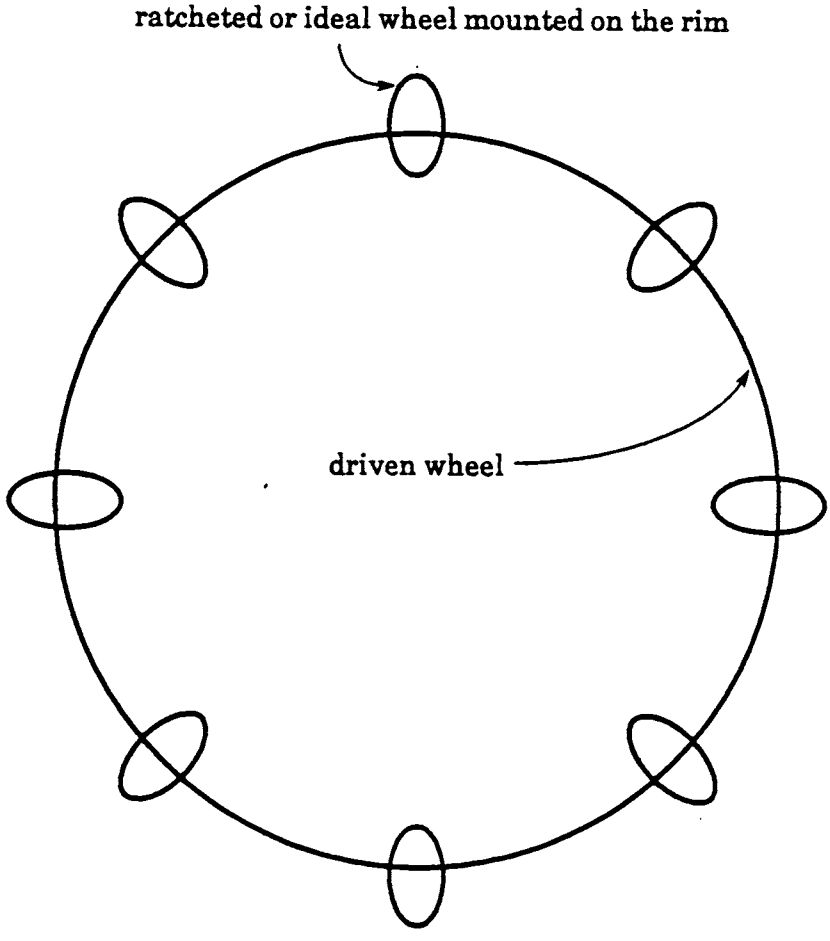

Figure 35: Driven Wheel With Continuous Distribution Of Mounted Wheels On Its Rim

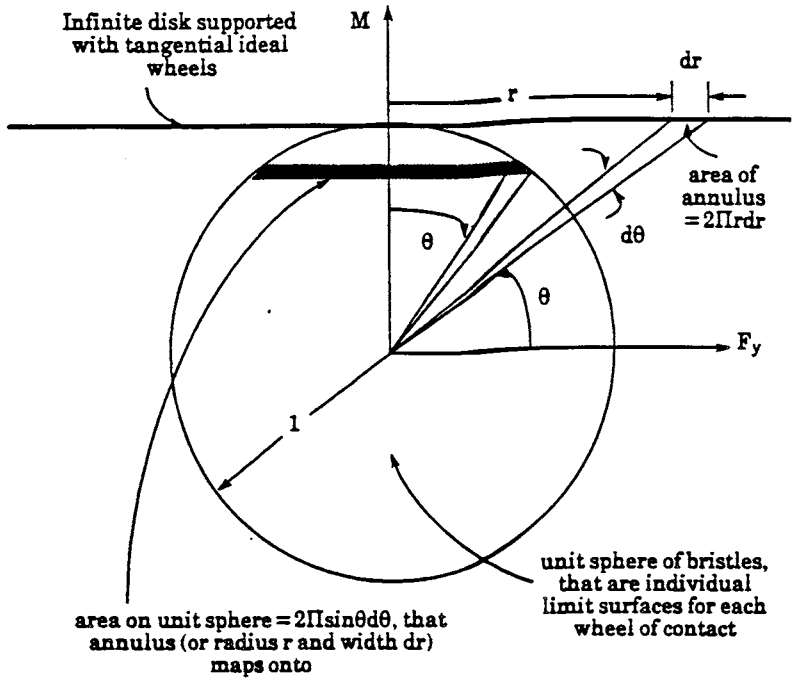

Figure 36: Pressure Distribution Leading To Spherical LS

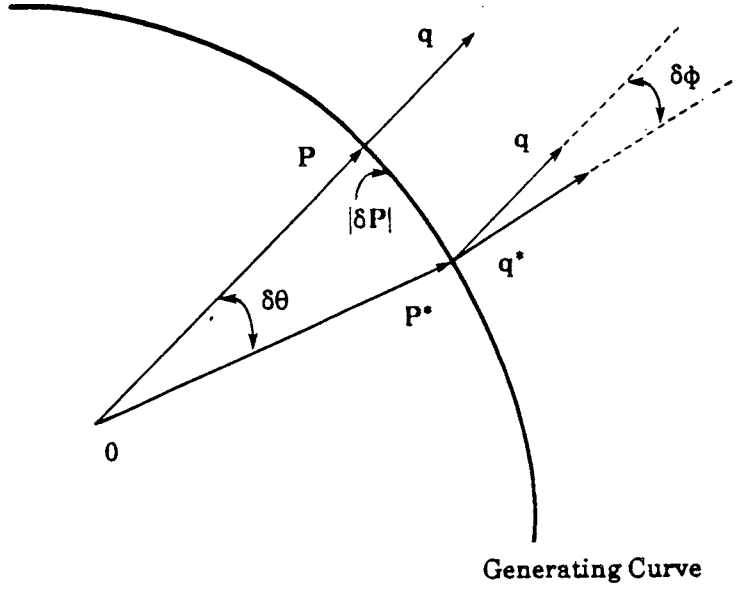

Figure 37: 'Eigen Direction' And Perturbed Motion On Generating Curve

Appendix A

A.1 Relation Between Motion Vector And COR

Referring back to figs. 1 and 2, and from the definition of the motion vector q, we have:

$$\mathbf{q} = \frac{\mathbf{Q}}{|\mathbf{Q}|} = \left[\frac{V_x}{(V_x^2+V_y^2+\omega^2)^{\frac{1}{2}}}, \frac{V_y}{(V_x^2+V_y^2+\omega^2)^{\frac{1}{2}}}, \frac{\omega}{(V_x^2+V_y^2+\omega^2)^{\frac{1}{2}}}\right]$$

From the definition of the COR, we get:

$$\mathbf{V} = \omega \times (-\mathbf{r_c})$$

or

$$\mathbf{r_c} = [x_c, y_c] = \left[\frac{-V_y}{\omega}, \frac{V_x}{\omega}\right] = \left[\frac{-q_y}{q_\omega}, \frac{q_x}{q_\omega}\right]$$

The above is the algebraic relation between $\mathbf{q}$ and $\mathbf{r_c}$, which is also obtained by using the properties of similar triangles on the construction of fig. 2.

Hence the set of all possible CORs, $C \in (\Re^2 \times \{+,-\}) \bigcup S^1$ and the motion vectors $\mathbf{q} \in S^2$ are related:

$$(\Re^2 \times \{+,-\}) \bigcup S^1 \leftrightarrow S^2.$$

A.2 Normal Vector To LS Obtained From Moment Function

We show here that the unit normal to the LS at a point $\mathbf{P}(x_c, y_c)$, obtained through equation 4.4, is indeed the motion vector q associated with $\mathbf{P}(x_c, y_c)$. The motion vector $\mathbf{q} = [q_x, q_y, q_\omega]$ corresponding to any COR positioned at $\mathbf{r_c} = [x_c, y_c]$ and a positive sense of rotation is given by:

$$\mathbf{q} = [\frac{y_c}{(x_c^2+y_c^2+1)^{\frac{1}{2}}}, \frac{-x_c}{(x_c^2+y_c^2+1)^{\frac{1}{2}}}, \frac{1}{(x_c^2+y_c^2+1)^{\frac{1}{2}}}]$$

From differential geometry, we have that the normal vector $\mathbf{N}$, at a point $\mathbf{P}(x_c, y_c) = [F_x(x_c, y_c), F_x(x_c, y_c), M(x_c, y_c)]$, on a parametric surface, is given by:

$$\mathbf{N} = [(\frac{\partial F_y}{\partial x_c}\frac{\partial M}{\partial y_c} - \frac{\partial F_y}{\partial y_c}\frac{\partial M}{\partial x_c}), (\frac{\partial M}{\partial x_c}\frac{\partial F_x}{\partial y_c} - \frac{\partial M}{\partial y_c}\frac{\partial F_x}{\partial x_c}), (\frac{\partial F_x}{\partial x_c}\frac{\partial F_y}{\partial y_c} - \frac{\partial F_x}{\partial y_c}\frac{\partial F_y}{\partial x_c})]$$

$$\Rightarrow \mathbf{N} = \left(\frac{\partial^2 M_c}{\partial y_c^2}\frac{\partial^2 M_c}{\partial y_c^2} - \frac{\partial^2 M_c}{\partial x_c y_c}\frac{\partial^2 M_c}{\partial x_c y_c}\right)[y_c, -x_c, 1]$$

$$\Rightarrow \mathbf{q} = \frac{\mathbf{N}}{|\mathbf{N}|} = \left[\frac{y_c}{(x_c^2+y_c^2+1)^{\frac{1}{2}}}, \frac{-x_c}{(x_c^2+y_c^2+1)^{\frac{1}{2}}}, \frac{1}{(x_c^2+y_c^2+1)^{\frac{1}{2}}}\right]$$

This shows that the unit normal $\mathbf{q}$, at a point $\mathrm{P}(x_c, y_c)$ on the LS obtained through equation 4.4, is the motion vector associated with the COR at $\mathbf{r_c} = [x_c, y_c]$.

A.3 LS For Point Of Isotropic Support Is An Ellipse

We show here (by a simple transformation of coordinates using Euler angles) that the LS obtained for one point of isotropic support (fig. 14) is a planar ellipse. This LS, it may be recollected, is constructed by mapping the frictional force $\mathbf{f_a}$ at the contact point 'a' corresponding to any direction of slip velocity $\mathbf{v_a}$ at 'a' to an equipollent load vector $\mathrm{p_a}$ at O. If the angle made by $\mathbf{r_a}$ with the X-axis is Φ, and the Euler angles [Meirovitch 1970] given as: precession=Φ, nutation=β, and spin=0. Then a transformation matrix $\underline{\mathrm{R}}$ can be obtained as:

$$\underline{\mathrm{R}} = \begin{bmatrix} \cos\Phi & \sin\Phi & 0 \\ -\sin\Phi\cos\beta & \cos\Phi\cos\beta & \sin\beta \\ \sin\Phi\sin\beta & -\cos\Phi\cos\beta & \cos\beta \end{bmatrix}$$

Load $\mathbf{P}$ on the LS that is obtained as a mapping of the friction force $\mathbf{f_a}$ that makes an angle θ with $\mathbf{r_a}$ at 'a' is given as:

$$\mathbf{P} = \begin{bmatrix} f_a\cos(\theta+\Phi) \\ f_a\sin(\theta+\Phi) \\ r_a f_a \sin\theta \end{bmatrix}$$

Now

$$\mathbf{P^R} = \underline{\mathrm{R}}\mathbf{P} = \begin{bmatrix} f_a\cos\theta \\ f_a(1+r_a^2)^{\frac{1}{2}}\sin\theta \\ 0 \end{bmatrix}$$

The coordinates of $\mathbf{P^R}$ as obtained above are the parametric equations of an ellipse in a plane, with its two semi-axes being f_a and $f_a(1+r_a^2)^{\frac{1}{2}}$, parameter θ, which proves that our LS of fig. 14 is an ellipse.

A.4 LS For Ring Of Isotropic Support As Elliptic Integrals

As also shown by Ishlinskii et al. [1980], equation 7.8 (parameterizing the LS for the uniformly supported ring of isotropic friction) can be obtained in the form of elliptic integrals, by rewriting the expressions for $F_y(r_c)$ and $M(r_c)$ as follows, and by using the formulae in Gradshteyn [1980].

$$F_y(r_c) = \frac{1}{\Pi}\int_0^{\Pi} \frac{\cos\theta - r_c}{\sqrt{1+r_c^2-2r_c\cos\theta}}d\theta$$

$$\Rightarrow F_y(r_c) = -\frac{1}{2\Pi r_c}\int_0^{\Pi}\sqrt{1+r_c^2-2r_c\cos\theta}\,d\theta + \frac{1-r_c^2}{2\Pi r_c}\int_0^{\Pi}\frac{1}{\sqrt{1+r_c^2-2r_c\cos\theta}}d\theta$$

$$\Rightarrow F_y(r_c) = -\frac{1+r_c}{\Pi r_c}E(\frac{2\sqrt{r_c}}{1+r_c}) + \frac{1-r_c}{\Pi r_c}K(\frac{2\sqrt{r_c}}{1+r_c})$$

$$\Rightarrow F_y(r_c) = \frac{2(1-r_c^2)}{\Pi r_c}K(r_c) - \frac{2}{\Pi r_c}E(r_c) \qquad \text{(A.1)}$$

$$M(r_c) = \frac{1}{\Pi}\int_0^{\Pi}\frac{1-r_c\cos\theta}{\sqrt{1+r_c^2-2r_c\cos\theta}}d\theta$$

$$\Rightarrow M(r_c) = \frac{1}{2\Pi}\int_0^{\Pi}\sqrt{1+r_c^2-2r_c\cos\theta}\,d\theta + \frac{1-r_c^2}{2\Pi}\int_0^{\Pi}\frac{1}{\sqrt{1+r_c^2-2r_c\cos\theta}}d\theta$$

$$\Rightarrow M(r_c) = \frac{1+r_c}{\Pi}E(\frac{2\sqrt{r_c}}{1+r_c}) + \frac{1-r_c}{\Pi}K(\frac{2\sqrt{r_c}}{1+r_c})$$

$$\Rightarrow M(r_c) = \frac{2}{\Pi}E(r_c) \qquad \text{(A.2)}$$

The LS for the ring of isotropic support can be obtained completely from equations A.1 and A.2, for $0 \le r_c \le 1$, with K and E being the complete elliptic integrals of the first and second kind respectively.

A.5 LS For Disk Of Isotropic Support As Elliptic Integrals

As also shown by Ishlinskii et al. [1980], equation 7.11 (parameterizing the LS for the uniformly supported disk of isotropic friction) can be obtained in the form of elliptic integrals, by rewriting the expressions for $F_y(r_c)$ and $M(r_c)$ as follows, and by using the formulae in Gradshteyn [1980]. The substitutions of variables $s = r/r_c$ and $w = 1/s = r_c/r$ have also been resorted to, wherever appropriate.

$$F_y(r_c) = \frac{2}{\Pi}\int_0^1\int_0^{\Pi}\frac{r(r\cos\theta - r_c)}{\sqrt{r^2+r_c^2-2rr_c^2\cos\theta}}d\theta dr,$$

$$\Rightarrow F_y(r_c) = -\frac{1}{\Pi r_c}\int_0^1 r\int_0^{\Pi}\left(\sqrt{r^2+r_c^2-2rr_c^2\cos\theta} + \frac{r_c^2-r^2}{\sqrt{r^2+r_c^2-2rr_c^2\cos\theta}}\right)d\theta dr$$

$$\Rightarrow F_y(r_c) = -\frac{2}{\Pi r_c}\int_0^1 r\left((r+r_c)E(\frac{2\sqrt{rr_c}}{r+r_c}) + (r_c-r)K(\frac{2\sqrt{rr_c}}{r+r_c})\right)dr$$

$$F_y(r_c) = -\frac{2r_c^2}{\Pi}\int_0^{\frac{1}{r_c}} s\left((s+1)E(\frac{2\sqrt{s}}{s+1}) + (1-s)K(\frac{2\sqrt{s}}{s+1})\right)ds \qquad \text{(A.3)}$$

$$M(r_c) = \frac{2}{\Pi}\int_0^1\int_0^{\Pi}\frac{r^2(r-r_c\cos\theta)}{\sqrt{r^2+r_c^2-2rr_c^2\cos\theta}}d\theta dr$$

$$\Rightarrow M(r_c) = \frac{1}{\Pi}\int_0^1 r \int_0^{\Pi} \left(\sqrt{r^2 + r_c^2 - 2rr_c^2\cos\theta} - \frac{r_c^2 - r^2}{\sqrt{r^2 + r_c^2 - 2rr_c^2\cos\theta}} \right) d\theta dr$$

$$\Rightarrow M(r_c) = \frac{2}{\Pi}\int_0^1 r \left((r + r_c)E(\frac{2\sqrt{rr_c}}{r + r_c}) - (r_c - r)K(\frac{2\sqrt{rr_c}}{r + r_c}) \right) dr$$

$$M(r_c) = \frac{2r_c^3}{\Pi}\int_0^{\frac{1}{r_c}} s \left((s+1)E(\frac{2\sqrt{s}}{s+1}) - (1-s)K(\frac{2\sqrt{s}}{s+1}) \right) ds \qquad (A.4)$$

Further simplification is achieved depending on the value of r_c. First we consider $r_c \geq 1$. Then from equations A.3 and A.4, we have:

$$F_y = -\frac{4r_c^2}{\Pi}\int_0^{\frac{1}{r_c}} sE(s)ds$$

$$\Rightarrow F_y = -\frac{4r_c^2}{3\Pi}\left((s^2+1)E(s) + (s^2-1)K(s) \right)_0^{\frac{1}{r_c}}$$

$$\Rightarrow F_y = -\frac{4r_c^2}{3\Pi}\left((\frac{1}{r_c^2}+1)E(\frac{1}{r_c}) + (\frac{1}{r_c^2}-1)K(\frac{1}{r_c}) \right) \qquad (A.5)$$

$$M = \frac{4r_c^3}{\Pi}\int_0^{\frac{1}{r_c}} (sE(s) + s(s^2-1)K(s))ds$$

$$\Rightarrow M = \frac{4r_c^3}{\Pi}[\quad \tfrac{1}{3}((1+s^2)E(s) + (s^2-1)K(s)) + \tfrac{1}{9}((4+s^2)E(s) + (s^2-1)(4+3s^2)K(s)) - (E(s) + (s^2-1)K(s))]$$

$$\Rightarrow M = \frac{4r_c^3}{9\Pi}\left((\frac{4}{r_c^2} - 2)E(\frac{1}{r_c}) + (\frac{3}{r_c^2} - 2)(\frac{1}{r_c^2} - 1)K(\frac{1}{r_c}) \right) \qquad (A.6)$$

Equations A.5 and A.6 parameterize the LS for the disk for $r_c \geq 1$. For $0 \leq r_c < 1$, we split up the integration into two parts as:

$$\int_0^1 (\quad)dr = \int_0^{r_c} (\quad)dr + \int_{r_c}^1 (\quad)dr = \int_0^1 (\quad)ds + \int_{r_c}^1 (\quad)dw$$

Applying this to equations A.3 and A.4 we have:

$$F_y(r_c) = -\tfrac{2r_c^2}{\Pi}\int_0^1 s\left((s+1)E(\tfrac{2\sqrt{s}}{s+1}) + (1-s)K(\tfrac{2\sqrt{s}}{s+1}) \right) ds - \tfrac{4r_c^2}{\Pi}\int_{r_c}^1 \tfrac{1}{w^4}\left(E(w) - (1-w^2)K(w) \right) dw$$

$$\Rightarrow F_y(r_c) = -\frac{8r_c^2}{3\Pi} - \frac{4r_c^2}{3\Pi}\left(\frac{1-w^2}{3w^3}K(w) - \frac{1+w^2}{3w^3}E(w) \right)_{r_c}^1$$

$$F_y(r_c) = -\frac{4}{3\Pi r_c}\left((1+r_c^2)E(r_c) + (r_c^2-1)K(r_c) \right) \qquad (A.7)$$

$$M(r_c) = \tfrac{2r_c^3}{\Pi}\int_0^1 s\left((s+1)E(\tfrac{2\sqrt{s}}{s+1}) - (1-s)K(\tfrac{2\sqrt{s}}{s+1}) \right) ds + \tfrac{4r_c^3}{\Pi}\int_{r_c}^1 \tfrac{E(w)}{w^4}dw$$

$$\Rightarrow M(r_c) = \frac{8r_c^3}{9\Pi} + \frac{4r_c^3}{9\Pi}\left(\frac{2(w^2-2)}{w^3}E(w) + \frac{1-w^2}{w^3}K(w)\right)_{r_c}^{1}$$

$$M(r_c) = -\frac{4}{9\Pi}\left(2(r_c^2-2)E(r_c) + (1-r_c^2)K(r_c)\right) \tag{A.8}$$

Equations A.7 and A.8 parameterize the LS for the disk for $0 \leq r_c < 1$.

A.6 Spherical LS For Infinite Disk With Tangential Ideal Wheels

For an infinite disk with tangential ideal wheels, the individual limit surfaces for the elemental area of contact would appear as 'bristles' centered at the origin of load space and oriented in every possible direction. If the lengths of each of these bristles is the same and there is a uniform density of their distribution (for any given solid angle in load space), then their Minkowsky sum would lead to a spherical LS.

We derive below the pressure distribution $p(r)$ necessary to achieve a spherical LS of unit radius. From fig. 36, it can be seen that the pressure distribution (leading to equal length bristles of equal density) must satisfy:

$$p(r)\sqrt{1+r^2}(2\Pi r dr) = 2\Pi \sin\theta d\theta, \qquad \tan\theta = \frac{1}{r}$$

$$\Rightarrow p(r)\sqrt{1+r^2}(2\Pi r dr) = 2\Pi\left(\frac{1}{\sqrt{1+r^2}}\right)\left(\frac{1}{1+r^2}dr\right)$$

$$\Rightarrow p(r) = \frac{1}{r(1+r^2)^2}$$

To show that equations 7.25 and 7.26 parameterizing the generating curve for the LS for the infinite disk with the above pressure distribution, yields a semicircle, we prove that:

$$M^2(r_c) + F_y^2(r_c) = 1$$

$$\Rightarrow M(r_c)\frac{\partial M(r_c)}{\partial r_c} + F_y(r_c)\frac{\partial F_y(r_c)}{\partial r_c} = 0 \tag{A.9}$$

Besides, normality of the LS implies that:

$$\frac{\partial M(r_c)}{\partial r_c} = r_c\frac{\partial F_y(r_c)}{\partial r_c} \tag{A.10}$$

Substituting equation A.10 into A.9 implies that we have to show:

$$F_y(r_c) + r_c M(r_c) = 0 \tag{A.11}$$

Simplifying equations 7.25 and 7.26, we have:

$$F_y(r_c) = -\frac{2}{\Pi r_c}\int_0^{r_c}\frac{r^2}{\sqrt{r_c^2-r^2(1+r^2)}}dr - \frac{2}{\Pi r_c}\int_0^{r_c}\frac{r\tan^{-1}r}{\sqrt{r_c^2-r^2}}dr$$

$$M(r_c) = \frac{2}{\Pi}\int_0^{r_c} \frac{1}{\sqrt{r_c^2 - r^2}(1+r^2)}dr$$

$$\Rightarrow F_y(r_c) + r_c M(r_c) = -\frac{2}{\Pi r_c}\left(\int_0^{r_c} \frac{r\tan^{-1} r}{\sqrt{r_c^2 - r^2}}dr - \int_0^{r_c} \frac{\sqrt{r_c^2 - r^2}}{1+r^2}dr\right)$$

$$\Rightarrow F_y(r_c) + r_c M(r_c) = -\frac{2}{\Pi r_c}\left(\int_0^{r_c} \frac{r\tan^{-1} r}{\sqrt{r_c^2 - r^2}}dr - \int_0^{r_c} \frac{r\tan^{-1} r}{\sqrt{r_c^2 - r^2}}dr\right)$$

$$\Rightarrow F_y(r_c) + r_c M(r_c) = 0$$

A.7 Relation Between Velocity And Acceleration At Start And Finish

If we assume that the acceleration $d\mathbf{Q}(t)/dt$ of the slider is continuous, sufficiently smooth and bounded, then the direction of its velocity $\mathbf{Q}(t)$ is parallel to $d\mathbf{Q}(t)/dt$, both when the slider just begins to move and when it just comes to rest. If the times at which the slider just begins to move or just comes to rest are considered as zero, then the velocity at a time ϵ (very small number) away from zero is given as:

$$\mathbf{Q}(t) = \int_0^{\epsilon} \frac{d\mathbf{Q}(t)}{dt}dt$$

Applying the mean value theorem [Thomas 1985], we get:

$$\mathbf{Q}(\epsilon) = c\frac{d\mathbf{Q}(\epsilon^*)}{dt}, \qquad \epsilon^* \in [0, \epsilon]$$

where c is a constant. The Taylor series expansion of $d\mathbf{Q}(\epsilon^*)/dt$ about $d\mathbf{Q}(0)/dt$, as $\epsilon \to 0$ and hence $\epsilon^* \to 0$, gives us:

$$\lim_{\epsilon^* \to 0} \frac{d\mathbf{Q}(\epsilon^*)}{dt} = \lim_{\epsilon^* \to 0}\left(\frac{d\mathbf{Q}(0)}{dt} + \epsilon^*\frac{d^2\mathbf{Q}(0)}{dt^2} + \ldots\right) \approx \frac{d\mathbf{Q}(0)}{dt}$$

This implies that:

$$\lim_{\epsilon \to 0} \mathbf{Q}(\epsilon) = \mathbf{Q}(0) = c\frac{d\mathbf{Q}(0)}{dt}$$

or $\mathbf{Q}(0)$ is parallel to $d\mathbf{Q}(0)/dt$.

A.8 Equilibrium Point For Final Motion During 'Free Sliding'

We show that for the governing equation 8.9, an eigen direction ($\mathbf{P} \parallel \mathbf{q}$) is an equilibrium point. At an eigen direction, we have:

$$\mathbf{Q}(t) = Q(t)\mathbf{q}(t), \qquad \mathbf{P}(t) = P(t)\mathbf{q}(t) \tag{A.12}$$

where $Q(t)$ and $P(t)$ are the magnitudes of $\mathbf{Q}(t)$ and $\mathbf{P}(t)$ respectively. Substituting these in equation 8.9 gives:

$$\left(\frac{dQ(t)}{dt} + P(t)\right)\mathbf{q}(t) + Q(t)\frac{d\mathbf{q}(t)}{dt} = 0 \tag{A.13}$$

Dotting the above equation with $\mathbf{q}(t)$ and remembering that $\mathbf{q}(t) \cdot \mathbf{q}(t) = 1$, we get:

$$\frac{dQ(t)}{dt} = -P(t) \tag{A.14}$$

Since $P(t) \geq 0$, equation A.14 proves that the magnitude of the motion $Q(t)$ decreases monotonically at the eigen direction. Also, substitution of equation A.14 into A.13 gives that:

$$\frac{d\mathbf{q}(t)}{dt} = 0 \tag{A.15}$$

Equations A.12, A.13, A.14 and A.15 prove that an eigen direction is an equilibrium point for the differential equation 8.9.

A.9 Stability Of Eigen Directions For Generating Curves For Axisymmetric Limit Surfaces

Consider the eigen direction $\mathbf{P}$ with associated motion vector $\mathbf{q}$ on the generating curve in fig. 37, and look at another load $\mathbf{P}^*$ (with associated motion vector $\mathbf{q}^*$) which is $\delta\mathbf{P}$ away from $\mathbf{P}$ on the curve. The angle $\delta\phi$ between $\mathbf{q}^*$ and $\mathbf{q}$ and the angle $\delta\theta$ between $\mathbf{P}^*$ and $\mathbf{P}$ are given as:

$$\delta\phi = \frac{|\delta\mathbf{P}|}{\rho_c}, \quad \delta\theta = \frac{|\delta\mathbf{P}|}{|\mathbf{P}|}$$

where ρ_c is the *meridional* radius of curvature in load space [O'Neill 1985] of the curve at $\mathbf{P}$. Applying simple geometric reasoning and from equation 8.9, we can conclude:

1. $\rho_c > |\mathbf{P}| \Rightarrow \delta\theta > \delta\phi \Rightarrow \mathbf{q}^*$ is attracted to $\mathbf{q}$ by $\mathbf{P}^*$.
2. $\rho_c < |\mathbf{P}| \Rightarrow \delta\theta < \delta\phi \Rightarrow \mathbf{q}^*$ is repelled away from $\mathbf{q}$ by $\mathbf{P}^*$.
3. $\rho_c = |\mathbf{P}| \Rightarrow \delta\theta = \delta\phi \Rightarrow \mathbf{P}^*$ is also an 'eigen direction' and motions near $\mathbf{q}$ are neutrally stable.

A.10 Presence Of Eigen Directions On Generating Curves

We now show that loads of minimum and maximum magnitude on the generating curve are eigen directions and additionally that the minimum load is either a stable or a neutrally stable eigen direction. Let the magnitude of the loads on the generating curve be parameterized as $P(\theta)$, where θ is the angle made by the load $\mathbf{P}$ with a reference axis. Then the angle α between the normal to $\mathbf{P}$ and the tangent to the curve at $\mathbf{P}$ is given as:

$$\alpha = \frac{1}{P(\theta)}\frac{dP(\theta)}{d\theta}$$

But at points of maximum $P(\theta)$ and minimum $P(\theta)$,

$$\frac{dP(\theta)}{d\theta} = 0 \Rightarrow \alpha = 0$$

This implies that the maximum and minimum load are 'eigen directions'.

Also, it can be derived that the *meridional* radius of curvature ρ_c to the generating curve at **P** is given as:

$$\frac{1}{\rho_c} = \frac{P^2(\theta) + 2\left(\frac{dP(\theta)}{d\theta}\right)^2 - P(\theta)\frac{d^2P(\theta)}{d\theta^2}}{\left(P^2(\theta) + \left(\frac{dP(\theta)}{d\theta}\right)^2\right)^{3/2}}$$

$$\frac{dP(\theta)}{d\theta} = 0 \Rightarrow \frac{1}{\rho_c} = \frac{1}{P(\theta)} - \frac{1}{P^2(\theta)}\frac{d^2P(\theta)}{d\theta^2}$$

But if $P(\theta)$ is the minimum load, then:

$$\frac{d^2P(\theta)}{d\theta^2} \leq 0 \Rightarrow \rho_c \geq P(\theta)$$

This implies that $P(\theta)$ is either a stable or a neutrally stable eigen direction. Because of convexity, vertices can only be maximas and never minimas.

A.11 Stability Of Eigen Directions For Limit Surfaces

We form a Lyapunov function [Hirsch and Smale 1974] to determine the stability of an eigen direction on the LS, which is an equilibrium point for the differential equation 8.9. Consider a motion $\mathbf{Q}^* = Q^*\mathbf{q}^*$ at the load $\mathbf{P}^*$, which is in the neighbourhood of the equilibrium point load **P** (with associated motion **q**) on the LS. Then $\mathbf{Q}^*$ and $\mathbf{P}^*$ can be given as:

$$\mathbf{Q}^* = Q^*(\mathbf{q} + \Delta\mathbf{q}), \quad \mathbf{P}^* = \mathbf{P} + \Delta\mathbf{P}$$

where $\mathbf{q}^* = \mathbf{q} + \Delta\mathbf{q}$ and $\Delta\mathbf{P}$ and $\Delta\mathbf{q}$ are small perturbations (on the LS) from the equilibrium point load **P** and motion **q** respectively.

Substituting the above in equation 8.9 gives us:

$$\frac{d(Q^*\mathbf{q})}{dt} + \frac{d(Q^*\Delta\mathbf{q})}{dt} = -\mathbf{P} - \Delta\mathbf{P}$$

Load **P** being an equilibrium point implies that:

$$\frac{d(Q^*\mathbf{q})}{dt} = -\mathbf{P} \Rightarrow \frac{dQ^*}{dt} = -P \tag{A.16}$$

The above equations give us:

$$\frac{dQ^*}{dt}\Delta\mathbf{q} + Q^*\frac{d\Delta\mathbf{q}}{dt} = -\Delta\mathbf{P} \tag{A.17}$$

From the geometry of the LS [O'Neill 1966] and normality, we have that:

$$\Delta \mathbf{q} = \underline{\kappa} \Delta \mathbf{P}, \quad \underline{\kappa} = \begin{bmatrix} \kappa_1 & 0 \\ 0 & \kappa_2 \end{bmatrix} \tag{A.18}$$

where κ_1 and κ_2 are the principal curvatures of the LS in load space at P; and $\Delta \mathbf{q}$ and $\Delta \mathbf{P}$ are expressed in a coordinate system with its principal axes along the principal directions of curvature. Substituting equation A.18 into equation A.17, and from equation A.16 we get:

$$-P\underline{\kappa}\Delta \mathbf{P} + Q^* \underline{\kappa} \frac{d\Delta \mathbf{P}}{dt} = -\Delta \mathbf{P}$$

$$\Rightarrow \frac{d\Delta \mathbf{P}}{dt} = -(\underline{\rho} - \underline{\mathbf{I}}P)\frac{\Delta \mathbf{P}}{\mathbf{Q}^*}, \qquad \underline{\rho} = \underline{\kappa}^{-1} = \begin{bmatrix} \rho_1 & 0 \\ 0 & \rho_2 \end{bmatrix} \tag{A.19}$$

where $\rho_1 = 1/\kappa_1$ and $\rho_2 = 1/\kappa_2$ are the principal radii of curvature of the LS at P and $\underline{\mathbf{I}}$ is the 2×2 identity matrix.

Now we form the Lyapunov function $V(\mathbf{P}^*)$ near the equilibrium point P, given as:

$$V(\mathbf{P}^*) = |\mathbf{P}^* - \mathbf{P}| = \Delta P \tag{A.20}$$

$$\frac{dV(\mathbf{P}^*)}{dt} = \frac{\frac{d\Delta \mathbf{P}}{dt} \cdot \Delta \mathbf{P}}{\Delta P} = -(\underline{\rho} - \underline{\mathbf{I}}P)\frac{\Delta \mathbf{P} \cdot \Delta \mathbf{P}}{Q^* \Delta P} \tag{A.21}$$

$V(\mathbf{P}^*)$ is an admissible Lyapunov function since it satisfies the requisite criterion [Hirsch and Smale 1974] and the sign of $dV(\mathbf{P}^*)/dt$, which determines the stability of the equilibrium point P depends on $\underline{\rho}$ and P, conclusible as follows:

1. $\rho_1, \rho_2 > |\mathbf{P}|$ implies that $dV(\mathbf{P}^*)/dt < 0$ and $|\mathbf{P}|$ is an attracting or stable eigen direction.
2. ρ_1 or $\rho_2 < |\mathbf{P}|$ implies that $dV(\mathbf{P}^*)/dt > 0$ and $|\mathbf{P}|$ is a repelling or unstable eigen direction.
3. $\rho_1 = \rho_2 = |\mathbf{P}|$ implies that $dV(\mathbf{P}^*)/dt = 0$ and $|\mathbf{P}|$ is a neutrally stable eigen direction.

The argument leading to equation A.19 is largely due to Jim Papadopoulos [private communication], who also suggested the following analogy. The limit surface is a slippery shell on which slides a bead which is attracted to the origin. Equilibrium points for this bead are eigen directions; stable equilibrium points (minimum radius points) are stable eigen directions.

A.12 Inner And Outer Bounds On ρ_g For Varying The Final Motions Of Ring Of Isotropic Support

We now find the inner and outer bounds for the radius of gyration ρ_g of the ring of isotropic support and unit radius (original $\rho_g = 1$), so that the only corresponding stable eigen directions are the loads associated with pure translation and pure rotation of the ring about its CM, respectively.

For calculating the inner bound on ρ_g, we need to calculate the radius of curvature ρ_c of the curve shown in fig. 19 at the F_y axis and equate it to the value of $|\mathbf{P}|$ at the F_y axis, as follows. From the geometry of this curve, we have that:

$$\lim_{r_c \to \infty} \rho_c = \lim_{s \to 0} \frac{\sqrt{\left(\frac{\partial M(s)}{\partial s}\right)^2 + \left(\frac{\partial F_y(s)}{\partial s}\right)^2}}{\sqrt{\left(\frac{\partial q_\omega(s)}{\partial s}\right)^2 + \left(\frac{\partial q_y(s)}{\partial s}\right)^2}}, \quad s = \frac{1}{r_c} \tag{A.22}$$

When non-dimensionalized with $l_r = \rho_g$, from equation 7.8 we have that:

$$M(s) = \frac{1}{\Pi \rho_g} \int_0^\Pi \frac{s - \cos\theta}{\sqrt{1 + s^2 - 2s\cos\theta}} d\theta$$

$$F_y(s) = \frac{1}{\Pi} \int_0^\Pi \frac{s\cos\theta - 1}{\sqrt{1 + s^2 - 2s\cos\theta}} d\theta \, .$$

$$q_y(s) = -\frac{1}{\sqrt{1 + s^2\rho_g^2}}, \quad q_\omega(s) = \frac{s\rho_g}{\sqrt{1 + s^2\rho_g^2}}$$

$$\lim_{s \to 0} \frac{\partial M(s)}{\partial s} = \lim_{s \to 0} \frac{1}{\Pi \rho_g} \int_0^\Pi \frac{\sin^2\theta}{(1 + s^2 - 2s\cos\theta)^{3/2}} d\theta = \frac{1}{2\rho_g}$$

$$\lim_{s \to 0} \frac{\partial F_y(s)}{\partial s} = \lim_{s \to 0} \frac{1}{\Pi} \int_0^\Pi \frac{s\sin^2\theta}{(1 + s^2 - 2s\cos\theta)^{3/2}} d\theta = 0$$

$$\lim_{s \to 0} \frac{\partial q_y(s)}{\partial s} = \lim_{s \to 0} \frac{s\rho_g^2}{(1 + s^2\rho_g^2)^{3/2}} = 0$$

$$\lim_{s \to 0} \frac{\partial q_\omega(s)}{\partial s} = \lim_{s \to 0} \frac{\rho_g}{(1 + s^2\rho_g^2)^{3/2}} = \rho_g$$

Substituting the above in equation A.22 and from equation 7.8, we have that:

$$\lim_{r_c \to \infty} \rho_c = \frac{1}{2\rho_g^2} = \lim_{r_c \to \infty} |\mathbf{P}| = 1$$

$$\Rightarrow \rho_g = \frac{1}{\sqrt{2}} \tag{A.23}$$

So the inner bound on ρ_g is $1/\sqrt{2}$ which implies that for all axisymmetric mass distributions of the unit radius ring of isotropic support, satisfying $\rho_g < 1/\sqrt{2}$, the final motion of the freely sliding ring is a pure translation.

Similarly for calculating the outer bound on ρ_g, we need to calculate again the radius of curvature ρ_c, this time at the M axis and equate it to the value of $|\mathbf{P}|$ at the M axis. Again from geometry, we have that:

$$\lim_{r_c \to 0} \rho_c = \lim_{r_c \to 0} \frac{\sqrt{\left(\frac{\partial M(r_c)}{\partial r_c}\right)^2 + \left(\frac{\partial F_y(r_c)}{\partial r_c}\right)^2}}{\sqrt{\left(\frac{\partial q_\omega(r_c)}{\partial r_c}\right)^2 + \left(\frac{\partial q_y(r_c)}{\partial r_c}\right)^2}} \tag{A.24}$$

From equation 7.8 we have that:

$$\lim_{r_c \to 0} \frac{\partial M(r_c)}{\partial r_c} = \lim_{r_c \to 0} \frac{1}{\Pi \rho_g} \int_0^{\Pi} \frac{-r_c \sin^2\theta}{(1 + r_c^2 - 2r_c \cos\theta)^{3/2}} d\theta = 0$$

$$\lim_{r_c \to 0} \frac{\partial F_y(r_c)}{\partial r_c} = \lim_{r_c \to 0} \frac{1}{\Pi} \int_0^{\Pi} \frac{-\sin^2\theta}{(1 + r_c^2 - 2r_c \cos\theta)^{3/2}} d\theta = -\frac{1}{2}$$

$$\lim_{r_c \to 0} \frac{\partial q_\omega(r_c)}{\partial r_c} = \lim_{r_c \to 0} \frac{-r_c \rho_g}{(r_c^2 + \rho_g^2)^{3/2}} = 0$$

$$\lim_{r_c \to 0} \frac{\partial q_y(r_c)}{\partial r_c} = \lim_{r_c \to 0} \frac{\rho_g^2}{(r_c^2 + \rho_g^2)^{3/2}} = \frac{1}{\rho_g}$$

Substituting the above in equation A.24 and from equation 7.8, we have that:

$$\lim_{r_c \to 0} \rho_c = \frac{\rho_g}{2} = \lim_{r_c \to 0} |\mathbf{P}| = \frac{1}{\rho_g}$$

$$\Rightarrow \rho_g = \sqrt{2} \tag{A.25}$$

Hence the outer bound on ρ_g is $\sqrt{2}$, which implies that for all axisymmetric mass distributions of the ring satisfying $\rho_g > \sqrt{2}$, the final attracting motion of the freely sliding ring is a pure rotation about its center.

A.13 Inner And Outer Bounds On ρ_g For Varying The Final Motions Of Disk Of Isotropic Support

Just like the ring (appendix A.11), we now find the inner and outer bounds on ρ_g for the unit radius disk of isotropic support (original $\rho_g = \frac{1}{\sqrt{2}}$), beyond which the only stable eigen directions are the loads associated with pure translation and pure rotation of the disk about its center, respectively.

Proceeding like before, from equation 7.11 we have:

$$F_y(s) = \frac{2}{\Pi} \int_0^1 \int_0^{\Pi} \frac{r(rs\cos\theta - 1)}{\sqrt{1 + r^2 s^2 - 2rs\cos\theta}} d\theta dr,$$

$$M(s) = \frac{2}{\Pi \rho_g} \int_0^1 \int_0^{\Pi} \frac{r^2(rs - \cos\theta)}{\sqrt{1 + r^2 s^2 - 2rs\cos\theta}} d\theta dr, \quad s = \frac{1}{r_c}$$

$$\lim_{s \to 0} \frac{\partial M(s)}{\partial s} = \lim_{s \to 0} \frac{2}{\Pi \rho_g} \int_0^1 \int_0^{\Pi} \frac{r^3 \sin^2\theta}{(1 + r^2 s^2 - 2s\cos\theta)^{3/2}} d\theta dr = \frac{1}{4\rho_g}$$

$$\lim_{s \to 0} \frac{\partial F_y(s)}{\partial s} = \lim_{s \to 0} \frac{2}{\Pi} \int_0^1 \int_0^{\Pi} \frac{r^3 s \sin^2\theta}{(1 + r^2 s^2 - 2s\cos\theta)^{3/2}} d\theta dr = 0$$

$$\Rightarrow \lim_{r_c \to \infty} \rho_c = \frac{1}{4\rho_g^2} = \lim_{r_c \to \infty} |\mathbf{P}| = 1$$

$$\Rightarrow \rho_g = \frac{1}{2} \tag{A.26}$$

Equation A.26 implies that the inner bound for ρ_g is $1/2$, i.e. for all axisymmetric mass distributions of the unit radius disk of isotropic support, satisfying $\rho_g < 1/2$, the final attracting motion of the freely sliding disk is a pure translation.

Again, from equation 7.11, we have:

$$\lim_{r_c \to 0} \frac{\partial M(r_c)}{\partial r_c} = \lim_{r_c \to 0} \frac{2}{\Pi \rho_g} \int_0^1 \int_0^{\Pi} \frac{-r_c r^3 \sin^2\theta}{(r^2 + r_c^2 - 2 r r_c \cos\theta)^{3/2}} d\theta dr = 0$$

$$\lim_{r_c \to 0} \frac{\partial F_y(r_c)}{\partial r_c} = \lim_{r_c \to 0} \frac{2}{\Pi} \int_0^1 \int_0^{\Pi} \frac{-r^3 \sin^2\theta}{(r^2 + r_c^2 - 2 r r_c \cos\theta)^{3/2}} d\theta dr = -1$$

$$\Rightarrow \lim_{r_c \to 0} \rho_c = \rho_g = \lim_{r_c \to 0} |\mathbf{P}| = \frac{2}{3\rho_g}$$

$$\Rightarrow \rho_g = \sqrt{\frac{2}{3}} \tag{A.27}$$

Hence the outer bound on ρ_g is $\sqrt{2/3}$, which implies that for all axisymmetric mass distributions of the disk satisfying $\rho_g > \sqrt{2/3}$, the final attracting motion of the freely sliding disk is a pure rotation about its center.

Bibliography

[1] Amontons, G., *De la Résistance Causée Dans Les Machines*, Mémories de L'Académie Royale A, Chez Gerard Kuyper, pp 257–282, 1699.

[2] Bishop, J. F. W., and Hill, R., *A Theory Of The Plastic Distortion Of A Polycrystalline Aggregate Under Combined Stresses*, Philosophical Magazine, Series 7, Vol. 42, pp 414–427, 1951.

[3] Coulomb, C. A., *Théorie Des Machines Simples, en Ayant égard au Frottement de Leurs Parties, et a la Roideur Des Cordages*, Mémoire de Mathématique et de Physique de L'Académie Royale, Paris, pp 161–342, 1785.

[4] Curnier, A., *A Theory Of Friction*, International Journal Solids Structures, Vol. 20, Number 7, pp 637–647, 1984.

[5] Dowson, D., *History Of Tribology*, Longman Group Limited, 1979.

[6] Drucker, D. C., *A More Fundamental Approach To Plastic Stress-Strain Relations*, Proceedings of the First National Congress of Applied Mechanics, pp 487–491, ASME, New York, 1951.

[7] Drucker, D. C., *Coulomb Friction, Plasticity, and Limit Loads*, Journal Of Applied Mechanics, pp 71–74, March 1954.

[8] Drucker, D. C., *A Definition Of Stable Inelastic Material*, Journal of Applied Mechanics, Vol. 26:1, pp 101–106, March 1959.

[9] Drucker, D. C.,*On The Postulate Of Stability Of Materials In The Mechanics Of Continuua*, Journal de Méchanique, Vol. 3, Number 2, pp 235-249, June 1964.

[10] Erdmann, M. A., *On Motion Planning With Uncertainity*, Technical Report 810, MIT Artificial Intelligence Laboratory, Cambridge, Massachusetts, 1984.

[11] Gradsteyn, I. S., and Ryzhik, I. M., *Table Of Integrals, Series And Products*, Academic Press, Inc., 1980.

[12] Hill, R., *Mathematical Theory of Plasticity*, Oxford University Press, 1950.

[13] Hill, R.,*The Essential Structure Of Constitutive Laws For Metal Composites And Polycrystals*, Journal of Mechanics of Physics of Solids, Vol. 15, pp 79–95, 1967.

[14] Hirsch, M. W., and Smale, S., *Differential Equations, Dynamiccal Systems, And Linear Algebra*, Academic Press, Inc., 1974.

[15] Ishlinskii, A. Yu., Sokolov, B. N. and Chernouśko, F. L., *Motion Of Plane Bodies With Dry Friction*, Izv. AN SSSR, Mechanics of Solids/Mechanika Tverdogo Tela, Vol. 16, Number 4, pp 17–28, 1981.

[16] Jean, M. and Pratt, E., *A System Of Rigid Bodies With Dry Friction*, Int. J. Engng. Sci., Vol. 23, Number 5, pp 497–513, 1985.

[17] Jean, M. and Moreau, M. M., *Dynamics In The Presence Of Unilateral Contacts And Dry Friction: A Numerical Approach*, to appear in Proceedings Of The 3^{rd} Meeting, Unilateral Problems In Structural Analysis, G. Del Piero and F. Maceri, ed., CISM Courses And Lectures, 1986.

[18] Jellett, J. H., *A Treatise On The Theory Of Friction*, Hodges, Foster, And Co., 1872.

[19] Kalker, J. J., *A Minimum Principle For The Law Of Dry Friction, With Application To Elastic Cylinders In Rolling Contact*, Journal Of Applied Mechanics, Transactions Of ASME, Series 38, Vol. 4, pp 875–887, December 1971.

[20] Lötstedt, P., *Coulomb Friction In Two-Dimensional Rigid Body Systems*, ZAMM, 61, pp 605–615, 1981.

[21] MacMillan, W. D., *Dynamics of Rigid Bodies*, Dover Publications, 1936.

[22] Mason, M. T., and Salisbury, J. K., *Robot Hands And The Mechanics Of Manipulation*, The MIT Press, 1985.

[23] McGuire, W., *Steel Structures*, Section 6.5, pp 812–820, Prentice-Hall Inc./Englewood Cliffs, N.J., 1968.

[24] Meirovitch, L., *Methods Of Analytical Dynamics*, Section 4.8, pp 140–143, McGraw Hill, Inc., 1970.

[25] Michalowski, R., and Mroz, Z., *Associated And Non-Associated Sliding Rules In Contact Friction Problems*, Archives of Mechanics, Vol. 30, Number 3, pp 259–276, Warszawa 1978.

[26] Moreau, J. J., *On Unilateral Constraints, Friction And Plasticity*, New Variational Techniques in Mathematical Physics, G. Capriz and G. Stampacchia (eds.), CIME, II ciclo 1973, Edizioni Cremonese, Roma, pp 175–322, 1974.

[27] Moreau, J. J., *Application Of Convex Analysis To Some Problems Of Dry Friction*, Trends In Applications Of Pure Mathematics To Mechanics, H. Zorski (Editor), Vol. 2, pp 263–280, 1979.

[28] Moszynski, W., *Frottement Des Corps Solides Dans le cas de L'Anisotropie Naturelle et Artificielle*, Bull. Acad. Polon. Sciences et Lettres, Serie 7, Suppl. 4, pp 447–486, 1951.

[29] Munkres, J. R., *Topology, A first Course*, Prentice Hall, Inc., Englewood Cliffs, New Jersey, 1975.

[30] Oden, J. T., and Martins, J. A. C., *Models And Computational Methods For Dynamic Friction Phenomena*, FENOMECH III, Stuttgart, West Germany, 1984.

[31] O'Neill, B., *Elementary Differential Geometry*, Academic Press Inc., 1966.

[32] Peshkin, M. A., *Planning Robotic Manipulation Strategies For Sliding Objects*, Ph.D. Thesis, Department Of Physics, Carnegie Mellon University, November 1986.

[33] Prager, W., *Introduction To Plasticity*, Addison Wesley, 1959.

[34] Prescott, J., *Mechanics of Particles and Rigid Bodies*, Longmans, Green and Co., London, 1923.

[35] Rice, J. R., *On The Structure Of Stress-Strain Relations For Time-Dependent Plastic Deformation In Metals*, Journal of Applied Mechanics, Transactions of the ASME, pp 728–737, September 1970.

[36] Ruina, A. L., *Slip Instabilities And State Variable friction Laws*, Journal Of Geophysical Research, Vol. 88, Number B12, pp 10,359–10,370, December 10, 1983.

[37] Ruina, A. L., *Constitutive Relations For Frictional Slip*, Mechanics Of Geomaterials, Edited by Z. Bâzant, Chapter 9, John Wiley & Sons Ltd., 1985.

[38] Savvin, A. P., *The Calculation Of Friction Joints*, Russian Engineering Journal, issue 12, 1962.

[39] Savvin, A. P., *Calculation Of Rectangular Shape Friction Joints*, Russian Engineering Journal, issue 12, 1969.

[40] Shvedenko, V. N., *Equilibrium Of a Plane System Of Friction Forces*, Izv. AN SSSR, Mekhanika Tverdogo Tela, Vol. 21, Number 1, pp 37–42, 1986.

[41] Tabor, D., *Friction – The Present State of Our Understanding*, Journal of Lubrication Technology, Vol. 103, April 1981.

[42] Thomas, G. B., and Finney, R. L., *Calculus and Analytical Geometry*, Addison-Wesley Publishing Company, 1985.

[43] Voyenli, K., and Eriksen, E., *On The Motion of An Ice Hockey Puck*, American Journal of Physics, Volume 53 (12), December 1985.

[44] Wittenburg, J., *Ebene Bewegungen Bei Flächenhaft Verteilten Reibungskräften*, Kleine Mitteilungen [in German], ZAMM, Bd. 50, pp 637–640, 1970.

[45] Zhukovskii, N. E., *Equilibrium Condition For a Rigid Body Resting On a Fixed Plane With Some Area Of Contact, And Capable Of Moving Along The Plane With Friction*, in: Collected Works, Vol. 1: General Mechanics [in Russian], Gostekhizdat, Moscow-Leningrad, pp 339–354, 1948.

[46] Ziegler, H., *Discussion of Some Objections to Thermomechanical Orthogonality*, Ingenieur-Archiv, Vol. 50, pp 149–164, 1981.

[47] Ziemba, S., *On Certain Cases Of Anisotropic Friction*, Archives Of Mechanics, pp 105–121, [in Polish], Vol. 4, 1952.

[48] Zmitrowicz, A., *A Theoretical Model of Anisotropic Dry Friction*, Wear, Vol. 73, pp 9–39, 1981.